

**A Study of Reservoir  
Characteristics of the  
Nanushuk and Colville Groups,  
Umiat Test Well 11,  
National Petroleum Reserve in Alaska**

By J. E. Fox, P. W. Lambert, J. K. Pitman, and C. H. Wu

---

**GEOLOGICAL SURVEY CIRCULAR 820**

**United States Department of the Interior**  
CECIL D. ANDRUS, *Secretary*



**Geological Survey**  
H. William Menard, *Director*

## CONTENTS

	Page
Abstract-----	1
Introduction-----	2
Location-----	2
Drilling history-----	4
Umiat test well 11-----	4
Objectives and procedures-----	4
Paleogeographic setting-----	4
Age-----	9
Core analysis-----	10
Introduction-----	10
Stratigraphy and depositional environments--Manushuk Group----	10
Tuktu and Grandstand Formations-----	10
Killik Tongue of the Chandler Formation-----	14
Ninuluk Formation-----	15
Stratigraphy and depositional environments--Colville Group----	17
Seabee Formation-----	17
Tuluwak Tongue of the Prince Creek Formation-----	18
Petrography-----	21
Manushuk Group-----	25
Grandstand Formation and Killik Tongue of the Chandler Formation-----	25
Detrital grains-----	25
Matrix-----	29
Authigenic minerals-----	29
Porosity-----	30
Ninuluk Formation-----	30
Detrital grains-----	30
Matrix-----	31
Authigenic minerals-----	31
Porosity-----	31
Colville Group-----	31
Seabee Formation and Tuluwak Tongue of the Prince Creek Formation-----	31
Detrital grains-----	32
Matrix and authigenic minerals-----	33
Porosity-----	34
Factors affecting porosity and permeability-----	35
Core and well-log analyses-----	38
Average porosity of each formation-----	39
Average permeability of each formation-----	40
Formation-water resistivity-----	43
Results of porosity and permeability analyses-----	44
Summary-----	45
References cited-----	46

## ILLUSTRATIONS

	Page
Figure 1. Index map of northern Alaska outlining location of National Petroleum Reserve in Alaska and showing Umiat Anticline-----	2
2. Structure contour map of the top of the Grandstand Formation and cross section of Umiat Anticline-----	3

ILLUSTRATIONS (Continued)

	Page
3. Stratigraphic section of Umiat test well 11-----	5
4. Cross section showing stratigraphic relationships of Lower Cretaceous deltaic facies, Umiat area, Alaska--	9
5. Index map of Umiat-Maybe Creek region, northern Alaska, including line of section-----	11
6-12. Lithology, sedimentary structures, texture, inferred environment of deposition, and reservoir properties, Umiat test well 11	
6. Core 60 (911.0-915.6 m), Grandstand Formation----	12
7. Cores 56-58 (856.5-868.7 m), Grandstand Formation-----	13
8. Cores 52 and 53 (744.9-749.8 m), Grandstand Formation-----	14
9. Core 49 (723.6-729.4 m), Killik Tongue of the Chandler Formation-----	15
10. Cores 35-38 (623.9-639.2 m), Ninuluk Formation--	16
11. Cores 21-25 (402.9-419.7 m), Shale Wall Member of the Seabee Formation-----	18
12. Cores 15 and 16 (227.1-239.3 m), Ayyiak Member of the Seabee Formation-----	19
13. Lithology, sedimentary structures, texture, and inferred environment of deposition, cores 11 and 12 (157.0-167.6 m), Tuluvak Tongue of the Prince Creek Formation-----	20
14. Lithology, sedimentary structures, texture, inferred environment of deposition, and reservoir properties, cores 1 and 2, (35.1-47.2 m), Tuluvak Tongue of the Prince Creek Formation-----	21
15. Primary arenite triangle showing composition of samples listed in table 2-----	25
16. Litharenite triangle showing composition of samples listed in table 2-----	26
17-20. Photomicrographs:	
17. Grandstand Formation, 860.8 m (2824 ft). Chert arenite showing excellent porosity and permeability-----	27
18. Grandstand Formation, 860.8 m (2824 ft). Chert arenite showing excellent porosity and permeability-----	27
19. Grandstand Formation, 913.5 m (2997 ft). Phyllarenite with poor porosity and permeability-----	27
20. Grandstand Formation, 868.4 m (2849 ft)-----	27
21. Scanning electron micrograph of Grandstand Formation 868.4 m (2849 ft)-----	28
22. Photomicrograph of Killik Tongue of the Chandler Formation, 700.4 m (2298 ft)-----	28
23. Scanning electron micrograph of Killik Tongue of the Chandler Formation, 700.4 m (2298 ft)-----	28
24. Photomicrograph of Grandstand Formation, 868.4 m (2849 ft)-----	28
25. Scanning electron micrograph of Grandstand Formation, 745.2 m (2445 ft). Deformation of compressible grain by noncompressible grain-----	29
26-30. Photomicrographs:	
26. Killik Tongue of the Chandler Formation, 670.6 m (2200 ft). Sparry anhedral to euhedral calcite crystals-----	30
27. Ninuluk Formation, 637.9 m (2093 ft). Very tightly packed phyllarenite-----	30

ILLUSTRATIONS (Continued)

	Page
28. Seabee Formation, 409.3 m (1343 ft). Tightly packed phyllarenite with authigenic chlorite matrix-----	31
29. Seabee Formation, 409.3 m (1343 ft). Typical volcanic rock fragment-----	32
30. Seabee Formation, 235.0 m (771 ft). Phyllarenite with authigenic smectite matrix--	33
31. Scanning electron micrograph of Seabee Formation, 409.3 m (1343 ft). Mass of intergrown flakes of authigenic phyllosilicate, presumably chlorite, filling an intergranular pore-----	33
32. Photomicrograph of Seabee Formation, 409.3 m (1343 ft). Chlorite-filled pore-----	33
33. Photomicrograph of Tuluvak Tongue of the Prince Creek Formation, 156.7 m (514 ft). Phyllarenite with authigenic smectite matrix-----	34
34. Scanning electron micrograph of Tuluvak Tongue of the Prince Creek Formation, 156.7 m (514 ft). Dense masses and coatings of smectite with bifurcating and anastomosing fractures-----	34
35. Scanning electron micrograph of Seabee Formation, 229.8 m (754 ft). Dense masses and coatings of smectite with bifurcating and anastomosing fractures--	34
36. Photomicrograph of Seabee Formation, 229.8 m (754 ft). Smectite coatings on detrital grains-----	35
37-40. Charts:	
37. Effective porosity versus depth-----	35
38. Air permeability versus depth-----	36
39. Effective porosity versus modal grain size-----	36
40. Air permeability versus modal grain size-----	36
41. Air permeability of samples listed in table 2 plotted on primary arenite triangle-----	37
42. Air permeability of samples listed in table 2 plotted on litharenite triangle-----	38
43-46. Charts:	
43. Effective porosity versus percent phyllite plus schist-----	39
44. Air permeability versus percent phyllite plus schist-----	39
45. Effective porosity versus percent matrix-----	40
46. Air permeability versus percent matrix-----	40
47. Correlation of core porosity and $R_{64}$ " for beds stratigraphically above 610 m (2000 ft)-----	41
48. Correlation of core porosity and $R_{64}$ " for beds stratigraphically below 610 m (2000 ft)-----	41
49. Correlation of core porosity and $R_{16}$ " for beds stratigraphically above 610 m (2000 ft)-----	42
50. Correlation of core porosity and $R_{16}$ " for beds stratigraphically below 610 m (2000 ft)-----	42
51. Correlation of core and microlog porosities-----	42
52. Core permeability and porosity correlation-----	42

TABLES

	Page
Table 1. Summary of drilling and production history of Umiat Anticline-----	4
2. Petrography and reservoir properties of selected core samples from Umiat test well 11-----	22

TABLES (Continued)

	Page
3. Core-analysis and well-log data-----	41
4. Weighted average porosity, Umiat test well 11-----	43
5. Core permeability and porosity data-----	44
6. Weighted average permeability-----	44
7. Water analysis and formation-water resistivity from 724 to 735 m-----	44
8. Water analysis and formation-water resistivity from 746 to 751 m-----	45
9. Water analysis and formation-water resistivity from 864 to 869 m-----	45
10. Formation-water resistivity from well-log analyses using SP and $R_{16''}$ -----	45
11. Formation-water resistivity from well-log analyses using $R_{16''}$ and $R_{64''}$ -----	45
12. Formation-water resistivity from well-log analyses using core porosity and $R_t$ method-----	45

# A Study of Reservoir Characteristics of the Nanushuk and Colville Groups, Umiat Test Well 11, National Petroleum Reserve in Alaska

By J. E. Fox, P. W. Lambert, J. K. Pitman, and C. H. Wu

## ABSTRACT

Cretaceous sandstones in the Umiat Anticline contain the largest volume of oil discovered to date in the National Petroleum Reserve in Alaska. Umiat test well 11, although dry and abandoned, penetrated the most complete sequence of Cretaceous rocks in the Umiat area. Cretaceous formations cored (oldest to youngest) were the Grandstand, Chandler, and Ninuluk Formations of the Nanushuk Group and the Seabee and Prince Creek Formations of the Colville Group. Cores from sandstone beds in each of the formations penetrated were studied to identify the factors influencing porosity and permeability.

Based on lithologic, textural, sedimentary-structural, faunal and floral, and regional paleogeographic evidence, the Cretaceous stratigraphic sequence in the Umiat area can be described as complexly interbedded delta-front and delta-plain facies (named the Umiat delta). The Grandstand Formation and Killik Tongue of the Chandler Formation represent one thick progradational sequence of delta-front and delta-plain facies, respectively. This sequence was followed by deposition of transgressive marine facies of the Ninuluk and Seabee Formations, which were in turn overlain by another progradational delta-plain facies, the Tuluva Tongue of the Prince Creek Formation.

The delta-front sandstone of the Grandstand Formation is well-sorted, fine-grained to very fine grained, angular to subangular chert arenite and phyllarenite. Authigenic cements include dolomite, calcite, siderite, quartz overgrowth, kaolinite, chert, pyrite, and possibly some small flakes of chlorite. The source terrane was southwest of Umiat and, on the basis of the aforementioned petrographic evidence, consisted of low-grade metamorphic rocks and possibly sandstone and cherty limestone. The weighted average porosity, based on well-log analyses, for the lower part of the Grandstand Formation is 15.1 percent

and for the upper part is 15.6 percent; the weighted average permeability is 58.6 md for the lower part and 167 md for the upper part. The average size of visible pores is about 50  $\mu\text{m}$ . A linear relationship was established between permeability and porosity for sandstone samples from depths less than 405 m and greater than 644 m; the average permeability of these intervals can be estimated with reasonable accuracy not only for the Grandstand but also for the Tuluva, Seabee, and Killik.

The delta-front, delta-plain marginal facies of the Killik Tongue of the Chandler Formation includes sandstone, siltstone, shale, and coal. Sandstone samples studied petrographically are similar to those of the Grandstand Formation; the delta prograded northeasterly across the Umiat area and the source terrane for the sediments remained the same. Well-log analyses indicate that the weighted average porosity for the Killik Tongue is 16.4 percent and the weighted average permeability is 96.2 md.

The delta-front sandstone of the Ninuluk Formation is similar to that of the Grandstand and Killik, but is moderately sorted and contains less detrital quartz and significantly more metamorphic rock fragments than chert fragments. Sandstone in the upper part of the formation contains a considerable amount of calcite. Visible pores average about 35  $\mu\text{m}$  in size. The weighted average porosity for the Ninuluk Formation, based on well-log analyses, is 12.6 percent; the weighted average permeability is 10.7 md.

The Seabee Formation is primarily shale deposited in an open-marine environment; sandstone units in the Seabee overlie and are overlain by black marine shale. The mineralogy of these sandstone units differs markedly from that of the older formations. The sandstones are characterized by an abundance of volcanic rock fragments, high content of volcanic plagioclase feldspar, and low content of detrital quartz. Quartz, chert, phyllite, and metaquartzite all appear to be the same

petrographically as in the Nanushuk Group. Abundant chlorite and smectite reduce permeability and make sandstones of the Seabee inadequate reservoir rocks. Well-log analyses indicate that the weighted average porosity of the Seabee Formation is 11.5 percent; the weighted average permeability is 3.1 md.

The Tuluva Tongue of the Prince Creek Formation in the Umiat area is composed of predominantly delta-plain sandstone, siltstone, shale, bentonite, and coal. The source terrane was to the southwest and the marine shoreline was to the northeast of the Umiat area. Sandstone samples studied petrographically have a composition similar to those of the Seabee Formation except for a slightly higher content of quartz and slightly fewer volcanic and metamorphic rock fragments. Abundant authigenic smectite in these sandstones reduces permeability to very low values. Well-log analyses indicate that the weighted average porosity is 14.6 percent; the weighted average permeability is 3.9 md.

Modal grain size is a minor factor affecting porosity and permeability; in all formations, porosity and permeability tend to increase with increasing grain size. A minimum grain size of about 175  $\mu\text{m}$  is necessary for good (>50 md) permeability. Composition of the rock has a major effect on porosity and permeability; rocks that have a higher content of compressible grains (phyllite, schist, mica, and, rarely, chert and micaceous metaquartzite) and rocks that have greater matrix and cement content generally have lower porosity and permeability. In general, rocks having the best permeability are chert arenites, and those with the poorest permeability are phyllarenites. Phyllite and matrix abundance are related to the mineralogy of the source terrane and to energy conditions at the site of deposition. Porous and permeable reservoirs in the Grandstand Formation and Killik Tongue should exist in those depositional areas that received only sparse amounts of metamorphic rock debris and in areas where energy conditions at the site of deposition facilitated sorting and winnowing of the sediment.

In general, a large amount of expandable clay matrix has an adverse effect on effective porosity and permeability of reservoir rocks. Expandable clays are essentially absent in the Grandstand Formation, Killik Tongue of the Chandler Formation, and Ninuluk Formation; these units have good porosity and permeability. The Seabee Formation and the Tuluva Tongue of the Prince Creek Formation, however, have abundant smectite matrix; porosity in these sandstones is in large part fracture porosity in this matrix. These fractures may have been formed by swelling and shrinking of the smectite due to wetting and drying or by freezing and

chawing of ice crystals in the permafrost zone. When these sandstones come into contact with water, the clay matrix expands and chokes off the porosity and permeability.

## INTRODUCTION

Cretaceous sandstones in the North Slope basin of Alaska have proven hydrocarbon accumulations. Umiat Anticline, drilled and tested by the U.S. Navy between 1945 and 1952, contains the largest volume of oil discovered to date in the National Petroleum Reserve in Alaska (Brosge and Whittington, 1966). The quantity of recoverable reserves has been estimated to be as great as 122 million barrels of oil and an undetermined volume of gas (Espach, 1951). A large range in estimates is due to the use of different recovery factors and reservoir parameters in calculating the recoverable reserves. Most of the oil and gas occurs in the Grandstand Formation of the Nanushuk Group. This study investigates the reservoir characteristics of Cretaceous sandstones in Umiat test well 11, located on Umiat Anticline. (All measurements in Umiat test well 11 were made in the foot-pound system and have been converted to metric and rounded off to the nearest tenth of a unit in this report. No increase in the precision of the basic measurements is implied.)

## LOCATION

Umiat Anticline is located near Umiat, Alaska, near the southeastern edge of NPRA, just north of the Colville River (fig. 1). The anticline is a west-trending structure that has a total structural closure of approximately 610 m (fig. 2) (Brosge and Whittington, 1966). Two major west-trending,

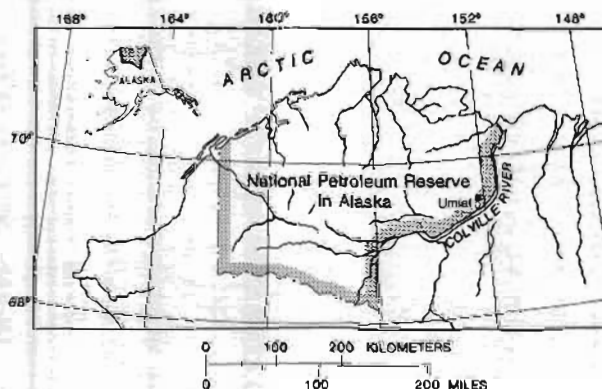


Figure 1.--Index map of northern Alaska outlining location of National Petroleum Reserve in Alaska.

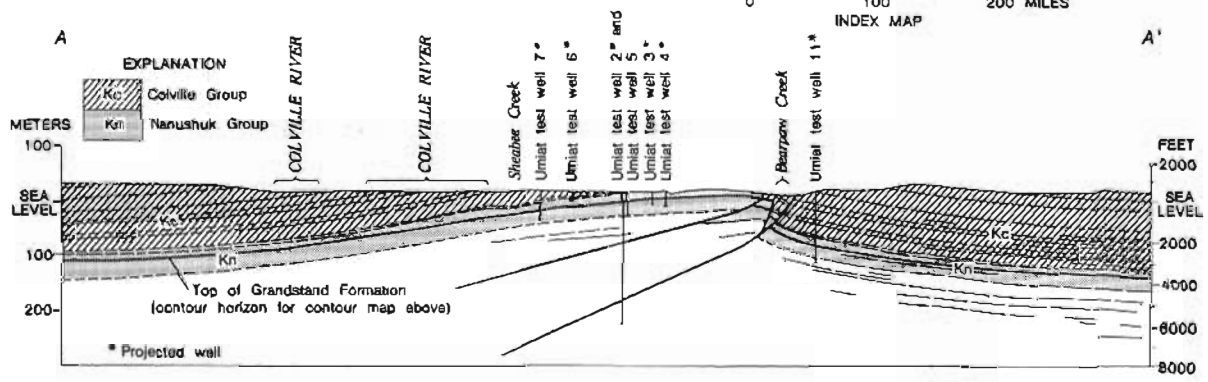
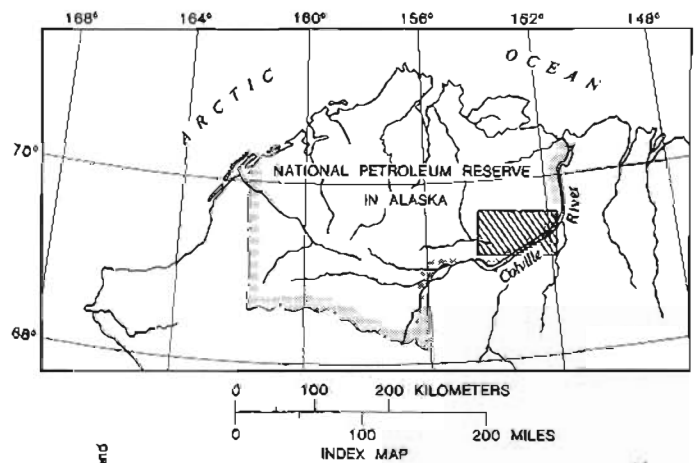
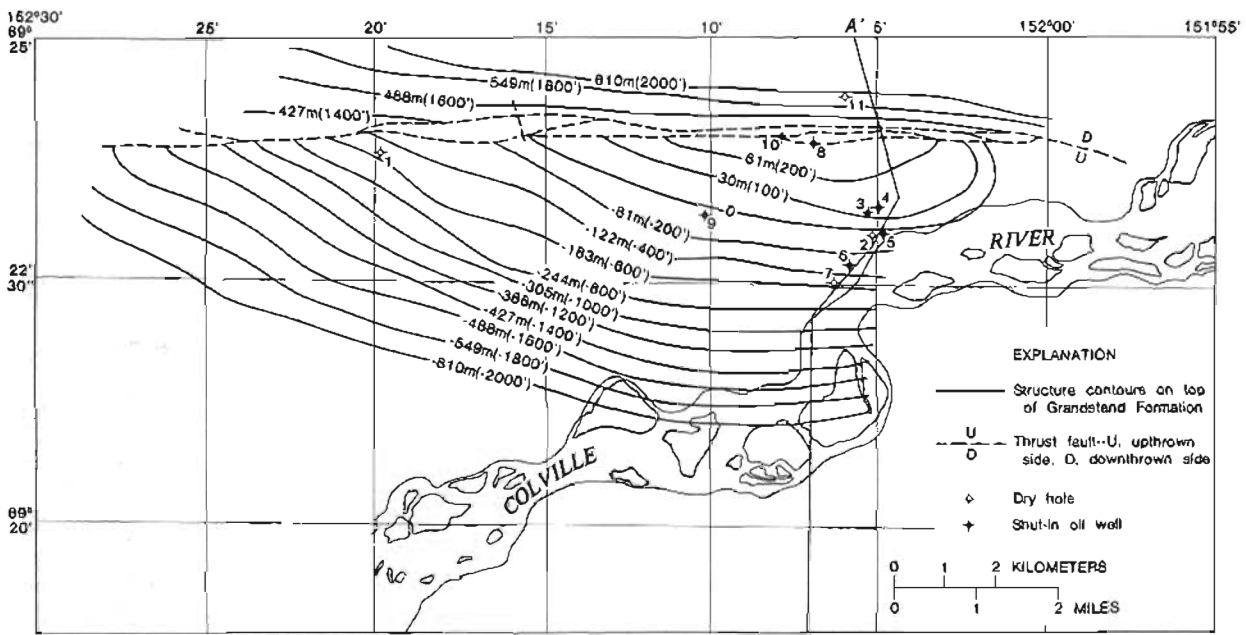


Figure 2.--Structure contour map of the top of the Grandstand Formation and cross section of Umiat Anticline. Area of structure contour map is shown by crosshatching on index map. Modified from Brosge and Whittington (1966).

southward-dipping thrust faults bisect the anticline. Strata on the south limb have been upthrown at least 610 m relative to strata on the north limb; structural closure of about 275 m exists on the south limb against the fault (Brosgé and Whittington, 1966) (fig. 2).

## Umiat Test Well 11

Umiat test well 11 was spudded on June 3, 1952, and was subsequently drilled to a total depth of 1,007 m. Numerous shows of oil and gas were reported. In test well 11, water was found in the two sandstone beds of the Grandstand Formation that were the most oil-productive beds in other Umiat test wells. On August 29, 1952, well 11 was listed as dry and was abandoned. Although rocks of both Early and Late Cretaceous age are found in the subsurface throughout the Umiat area, well 11 penetrated the most complete Cretaceous stratigraphic section because of its location on the lower block of the faulted anticline (fig. 2). For this reason, and because it is an unfaulted sequence, Umiat test well 11 was chosen for detailed study. (Refer to figure 3 for the complete stratigraphic sequence for well 11; also note the shape of the electric log.)

### Drilling History

Eleven test wells were drilled on Umiat Anticline during the period from 1945 to 1952 (fig. 2); cores were cut during the drilling of all of the wells. The first 10 wells were drilled on the south flank (overthrust block) and test well 11 was drilled on the north flank (lower fault block). Test wells 1, 2, and 3 were drilled with rotary rigs using freshwater mud. Thin-section analysis of these cores by Krynine (1947, 1948) revealed expandable interstitial clays in several of the target Cretaceous sandstone beds. Krynine believed that these clays may have swelled upon contact with the mud filtrate and "choked off" the permeability. Beginning with test well 4, and for the remainder of the wells, cable drilling, using brine, or rotary drilling, using oil-base or oil-emulsion mud, was employed. Test wells 1, 2, 7, and 11 were dry; therefore, they were abandoned. Table 1 presents a summary of production tests from each of the test wells. The oil in productive wells has a gravity of 36.0° to 37.2° API, a pour point ranging from less than 15° to -32° C, and a sulfur content of less than 0.1 percent; it contains about 35 percent gasoline and naphtha (Brosgé and Whittington, 1966). The reader is referred to Collins (1958) for more detailed production information for each well.

### OBJECTIVES AND PROCEDURES

The major objective of this study was to identify factors influencing porosity and permeability of Cretaceous sandstone units in Umiat test well 11. The information presented in this report should be useful in future reservoir studies of Cretaceous rocks throughout the area.

A multiphase procedure was used in this study. One phase involved a sedimentologic study of selected cores from well 11. Sedimentologic information obtained from the cores was incorporated into the regional paleogeographic setting in order to make interpretations as to the environment in which sediment in each of the selected cored intervals was deposited. A second phase was a detailed petrographic study documenting the influence of texture and fabric properties and mineralogic and diagenetic factors on reservoir quality. Because of the abundance of swelling clays in this area and their demonstrated effects on drilling and recovery techniques, a third phase was implemented: identification, using X-ray diffraction, of the kinds of interstitial clay in the various sandstone units. The fourth phase of the study was the examination of electric logs to learn whether porosity of uncored zones could be determined from the available well logs and whether formation-water salinity could be determined so that water saturation could be estimated from the logs.

Table 1.--Summary of drilling and production history of Umiat Anticline

[Modified from Brosgé and Whittington (1966)]

Umiat test well	drilling data		Total depth (meters)
	Status	Type of drill	
1	Dry and abandoned	Rotary	1,832
2	do	do	1,895
3	Pumped 24 bbl oil per day; abandoned.	Rotary (core test)	174
4	Pumped 100 bbl oil per day; shut in.	Cable tool	256
5	Pumped 400 bbl oil per day; shut in.	do	328
6	Pumped estimated 80 bbl oil per day; junked and abandoned.	do	252
7	Dry and abandoned	do	422
8	Pumped 60-100 bbl oil per day; gas estimated 169,923.5 cu m (6 million cu ft) per day; shut in.	do	405
9	Pumped average 217 bbl oil per day; abandoned.	Rotary	363
10	Failed 222 bbl oil in 24 h; plugged and abandoned.	Cable tool	480
11	Dry and abandoned	Rotary	1,007

### PALEOGEOGRAPHIC SETTING

Cretaceous strata in the Umiat area of the North Slope consist of detrital clastic sediments derived from the ancestral Brooks

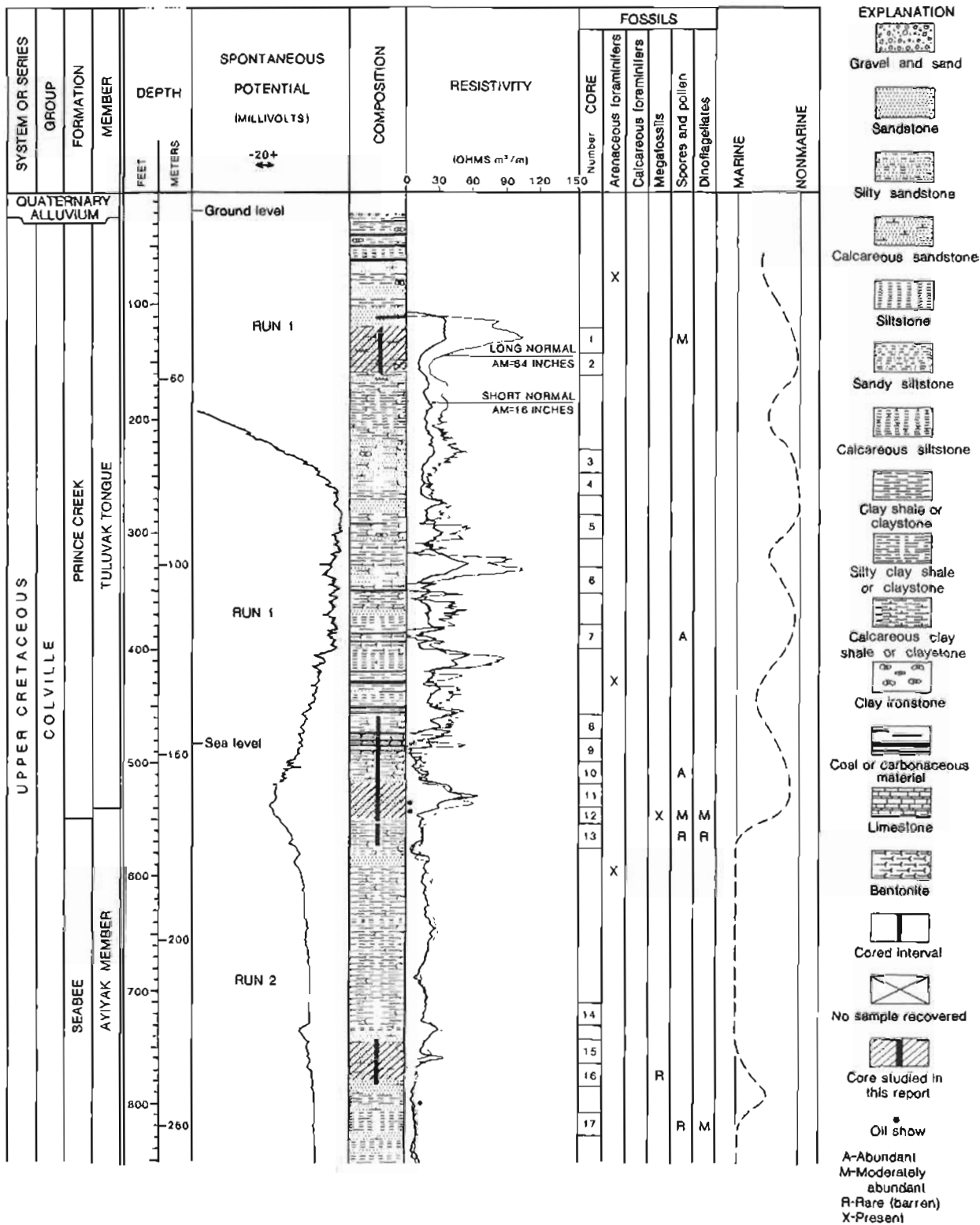


Figure 3.--Stratigraphic section of Umiat test well 11. Modified from Collins (1958).

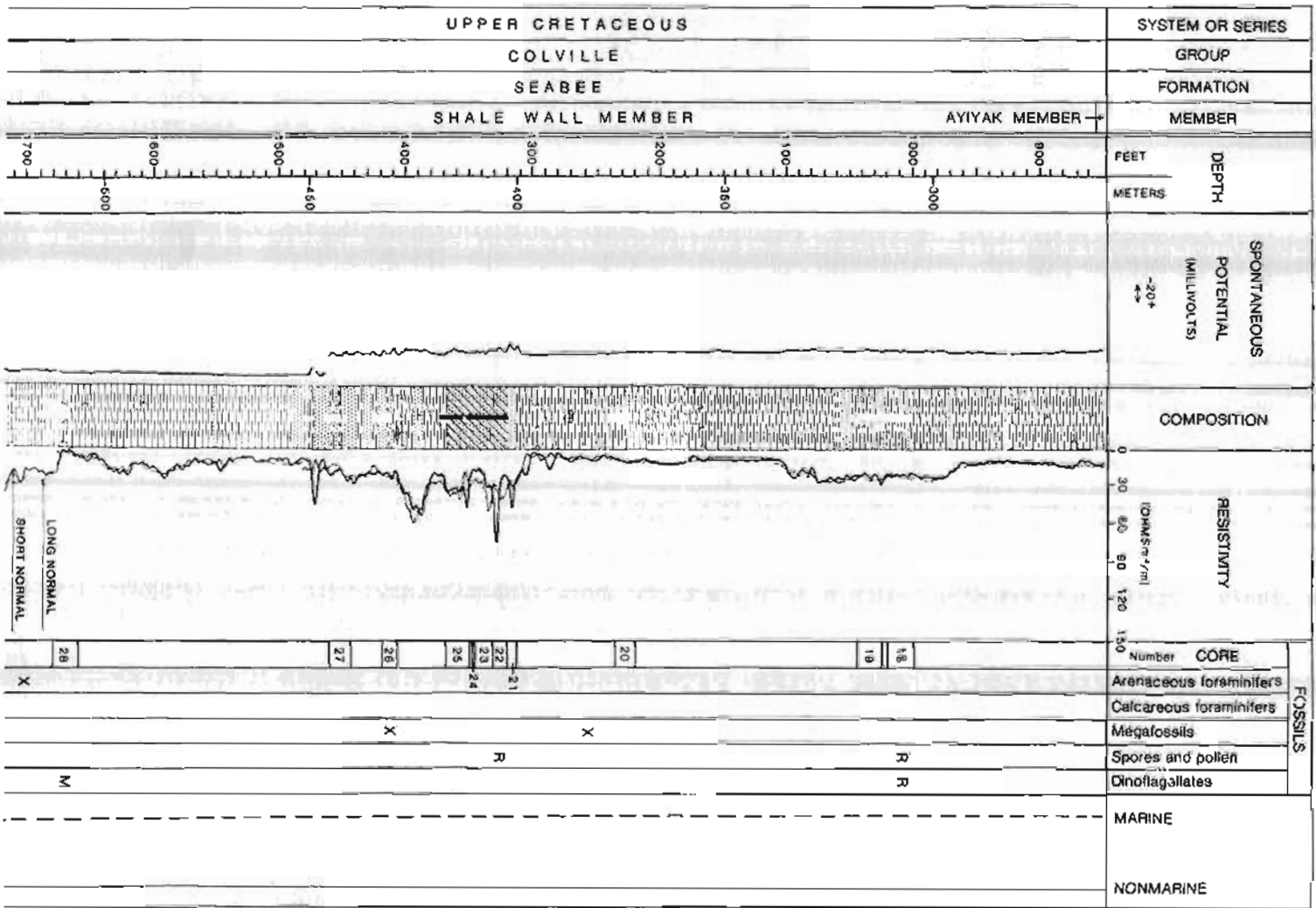


Figure 3.--Stratigraphic section of Uinta test well 11. Modified from Collins (1958)--Continued.

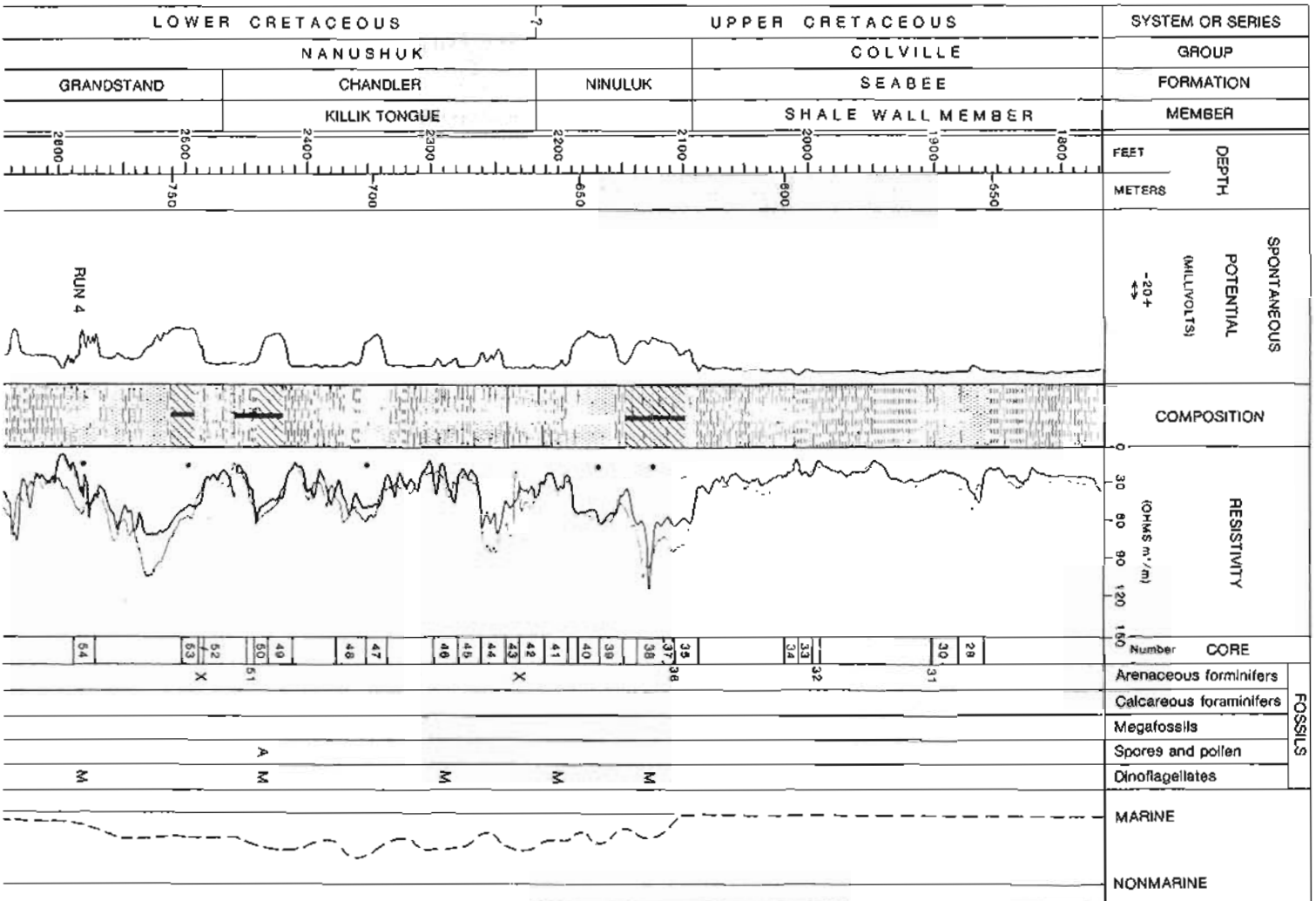
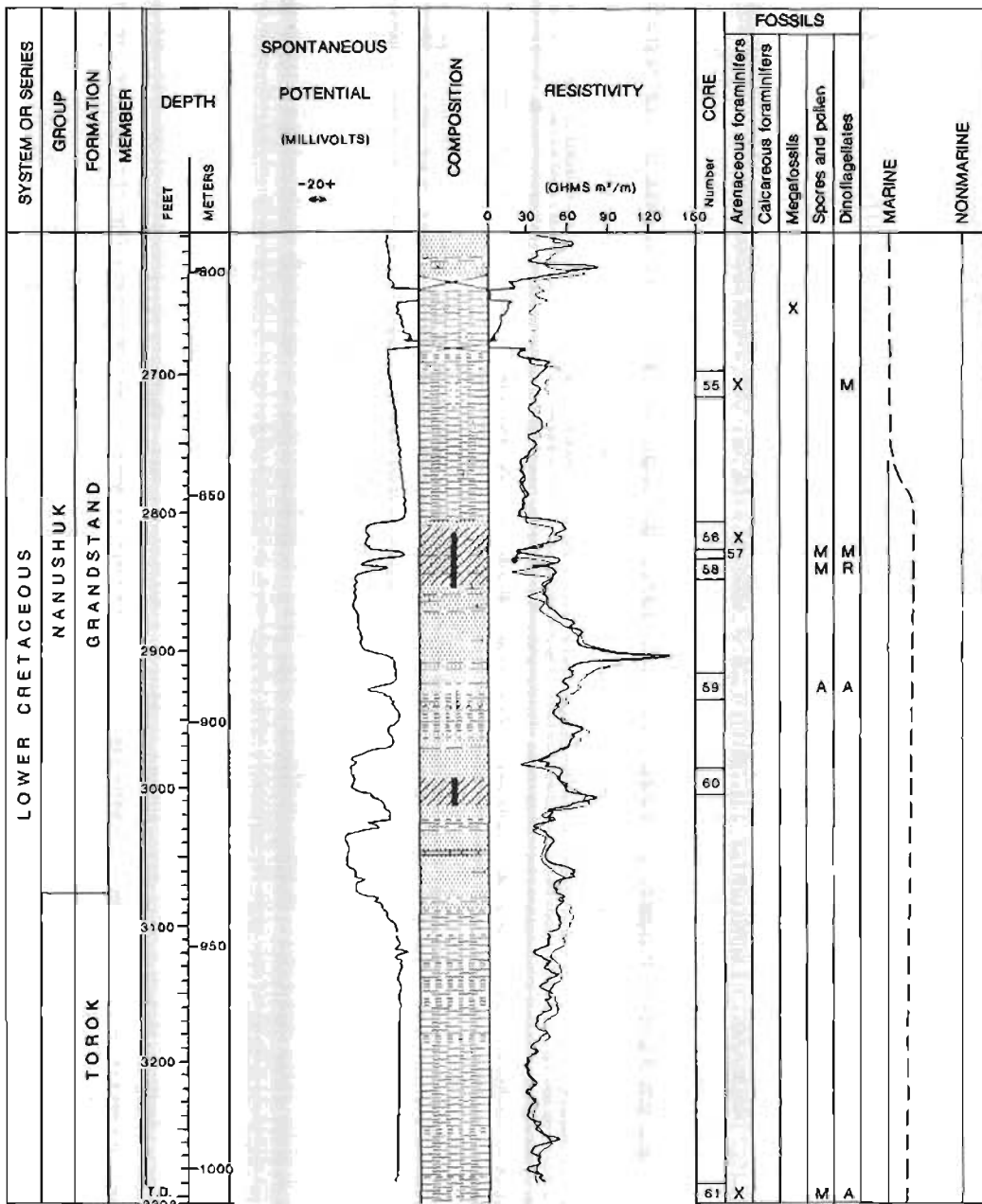


Figure 3.--Stratigraphic section of Umist test well 11. Modified from Collins (1958)--Continued.



Location Lat 89°24'29" N.  
Long 152°05'58" W  
Elevation Kelly Bushing 481 feet  
Ground 464 feet  
Total depth 3303 feet  
Status Dry and abandoned

Spudded June 3, 1952  
Completed August 29, 1952  
Electric log by Schlumberger Well  
Surveying Corporation  
All depths are measured from  
the top of the Kelly Bushing

Figure 3.--Stratigraphic section of Umiat test well 11. Modified from Collins (1958)--Continued.

Range to the south. These sediments were deposited in continental alluvial fans and delta plains, and in nearshore- and offshore-marine environments. The sedimentary

environments generally prograded from southwest to northeast as the Cretaceous seas retreated from the area. Periodic transgressions of the sea caused a complex intertonguing of the

nearshore-marine and continental facies (fig. 3). Fisher and others (1969), basing their conclusions on work by Brosgé and Whittington (1966), presented a deltaic interpretation of Lower Cretaceous rocks in the Umiat area, as shown on figure 4. They interpreted the Grandstand Formation as consisting of delta-front sands that overlie and intertongue with prodelta muds of the Torok Formation. The upper contact of these delta-front sands intertongues with the overlying Killik Tongue of the Chandler Formation, interpreted to be delta-plain deposits of mud and sand, rich in organic matter. As shown on figure 4, the delta-plain facies of the Killik Tongue thins to the east-northeast. Near Umiat, at the far east end of the section, very little of the delta-plain facies is present. This facies of Lower Cretaceous rocks eventually pinches out to the east and northeast of Umiat Anticline.

Transgression of the sea is indicated by deposits of sandstone of the Upper Cretaceous Ninuluk Formation (fig. 3). Continued transgression resulted in deposition of marine shale of the Seabee Formation. Near the end of Seabee deposition, the shoreline again prograded. Deposition was again deltaic; sands and silts grade vertically into nearshore marine-to-continental sands, silts, shale, and coal of the Tuluvak Tongue of the Prince Creek Formation. These facies relationships are similar to those of the Lower Cretaceous strata of this area.

#### AGE

The stratigraphic position of fossils in test well 11 is shown on figure 3. In his study of microfossils of the Umiat area, Bergquist (in Collins, 1958) noted that the

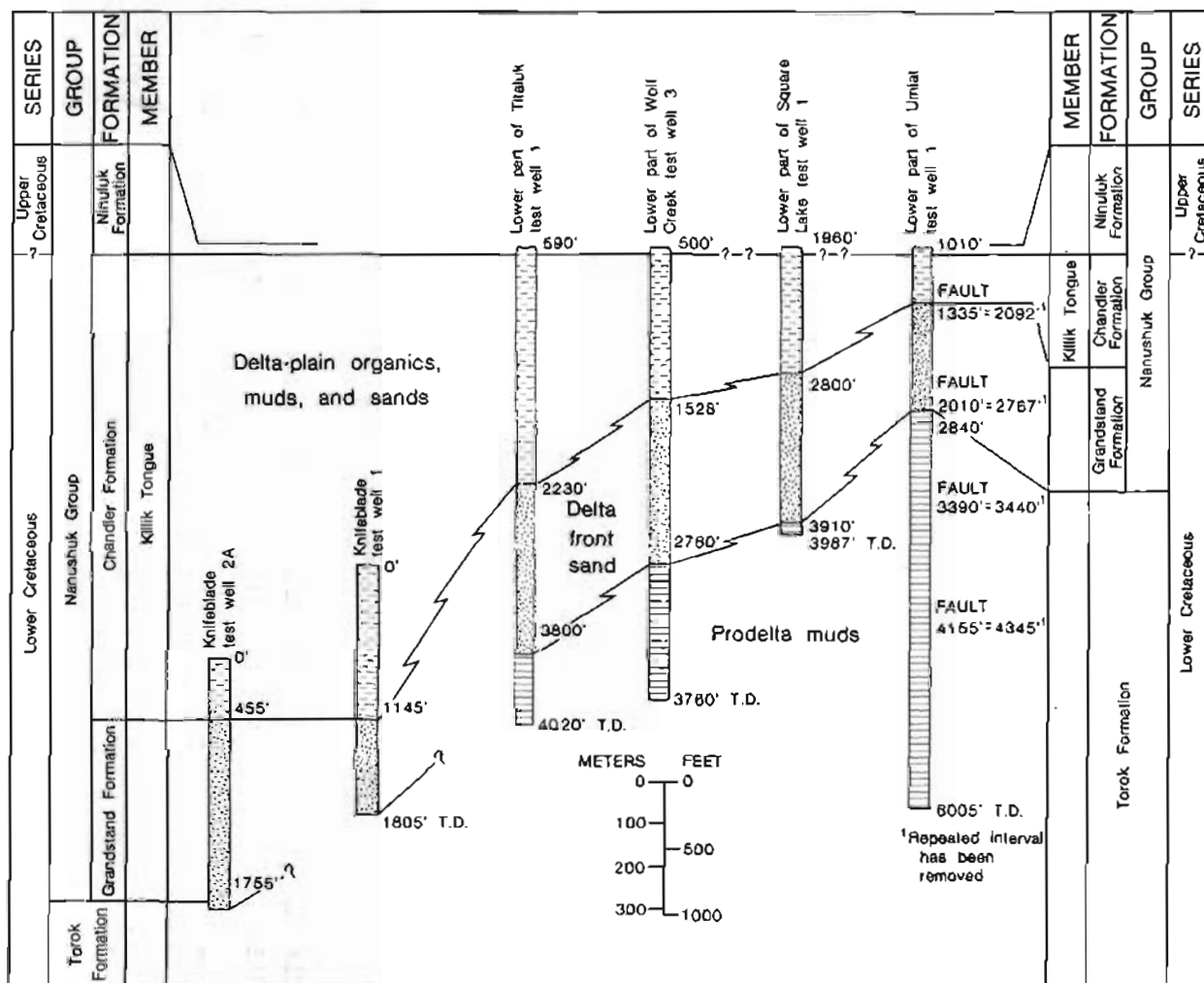


Figure 4.--Cross section showing stratigraphic relationships of Lower Cretaceous deltaic facies, Umiat area, Alaska. From Fisher and others (1969). Line of cross section is indicated on figure 5.

Grandstand Formation contains a number of beds having a fauna rich in arenaceous foraminifers of the *Verneuilinoides borealis* Zone. He reported that the microfauunal assemblage of this zone consists of about 60 species of forams mostly of the arenaceous type. He also reported the presence of a few calcareous foraminifers of the same species as those found in Albian beds of Europe. Some of the arenaceous species have also been described by Bergquist from Albian beds in western Canada. Bergquist reported that R. W. Imlay (oral commun., 1956) identified certain mollusks from beds of the Grandstand, Tuktu, and upper part of the Torok that are of middle Albian age. Dinoflagellates and acritarchs also suggest a middle to late Albian age for the Grandstand (May, in Ahlbrandt, 1979).

The Killik Tongue contains a moderate to very rich flora of dinoflagellates, acritarchs, spores, and pollen (E. I. Robbins, oral commun., 1976). This flora has been dated as middle Albian to early Cenomanian(?) (May, in Ahlbrandt, 1979). Shallow-marine beds occur in the lower part and contain a few arenaceous foraminifers that are part of the *Verneuilinoides borealis* Zone already described.

The Ninuluk Formation is characterized by an abundance of arenaceous foraminifers, as identified by Bergquist (in Collins, 1958). He considered one of the species, *Trochammina rutherfordia*, to be indicative of a Cenomanian Age for the Ninuluk Formation. A moderately abundant assemblage of dinoflagellates was recovered from core 38 in the Ninuluk. These dinoflagellates were not datable, but they are similar to those of the underlying Killik Tongue (May, in Ahlbrandt, 1979).

A small ammonite, *Borissiakoceras* sp., occurs in the shale beds of the Seabee Formation. Because of the presence of this ammonite, the age of the Seabee is considered to be Turonian (Gryc, in Payne and others, 1951).

## CORE ANALYSIS

### Introduction

Twenty-two cores, representative of sandstone units from the Nanushuk and Colville Groups and constituting 83.8 m of strata, were borrowed from the U.S. Geological Survey core storage facility in Fairbanks, Alaska. The stratigraphic position of each of the cores studied is shown on figure 3. A thin slice (1.25 cm) was cut from each of these cores for detailed sedimentologic study. Sandstone beds make up a relatively small proportion of the overall lithotype of the total cored interval. Interbedded with the thin sandstone units are claystone, siltstone, and coal beds which were not studied. The following aspects were studied in the core analysis: visual porosity, lithology, color, grain size, bedding type, sedimentary structures, biologic constituents,

sorting, roundness, oil shows, and inferred environment of deposition.

Data were gathered from the core specimens using a hand lens, binocular microscope, and black-light (fluorescence) apparatus. Interpretation of depositional environments was primarily dependent upon the identification of sedimentary structures. Because of the fine-grained, homogeneous nature of most of the sediments and the abundance of interstitial clay, the sedimentary structures were difficult to see clearly. For this reason each of the thin slices of core was photographed using an X-radiography apparatus, and an X-radiograph photograph was printed to assist in interpretation. These prints revealed structures not otherwise clearly distinguished.

A paleontologic study primarily concerned with foraminifers was made by Bergquist (in Collins, 1958). Fred May (U.S. Geological Survey, Denver, Colo.) and Eleanora Robbins (U.S. Geological Survey, Reston, Va.) examined slides prepared for identification of spores, pollen, and dinoflagellates. These paleontologic studies were used to assist in the interpretation of the ages and environments of deposition.

Although visual estimates of the grain size, sorting, roundness, and porosity were made from hand-specimen samples of the core, the reader is referred to the petrography section for detailed discussion of these aspects based on thin-section studies.

## Stratigraphy and Depositional Environments--Nanushuk Group

Detterman (1956a) revised the nomenclature of formations of the Nanushuk Group, originally named the Nanushuk Series by Schrader (1902). Detterman divided predominantly marine rocks of the Nanushuk Group into three formations: Tuktu, Grandstand, and Ninuluk (fig. 3). The Tuktu is not distinguished from the Grandstand in the Umiat 11 test well. Predominantly nonmarine rocks were placed in the Killik Tongue of the Chandler Formation.

### TUKTU AND GRANDSTAND FORMATIONS

Detterman (1956a) named the Grandstand Formation for a 518.2-m-thick sequence of predominantly marine rocks at Grandstand Anticline, approximately 56 km south of Umiat. In this area the Grandstand rests on the Tuktu Formation and interfingers with the Killik Tongue of the overlying Chandler Formation.

Throughout the area of this study, the stratigraphic relationships between the Grandstand Formation and overlying and underlying formations are not completely established. According to Chapman and others (1964), the Grandstand at Knifeblade Ridge (fig. 5), just north of the Colville River about 105 km west-southwest of Umiat, is stratigraphically the same formation as the

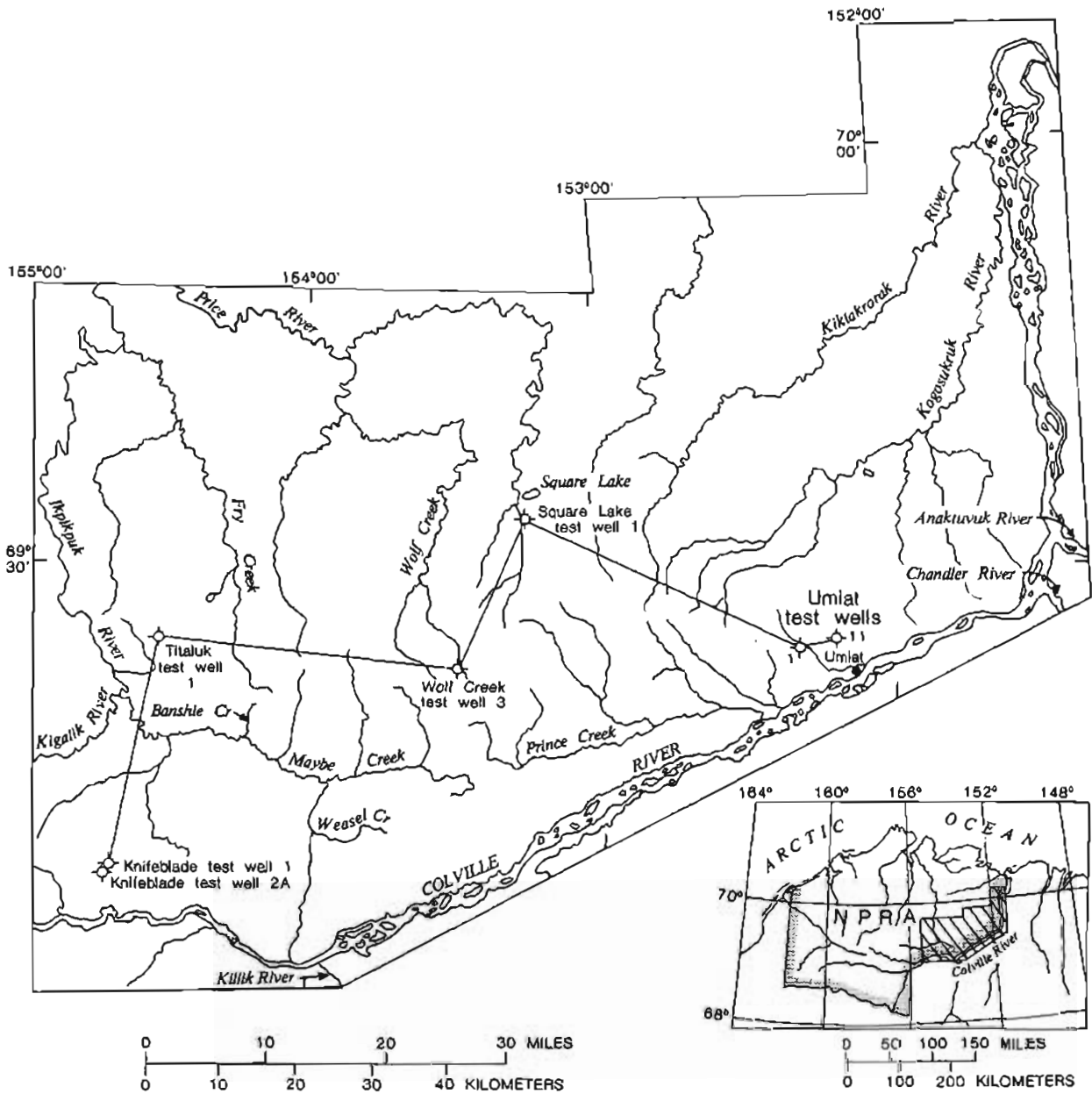


Figure 5.--Index map of Umiat-Maybe Creek region, northern Alaska, including line of section. Crosshatched area in small index map shows location of Umiat-Maybe Creek region within NPRA. Cross section shown in figure 4.

Tuktu mapped just south of the Colville River in this same area. On the other hand, Brosgé and Whittington (1966) pointed out that the Grandstand Formation of the Umiat-Maybe Creek region (fig. 5) is probably considerably younger than the type Tuktu of Tuktu Bluff about 80 km south of Umiat. The reader is referred to Brosgé and Whittington (1966) for a discussion of stratigraphic problems of the Grandstand Formation.

According to Brosgé and Whittington

(1966), the Grandstand occurs throughout most of the Umiat-Maybe Creek area but thins to the north and east. It is absent in the well at Fish Creek, about 113 km north of Umiat (Robinson and Collins, 1959). At Wolf Creek Anticline, about 32 km west of Umiat (fig. 5), the Grandstand is about 378 m thick. At Umiat, the Grandstand is about 195 m thick, having thinned about 183 m in 32 km.

Three lines of compositional and textural evidence are used to infer the depositional

setting of the Grandstand Formation. First, in the Knifeblade and Titaluk wells, 80-97 km to the west of Umiat (fig. 5), thin coal beds are common throughout the Grandstand (Brosge and Whittington, 1966); at Umiat, on the other hand, coal streaks and partings are rare, suggestive of a more marine condition in the Umiat area during deposition.

Second, sandstone beds in the Grandstand at Umiat Anticline are cleaner and better sorted than in the Wolf Creek and Square Lake wells to the west (fig. 5), possibly due to winnowing in the foreshore zone. Therefore, they have greater porosity and permeability than at other anticlines in the area (Brosge and Whittington, 1966).

Third, the grain size of the sandstone decreases eastward, ranging from very fine to coarse at Knifeblade, very fine to medium at Titaluk, and very fine to fine at Wolf Creek and Square Lake (fig. 5). These regional compositional, textural, and thickness relationships suggest that the depocenter of the delta system, of which the Grandstand sandstones are a part, lay to the west-southwest of the Umiat area. This delta was named the Umiat delta by Ahlbrandt (1979). Faunal evidence suggests a shallow-water nearshore-marine environment for deposition of the Grandstand sediments at Umiat. Nearly all shale beds and some of the sandstone beds contain abundant benthic arenaceous microfossils (*Vernanilinoides borealis* Zone), as identified by Bergquist (in Collins, 1958). Arenaceous foraminifers are commonly present in shallow nearshore-marine environments. A moderately rich assemblage of dinoflagellates, spores, and pollen also occurs throughout the Grandstand

(May, in Ahlbrandt, 1979; E. I. Robbins, oral commun., 1976), as would be expected in sediments deposited in a nearshore-marine environment. The dinoflagellate assemblage is of middle to late Albian age. Marine invertebrate megafossils (primarily mollusks) occur throughout the Grandstand sequence (Brosge and Whittington, 1966).

At Umiat test well 11, the Grandstand Formation is characterized by a lower unit of very fine grained to fine-grained sandstone (approximately 92 m thick), separated from an upper unit of similar sandstone (31 m thick) by about 92 m consisting predominantly of shale (fig. 3). Cores 56-58 and 60 are from the lower sandstone unit, and cores 52 and 53 are from the upper sandstone unit.

Cored interval 60 (911.0-915.6 m) is near the base of the Grandstand Formation and near the contact with marine shale of the underlying Torok Formation (fig. 3). The sandstone of this interval consists of medium-light-gray, very fine grained to fine-grained, well-sorted, subangular to angular quartz grains. Sedimentary structures include small-scale, thin, even-parallel, low-angle laminations; some interbedded homogeneous mottled units are especially prevalent in the lower half of the core (fig. 6). The sedimentary structures and lithologic and faunal evidence are interpreted as indicating delta-front sands deposited in an upper shoreface (mottled, bioturbated beds) and foreshore-marine (low-angle, parallel, thinly laminated) environment.

Cored intervals 56-58 (856.5-868.7 m) (fig. 7) are near the top of the basal sandstone unit of the Grandstand. The fine-grained, well-sorted nature of the sandstone and the

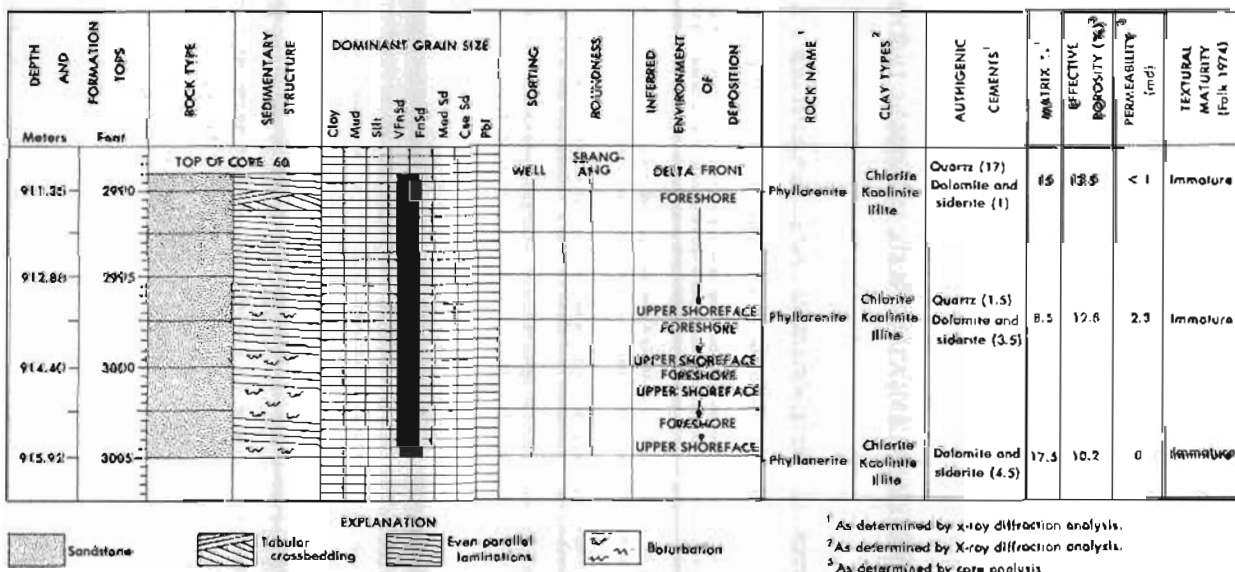
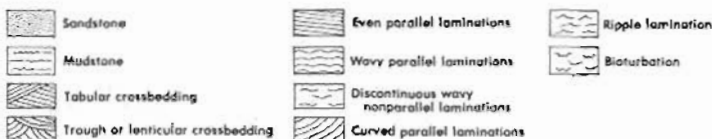


Figure 6.--Lithology, sedimentary structures, texture, inferred environment of deposition, and reservoir properties, core 60 (911.0-915.6 m), Grandstand Formation, Umiat test well 11. See table 2 for more detailed information regarding mineralogy and reservoir properties.

DEPTH AND FORMATION TOPS		ROCK TYPE	SEDIMENTARY STRUCTURE	DOMINANT GRAIN SIZE		SORTING	ROUNDNESS	INFERRED ENVIRONMENT OF DEPOSITION	ROCK NAME <sup>1</sup>	CLAY TYPES <sup>2</sup>	AUTHIGENIC CEMENTS <sup>1</sup>	MATRIX (%) <sup>1</sup>	EFFECTIVE POROSITY (%) <sup>2</sup>	PERMEABILITY (md) <sup>3</sup>	TEXTURAL MATURITY (Folk, 1974)		
METERS	FEET			Clay	Mud											Silt	Fine Sd
856.48	2810							WELL	ANG-SBANG	DELTA FRONT (FORESHORE)	Chert arenite	Chlorite Kaolinite Illite	Quartz (1%)	8	16.4	100	Immature
858.01	2815																
859.53	2820																
861.06	2825										Chert arenite	Chlorite Kaolinite Illite	Calcite (1%) Quartz (2%)	3	17.4	158	Mature
862.58	2830							WELL	SBANG ANG-SBANG	(UPPER SHOREFACE)	Chert arenite	Chlorite Kaolinite Illite	Quartz (2.5%)	3	17.1	280	Mature
864.10	2835									(FORESHORE)							
865.63	2840								ANG-SBANG		Phyll arenite	Chlorite Kaolinite Illite	Quartz (1%)	11	14.7	Too friable to test	Immature
867.15	2845								SBANG								
868.68	2850									(UPPER SHOREFACE)	Chert arenite	Chlorite Kaolinite Illite	Quartz (2%)	3	19.2	400	Mature



<sup>1</sup> As determined by petrographic analysis  
<sup>2</sup> As determined by X-ray diffraction analysis  
<sup>3</sup> As determined by core analysis

Figure 7.--Lithology, sedimentary structures, texture, inferred environment of deposition, and reservoir properties, cores 56-58 (856.5-863.7 m), Grandstand Formation, Umiat test well 11. See table 2 for more detailed information regarding mineralogy and reservoir properties.

presence of a thin (0.6 m), homogeneous, bioturbated sandstone interval near the base, which is overlain by a thicker interbedded interval (4.0 m) containing low-angle parallel laminae and small-scale lenticular crossbed sets, support the theory of deposition as delta-front sands in a dominantly foreshore zone. This sequence grades upward into another bioturbated homogeneous sandstone unit, reflecting a slight marine incursion and deposition of delta-front sands in a shoreface zone. A thin (0.3 m) shale bed separates the aforementioned sandstone interval from the overlying sequence of sandstone, which is of approximately the same thickness. This upper sandstone unit differs from the lower by having more carbonaceous laminae, more abundant rippled laminae (asymmetric), and near absence

of bioturbation. Occasional flooding during deposition of this upper sandstone unit may have been responsible for the abundant carbonaceous detritus being carried so far offshore and for the formation of asymmetric ripples. These thin carbonaceous laminae may be time-equivalent to thicker coal stringers to the west.

The sequence of predominantly nearshore-marine sandstone is overlain by a marine shale sequence (92 m), reflecting continued transgression of the sea. Abundant arenaceous and calcareous benthic foraminifera, abundant dinoflagellates, and some spores and pollen are present in the shale. This combination of fossils is commonly found in modern nearshore-marine environments. This shale sequence may have been deposited as prodelta muds.

Cores 52 and 53 (744.9-749.8 m) (fig. 8) are from about 6 m below the top of the Grandstand Formation. This sandstone interval is similar to the lower 4.0-m interval just described from cores 56-58 and is also interpreted as a delta-front sand deposited in a foreshore environment. However, correlation with coal stringers to the west-southwest of Umiat is not obvious. The only evidence is black carbon grains evenly disseminated throughout the sandstone and concentrated in thin laminations on bedding surfaces. As was the case with the foreshore sandstone of interval 60, the sandstone of this interval is also overlain by a transgressive shale. In this interval the shale is only 12.2 m thick and contains a rich fauna of arenaceous forams (Bergquist, in Collins, 1958).

#### KILLIK TONGUE OF THE CHANDLER FORMATION

The Chandler Formation is about 1,433 m thick at its type locality on the Chandler River and is predominantly nonmarine. It consists of two major tongues, the Killik Tongue and the Niakogon Tongue. The Niakogon Tongue is not differentiated from the Ninuluk Formation in the Umiat area (Brosgé and Whittington, 1966) (fig. 3).

Detterman (1956a) named the Killik Tongue from exposures of strata approximately 854 m thick along the Killik River near its confluence with the Colville River, about 80 km southwest of Umiat (fig. 5). The Killik Tongue progressively thins to the northeast; at the

Knifeblade Anticline it is about 1,036 m thick, at Titaluk Anticline it is about 488 m, at Wolf Creek Anticline it is about 305 m thick, and at Umiat Anticline it is about 92 m thick. In the area to the southwest where the Killik Tongue is thick, Brosgé and Whittington (1966) described it as consisting of stream-channel sandstone, siltstone, mudstone, and coal--a typical delta-plain facies.

The Killik Tongue is essentially barren of megafossils. However, Brosgé and Whittington (1966) reported the presence of marine assemblages near the top and bottom of the Killik Tongue in the Umiat-Maybe Creek area. Thin shallow-marine beds in the lower part of the Killik contain arenaceous forams of the *Verneuilinoides borealis* faunal zone. May (in Ahlbrandt, 1979) identified nearshore-marine assemblages containing abundant dinoflagellates and acritarchs from cores 41, 46, and 50 of the Killik Tongue at Umiat test well 11; an age of middle Albian to early Cenomanian(?) was established. Approximately 26 species were observed, most of which are new species. An abundant flora of spores and pollen was reported from core 50 (E. I. Robbins, oral commun., 1976).

The abundance of coal diminishes to the northeast, and only a few very thin (10 cm) stringers are present near the top of the Killik Tongue at Umiat. This decrease in abundance of coal, the predominance of a nearshore-marine fauna and flora, and the general thinning of the Killik to the northeast suggest a facies change from well-developed

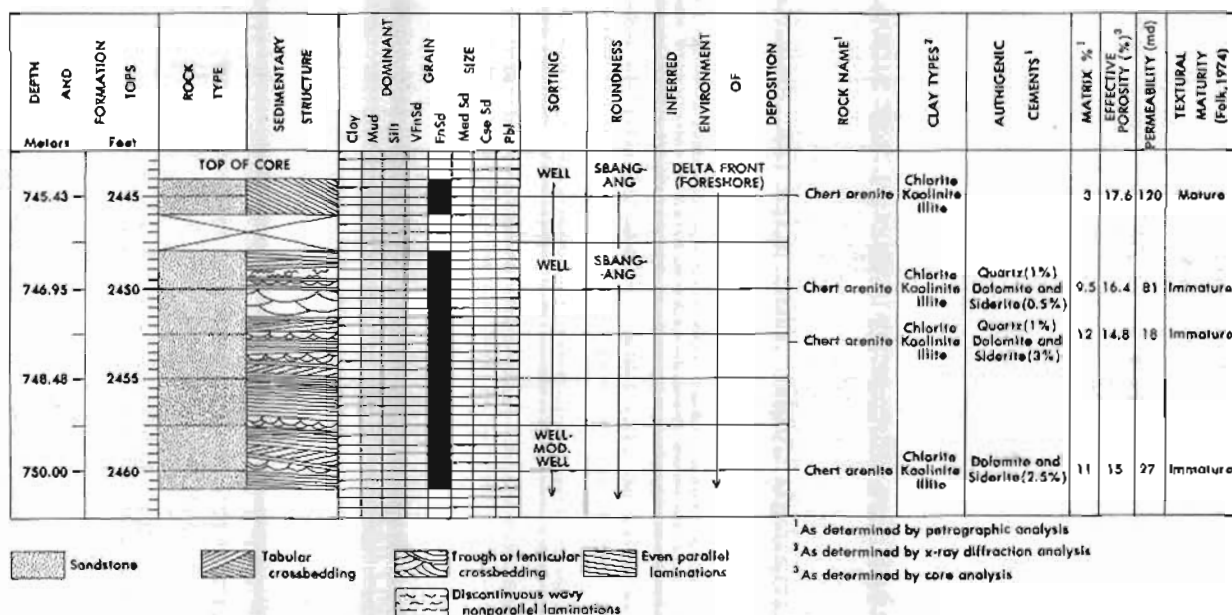


Figure 8.--Lithology, sedimentary structures, textures, inferred environment of deposition, and reservoir properties, cores 52 and 53 (744.9-749.8 m), Grandstand Formation, Umiat test well 11. See table 2 for more detailed information regarding mineralogy and reservoir properties.

delta-plain facies to the southwest to a dominantly nearshore-marine facies at Umiat.

Core 49 (723.6-729.4 m) is from the Killik Tongue (fig. 3). The sandstone in this core is light gray and fine to very fine grained; it contains well-sorted, subangular to angular grains (fig. 9). Analysis of the core indicates two major kinds of sedimentary structures: small-scale, lenticular, crossbed sets of thin laminae interbedded with small-scale, low-angle, even-parallel sets of thin laminae. A few thin, ripple-laminated beds are present near the base of this core. These sediments are interpreted to be foreshore sediments; the well-developed delta-plain facies lies to the west.

#### NINULUK FORMATION

In the Umiat area the Ninuluk Formation is mapped as a single unit with the Niakogon Tongue of the Chandler Formation. To the south of Umiat, south of the Colville River, the Ninuluk Formation and Niakogon Tongue of the Chandler Formation are separately defined and mapped (Brosgé and Whittington, 1966). The Ninuluk Formation contains abundant sandstone and is easily distinguished from the dominantly marine shale of the overlying Seabee Formation.

The thickness of the Ninuluk varies from a maximum of about 280 m just south of Weasel Creek Anticline (fig. 5) to about 29 m on

Umiat Anticline, a distance of about 64 km to the northeast (Brosgé and Whittington, 1966). This trend in direction of thinning is similar to that of the underlying rocks of the Nanushuk Group. In contrast, the overlying marine sequence of the Upper Cretaceous Seabee Formation thickens to the northeast (Brosgé and Whittington, 1966).

In the Maybe Creek area (fig. 5), approximately 64 km to the west of Umiat, the Ninuluk consists of complexly interbedded sediments containing nonmarine fossils and coal interbedded with beds containing shallow-marine fossils (Brosgé and Whittington, 1966).

Cores 35-38 (623.9-639.2 m) are from the Ninuluk Formation (fig. 3). These rocks are predominantly medium-light-gray, very fine grained to fine-grained, moderately well sorted to well-sorted, angular to subangular sandstone (fig. 10). About 1.5 m above the base of the core is a 1.5-m-thick sandstone interval that is moderately well to poorly sorted, is angular to rounded, and contains coaly laminae. In this basal unit are thin beds of poorly sorted clay-pebble conglomerate (clay clasts as large as 2.5 cm in diameter) in a clay matrix; these beds are interbedded with moderately well sorted, thin, very fine grained to fine-grained beds. Immediately above this basal 1.5-m-thick unit, small-scale, curved-parallel and discontinuous, wavy, nonparallel coaly laminations are present. The lower part of this interval contains a

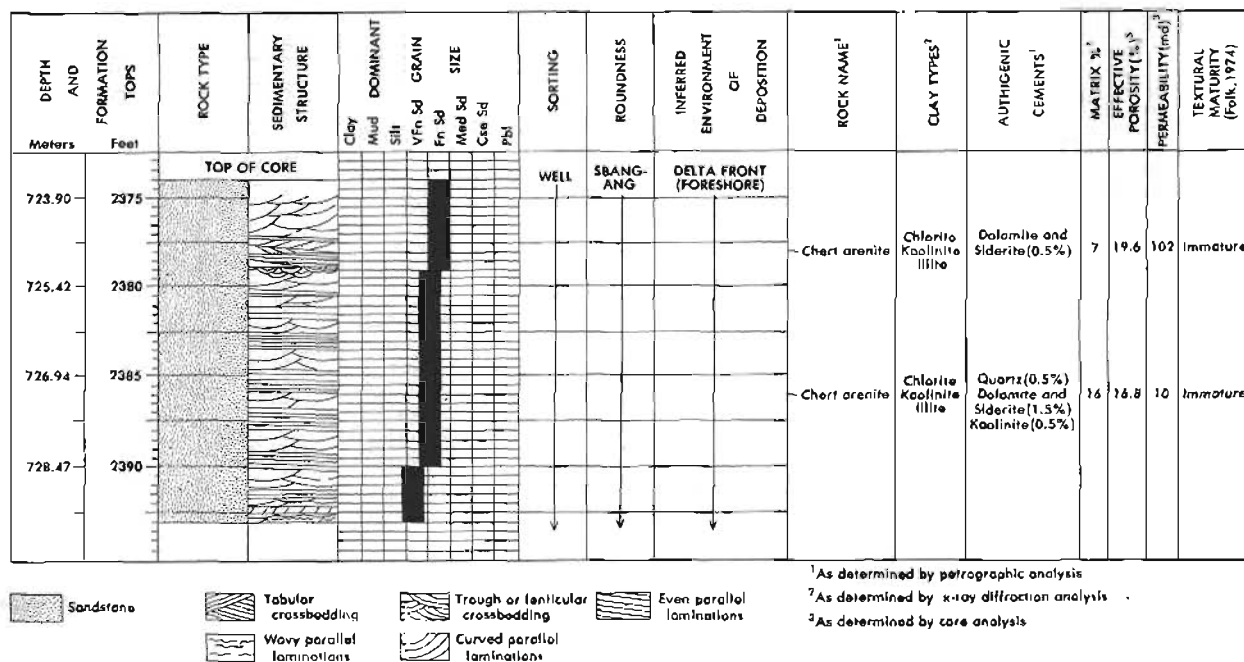


Figure 9.--Lithology, sedimentary structures, texture, inferred environment of deposition, and reservoir properties, core 49 (723.6-729.4 m), Killik Tongue of the Chandler Formation, Umiat test well 11. See table 2 for more detailed information regarding mineralogy and reservoir properties.

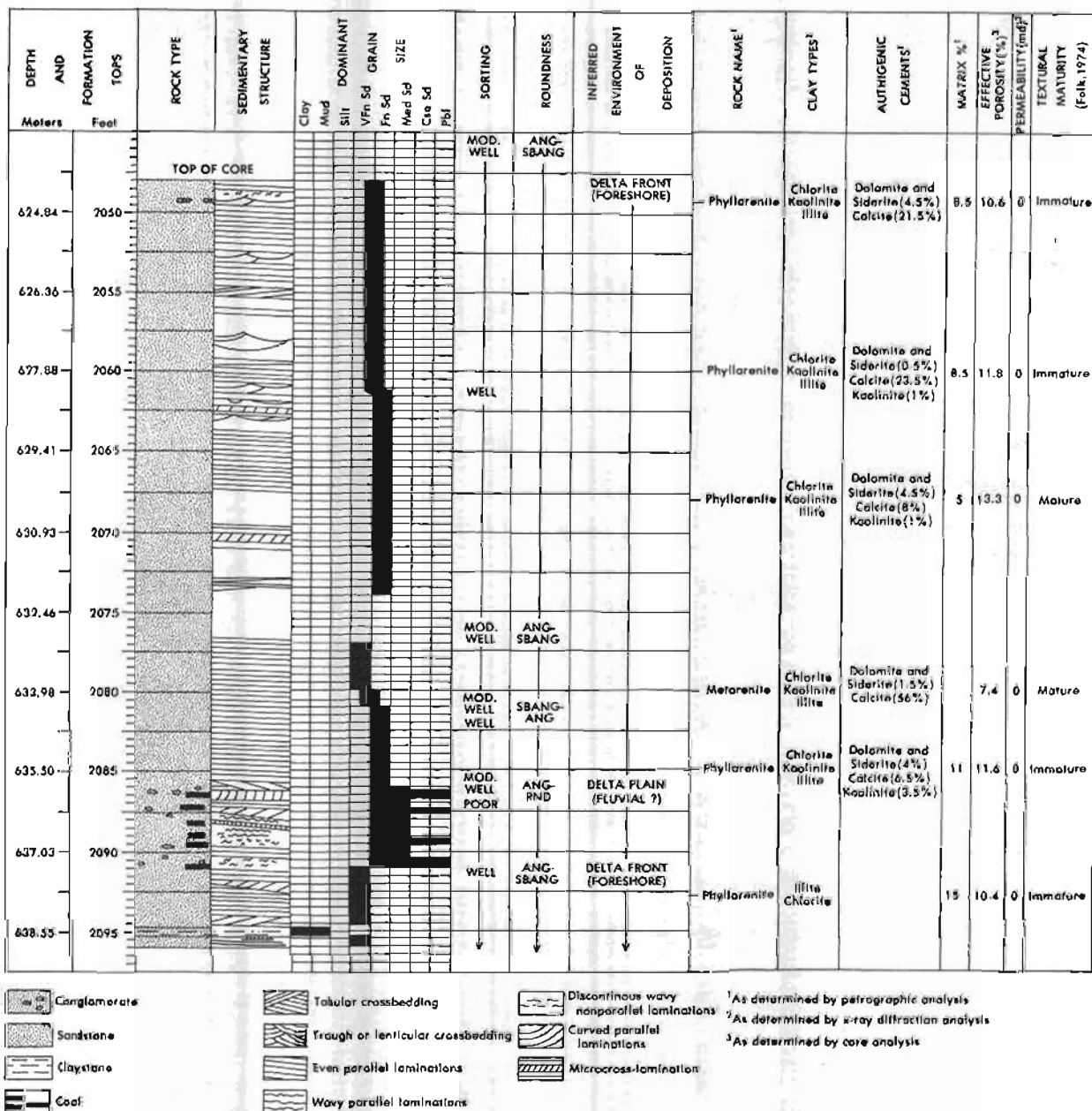


Figure 10.--Lithology, sedimentary structures, texture, inferred environment of deposition, and reservoir properties, cores 35-38 (623.9-639.2 m), Ninuluk Formation, Umiat test well 11. See table 2 for more detailed information regarding mineralogy and reservoir properties.

moderately abundant assemblage of dinoflagellates (F. E. May, oral commun., 1978). These were not datable, but they are similar to those of the underlying Killik Tongue (middle Albian to early Cenomanian(?)) (May, in Ahlbrandt, 1979). In turn, above that interval are small-scale, low-angle, parallel laminae of sandstone interbedded with homogeneous unstructured sandstone overlain by a few thin (15 cm) sandstone beds having

lenticular crossbeds. Also, small-scale, curved-parallel and discontinuous, wavy, nonparallel coaly laminations are present. The upper part of the cored interval was barren of fossils.

On the basis of sedimentary structures, fossils, and thickness trends the Ninuluk in the Umiat area was deposited, in large part, as delta-front sands in a shallow-marine foreshore environment, seaward from the typical

delta-plain facies of the Niduluk at the Maybe Creek area to the west.

#### Stratigraphy and Depositional Environments--Colville Group

The name Colville "Series" was first used by Schrader (1902) for rocks exposed along the Colville River below the mouth of the Anaktuvuk River (fig. 5). Later studies by Gryc and others (1951) resulted in the application of the name Colville Group to these rocks. They also included approximately 915 m of other Upper Cretaceous rocks underlying the originally defined Colville "Series" and overlying the Nanushuk Group.

In the Umiat area, the Colville Group is about 1,678 m thick and includes three formations: the marine Seabee, the overlying nonmarine Prince Creek, and the overlying marine Schrader Bluff (Brosgé and Whittington, 1966). Umiat test well 11 spudded in the upper part (Tuluvak Tongue) of the Prince Creek (fig. 3).

#### SEABEE FORMATION

The Seabee Formation of the Colville Group thickens eastward from about 250 m at Wolf Creek to about 458 m at Umiat test well 11 (fig. 5).

The Seabee was originally named for Seabee Creek by Gryc and others (1951) and was included as a member of the Schrader Bluff Formation. Later it was redefined as the Seabee Formation by Whittington (1956) to include all the dominantly marine strata of the Colville Group that underlie the Tuluvak Tongue of the Prince Creek Formation. The type Seabee is in Umiat test well 11; strata lie between 166.1 m and 621.8 m in this well. The Seabee has a very widespread distribution, extending from the Arctic coast to about 80 km south of the latitude of Umiat (Brosgé and Whittington, 1966).

The Seabee Formation has been subdivided into two members: The upper member is the Aiyiak Member (Detterman, 1956b); it is composed of about 92 m of greenish-gray siltstone and silty shale and light-tan to light-chocolate-brown sandstone. Detterman and others (1963) named the Seabee below the Aiyiak Member as the Shale Wall Member, consisting dominantly of shale.

Brosgé and Whittington (1966) recognized four distinct sandstone beds in the Seabee on the west part of the Titaluk Anticline near Titaluk test well 1 (fig. 5). These sandstone beds pinch out to the east, with younger ones extending progressively farther east; they all pinch out at about the area of Fry Creek and Banshee Creek, approximately 80 km west of Umiat. Brosgé and Whittington (1966) pointed out that the distribution of these sandstone beds suggests that they were deposited in a

nearshore-marine environment by a generally eastward-regressing sea. The shoreline configuration was probably northwest.

Cores 21-25 (402.9-419.7 m), from near the middle of the Shale Wall Member, consist of moderately well sorted, very fine grained to fine-grained, subangular to angular sandstone with some grading, especially near the top (fig. 11). This entire interval is dominated by homogeneous, generally structureless sandstone, indicating rapid deposition without development of laminae. Randomly distributed throughout the interval are thin (15-30 cm) stringers of sandstone exhibiting low-angle, even-parallel bedding. Ripple-laminated beds are rare. Two mudstone beds are present at the base of the cored sandstone interval; mudstone clasts and contorted mudstone laminations are present. This is the first (oldest) cored interval in which trace amounts of bentonitic clay matrix were observed. This sandstone interval is overlain and underlain by dark marine shale and includes mudstone clasts at the base, graded bedding, and occasional ripple laminae. These features suggest marine turbidite deposition. The sediment may have come from a delta to the west.

In shale beds approximately 23 m above and 15 m below the cored interval, Bergquist (in Collins, 1958) reported the occurrence of the Turonian ammonite *Borissiakoceras*. Approximately 46 m below the lower *Borissiakoceras*, Bergquist noted a shale interval that contains abundant radiolarians. Other marine invertebrates reported in the Seabee shales include the ammonite genera *Scapilites* and *Watenoceras* and the bivalve mollusk *Inoceramus labiatus* (Brosgé and Whittington, 1966). The marine fauna of the Seabee Formation shales at Umiat test well 11 is less diverse and typically more open marine than the Seabee Formation 64 km to the west at Maybe Creek (fig. 5). At Maybe Creek a very abundant and diverse mollusk assemblage is present (Brosgé and Whittington, 1966), indicating shallower marine conditions in this area than at Umiat during Seabee deposition.

Cores 15-16 (227.1-239.3 m) are from the Aiyiak Member of the Seabee Formation (fig. 3). Sedimentologic evidence (fig. 12) suggests that this very fine grained to fine-grained sandstone with a bentonitic clay matrix was probably deposited in a nearshore-marine (foreshore) environment. The abundance of low-angle, even-parallel laminae of fine-grained to very fine grained, moderately well sorted to well-sorted sandstone and the moderate abundance of tabular, small- to medium-scale crossbed sets with tangential lower contacts give rise to the above interpretation.

Whether these sandstones (cores 15-16) were deposited in a delta-front environment is difficult to ascertain. Broken fragments of pollen and spores have been identified

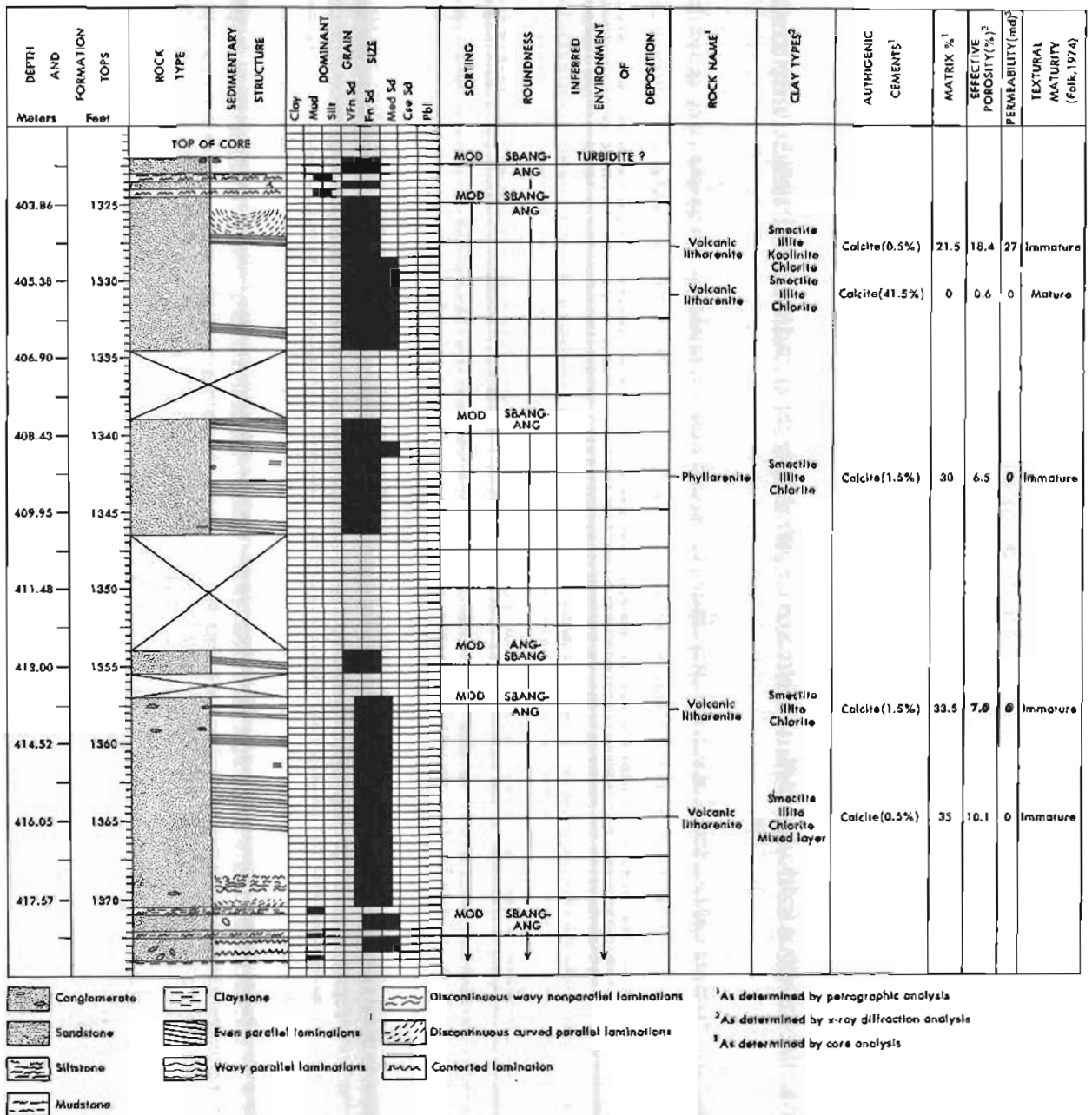


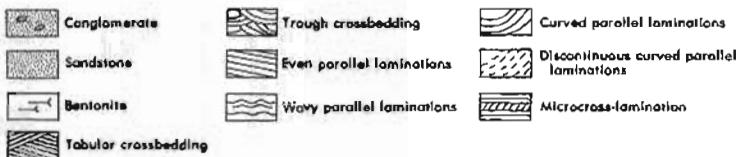
Figure 11.—Lithology, sedimentary structures, texture, inferred environment of deposition, and reservoir properties, cores 21-25 (402.9-419.7 m), Shale Wall Member of the Seabee Formation, Umiat test well 11. See table 2 for more detailed information regarding mineralogy and reservoir properties.

(E. I. Robbins, oral commun., 1976) and may have been carried into the area by distributaries of a delta plain. Core number 17 (245.4-248.4 m), from a shale bed approximately 6 m below the base of core 16, contains abundant dinoflagellates and some spores suggestive of a setting close to a marine shoreline. Abundant bentonitic clay matrix is present in these and younger strata.

#### TULUVAK TONGUE OF THE PRINCE CREEK FORMATION

Gryc and others (1951) named the Tuluvak Tongue for outcrops east of Umiat on the Chandler River (fig. 5). Here coal and conglomerate occur in abundance; they may represent a lobe of delta-plain sediments similar to lobes of equivalent age at Wolf Creek and Maybe Creek to the west of Umiat.

DEPTH AND FORMATION TOPS	ROCK TYPE	SEDIMENTARY STRUCTURE	GRAIN SIZE						SORTING	ROUNDNESS	INFERRED ENVIRONMENT OF DEPOSITION	ROCK NAME <sup>1</sup>	CLAY TYPES <sup>2</sup>	AUTHIGENIC CEMENTS <sup>1</sup>	MARTIX % <sup>3</sup>	EFFECTIVE POROSITY (%) <sup>3</sup>	PERMEABILITY (md) <sup>3</sup>	TEXTURAL MATURITY (Folk, 1974)
			Clay	Mud	Silt	Fn Sd	Med Sd	Coe Sd										
227.07 745		TOP OF CORE							MOD	ANG-SBANG	DELTA FRONT (FORESHORE)	Feldspatic phyllonite	Smectite Illite Kaolinite Chlorite	Dolomite and Siderite (0.5%) Calcite (2%)	14.5	18.2	5.1	Immature
228.6 750																		
230.12 755												Phyllonite	Smectite Illite Kaolinite Chlorite	Dolomite and Siderite (2%) Calcite (2%)	35.5	17.7	7.0	Immature
231.64 760									MOD-WELL	ANG-SBANG								
233.17 765									MOD-WELL	ANG-SBANG		Meraranite	Smectite Illite Chlorite	Dolomite and Siderite (1.5%) Calcite (14%)	17.0	12.7	0	Immature
234.69 770									MOD	ANG-SBANG								
									MOD-WELL	ANG-SBANG		Phyllonite	Smectite Illite Kaolinite Chlorite	Calcite (1%)	15.0	20.6	48	Immature



<sup>1</sup>As determined by petrographic analysis  
<sup>2</sup>As determined by x-ray diffraction analysis  
<sup>3</sup>As determined by core analysis

Figure 12.—Lithology, sedimentary structures, texture, inferred environment of deposition, and reservoir properties, cores 15 and 16 (227.1–239.3 m), Aiyak Member of the Seabee Formation, Umiat test well 11. See table 2 for more detailed information regarding mineralogy and reservoir properties.

There previous workers (Brosge and Whittington, 1966) noted the presence of conglomerate and conglomeratic sandstone units in the Tuluvak Tongue. These conglomeratic units grade eastward into sandstone, pinching out somewhere between Wolf Creek and Umiat test well 11, a distance of approximately 48 km (fig. 5). At Wolf Creek, the Tuluvak Tongue is about 171 m thick and contains at least three units of conglomerate and conglomeratic sandstone separated by finer grained clastics. Bentonite beds are also present. At Umiat test well 11, 160 m of Tuluvak is present; it is exposed at the surface and some of the upper part is missing due to erosion. At Umiat the Tuluvak Tongue consists of interbedded very fine grained sandstone, shale, and siltstone (all quite bentonitic) and thin coal beds (fig. 3).

In the Wolf Creek-Maybe Creek area west of Umiat, the Tuluvak Tongue was building northward (Brosge and Whittington, 1966). This is indicated by finer grained sandstone found in the lower strata and by successively

younger and coarser clastics being deposited farther north; gravel and plant material become increasingly more abundant. The eastward decrease in grain size from fluvial conglomerate to fine-grained sandstone suggests an increasing distance from the source, which was to the west-southwest, and a change in depositional environment from high energy fluvial to the west to lower energy fluvial, possibly delta-plain deposits, to the east. The number of coal beds and the abundant floras of spores and pollen suggest abundant plant life. A complexly interbedded, very nearshore marine to continental depositional environment existed in the Umiat area during deposition of the Tuluvak Tongue. This interpretation is supported by numerous spores, pollen, and dinoflagellates in the upper part of the Seabee and throughout the Tuluvak Tongue, by beds with many arenaceous foraminifers, and by abundant coal-rich beds interbedded with thin sandstone, siltstone, and organic-rich shale beds.

Cores 11-12 (157.0-167.6 m) contain strata from the base of the Tuluvak Tongue, very near but just above its contact with the underlying Aiyiak Member of the Seabee Formation (fig. 3). The lower 3.7 m of this cored sequence contains predominantly fine grained sandstone with a bentonitic clay matrix. Low-angle parallel laminations and tabular and wedge-planar crossbed sets are present (fig. 13). Beds with these characteristics may reflect deposition of delta-front sands in a foreshore environment. A moderately rich assemblage of spores, pollen, and

dinoflagellates occurs in this interval (E. I. Robbins, oral commun., 1976), attesting to the marginal-marine environment of deposition.

The upper 4.3 m of the core contains very fine grained to medium-grained sandstone having a bentonitic clay matrix. The dominant sedimentary structures are small-scale lenticular crossbed sets, interbedded with a few climbing ripple laminae and small-scale tabular and wedge-planar crossbed sets. Some coaly and partially oxidized plant fragments are also present. The upper part of the core represents more fluvial conditions of deposition

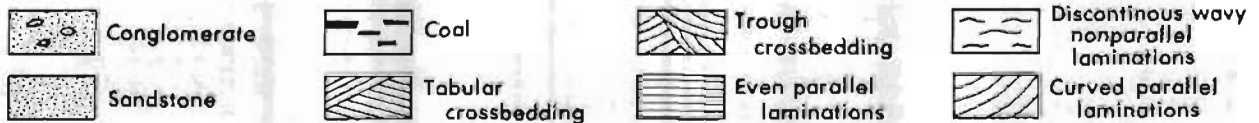
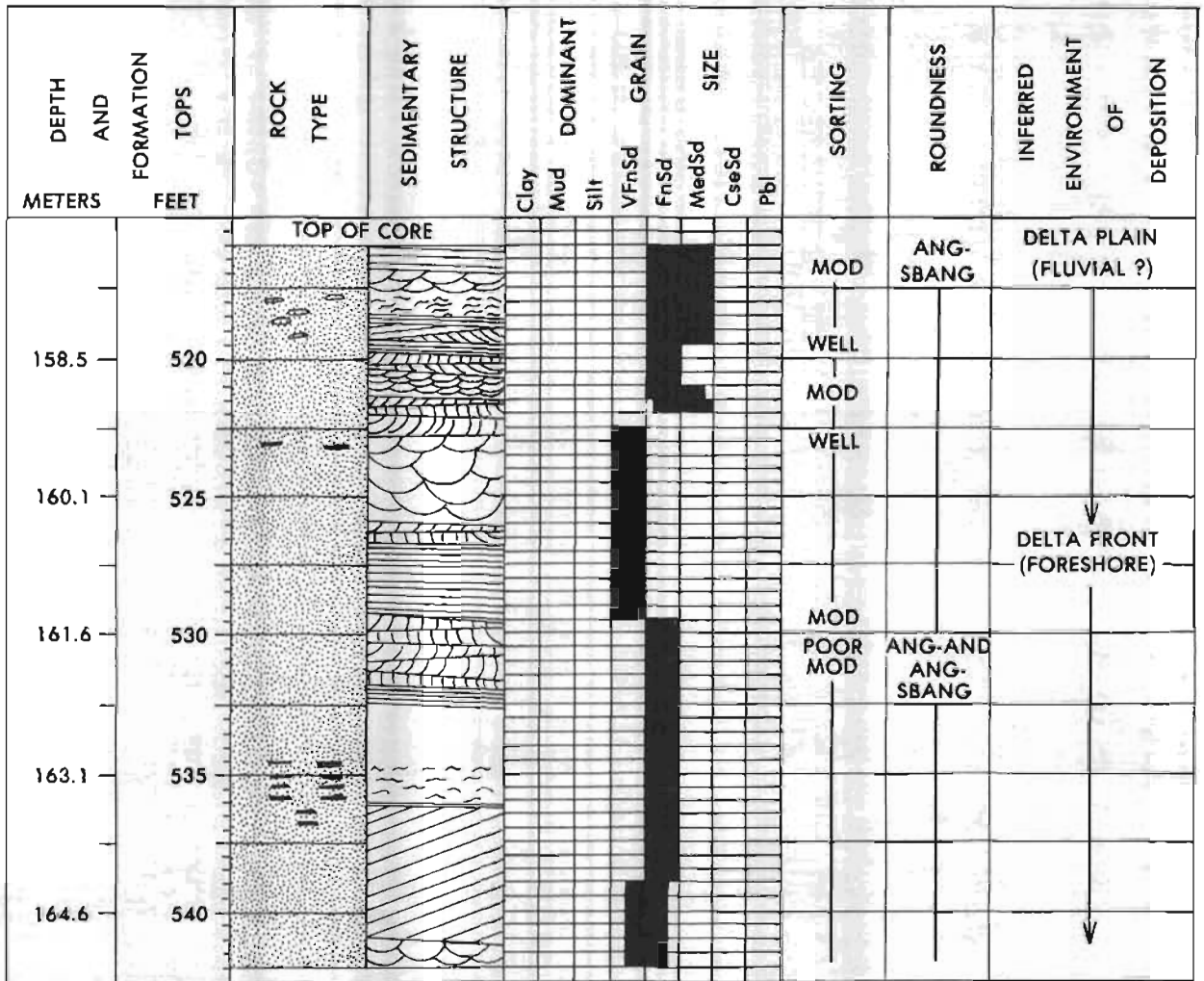


Figure 13.--Lithology, sedimentary structures, texture, and inferred environment of deposition, cores 11 and 12 (157.0-167.6 m), Tuluvak Tongue of the Prince Creek Formation, Umiat test well 11.

than the lower part. It probably represents an intertonguing of deltaic-marine-shoreline and fluvial deposits.

Cores 1-2 (35.1-47.2 m) (fig. 3) consist of very fine grained sandstone with a bentonitic clay matrix (fig. 14). Very low angle, parallel-laminated sets are interbedded with small-scale (5 cm thick) lenticular crossbed sets throughout the core. Bioturbation is common in silty to very fine grained sandstone beds containing coaly laminations near the base of the core. Ripple laminations occur in a few thin beds. These sands are interpreted as representing a low-energy, fluvial flood-plain system in a delta-plain environment.

The interval between cores 2 and 11 is composed of interbedded bentonite, sandstone, siltstone, shale, and coal. A very rich assemblage of spores and pollen was reported in several samples from this interval (E. I. Robbins, oral commun., 1976), supporting a continental setting for these sediments.

**Summary.**--The following summary of characteristics of the sandstone cores studied includes some data from table 2:

Characteristics	Nanushuk Group	Colville Group
Environment-----	Predominantly foreshore and shoreface sands deposited in a delta-front----	Variety of environments represented including turbidite, foreshore, and fluvial.
Volcanic rock fragments-----	Not abundant-----	Abundant.
Metamorphic rock fragments-----	Abundant-----	Not abundant.
Smectite-----	Absent-----	Abundant.
Quartz grains-----	Abundant-----	Not abundant.
Feldspar-----	Not abundant-----	Abundant.
Biotite-----	Not abundant-----	Abundant.
Detrital chert-----	Abundant-----	Not abundant.
Organic material-----	Not abundant-----	Abundant.
Quartz overgrowths-----	Abundant-----	Not abundant.
Calcite cement-----	Not abundant-----	Abundant.
Matrix material-----	Not abundant-----	Abundant.
Reservoir quality-----	Good-----	Poor.

### PETROGRAPHY

Forty-five core samples ("perm plugs") previously used for porosity and permeability analyses (Collins, 1958, p. 192) were thin-sectioned and studied petrographically in an effort to identify the factors affecting porosity and permeability. Except for one sample of siltstone, all samples are sandstone. X-ray diffraction analysis was used to identify clay and major mineral constituents in samples taken as closely as possible to 35 of the

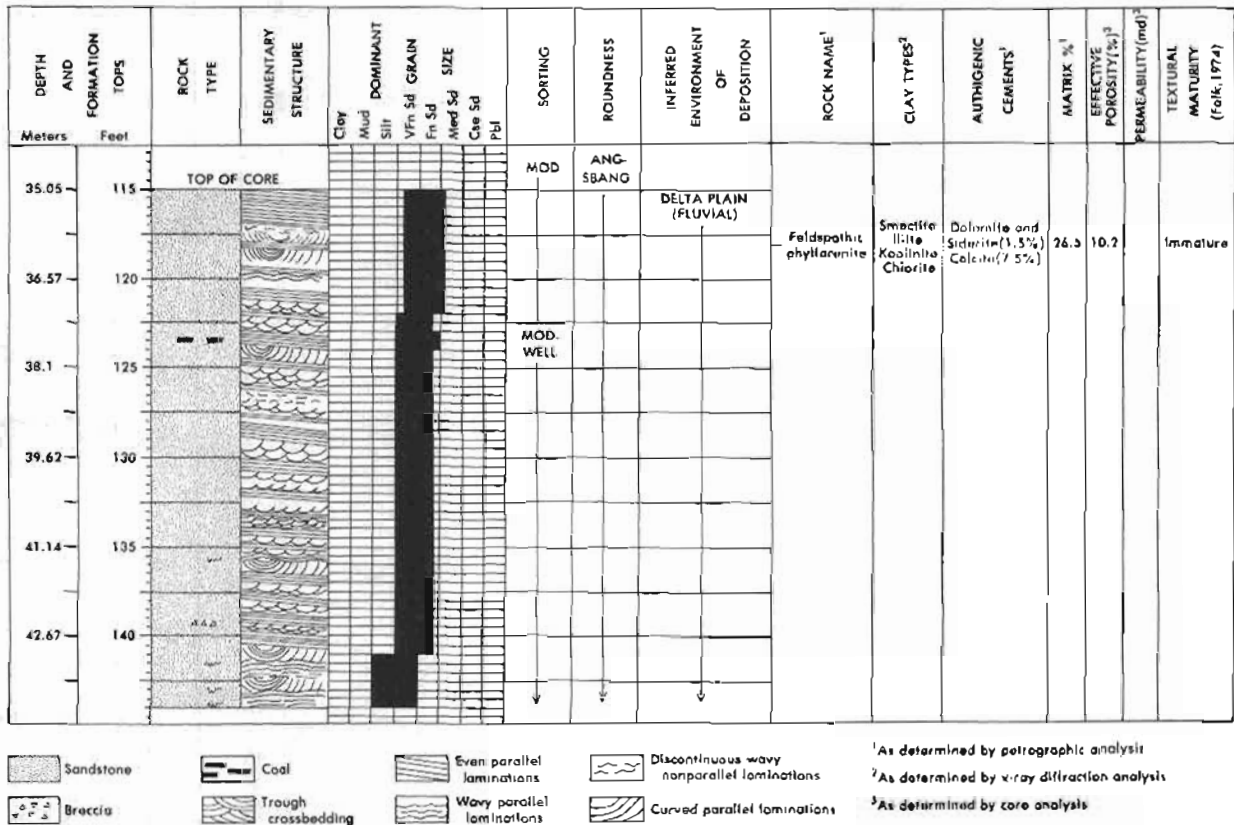


Figure 14.--Lithology, sedimentary structures, texture, inferred environment of deposition, and reservoir properties, cores 1 and 2 (35.1-47.2 m), Tuluwak Tongue of the Prince Creek Formation, Umiat test well 11. See table 2 for more detailed information regarding mineralogy and reservoir properties.

Table 2.--Petrography and reservoir properties

[Mod., modal; Max, maximum; Qm, monocrystalline quartz; Pq, polycrystalline quartz; P, plagioclase feldspar; K, alkalic feldspar; Mu, muscovite; B, biotite; metaquartzite; Cl, chlorite; Ph, phosphatic(?) nodules; Or, organic material; Og, quartz overgrowths; Ch, chert; Ka, kaolinite; D, dolomite and siderite; smectite; Ml, mixed layer; Ap, Air permeability; Ep, effective porosity; Vp, visible porosity; V po, modal size of visible pores; PWC, pore-wall coatings;

Sample No.	Depth m(ft)	Color <sup>1</sup>		Mod. grain size (µm)	Max. grain size (µm)	Sort- ing <sup>1</sup>	Stain <sup>1</sup>	Optical mineralogy <sup>1</sup>																	
		Dry	Wet					Qm	Pq	P <sup>1</sup>	K	Mu	B	Og	G	Z	T	R	Lv	Ch	Hp	Hq	Cl	Ph	
Tuluvak Tongue of the Prince Creek Formation																									
118	36.0(118)	N7	5Y4/1	90	570	mvs	s	22.0	1.5	10.0	1.5	tr	3.5	tr	0	0	0	0	1.5	11.0	8.5	3.0	tr	0	
128	39.0(128)	na	na	na	na	na	na	na	na	na	na	na	na	na	na	na	na	na	na	na	na	na	na	na	na
140	42.7(140)	na	na	na	na	na	na	na	na	na	na	na	na	na	na	na	na	na	na	na	na	na	na	na	na
233	71.0(233)	N7-N8	5Y4/1	225	722	ws	s	15.0	6.0	9.0	na	tr	.5	tr	0	0	0	0	15.0	12.5	7.5	5.5	tr	0	
331	100.9(331)	N7	N4	90	494	mvs	s	12.0	3.0	6.5	na	tr	tr	tr	0	0	0	0	10.5	13.0	8.5	7.0	0	0	
514	156.7(514)	N7	5Y4/1	80	456	vps	s	7.5	1.0	3.0	na	0	8.0	tr	0	0	0	0	5.0	4.5	3.5	3.0	0	0	
519	158.7(519)	na	na	na	na	na	na	na	na	na	na	na	na	na	na	na	na	na	na	na	na	na	na	na	na
532	162.2(532)	na	na	na	na	na	na	na	na	na	na	na	na	na	na	na	na	na	na	na	na	na	na	na	na
Mean	---	---	---	121.3	560.5	---	---	14.13	2.88	7.13	na	0.08	3.03	0.1	0.0	0.0	0.0	0.0	8.00	10.25	4.0	4.63	0.05	0.0	
Stan. dev.	---	---	---	69.3	117.6	---	---	6.09	2.25	3.12	na	.05	3.65	.0	.0	.0	.0	.0	5.96	3.93	2.38	1.97	.06	.0	
Seabee Formation																									
545	166.1(545)	N7-N8	5Y5/1	230	722	ws	s	12.5	4.5	4.0	2.5	tr	tr	tr	0	0	0	0	11.0	22.5	11.0	11.5	tr	0	
746	227.4(746)	N5	5Y4/1	150	608	mvs	s	10.0	6.5	11.5	6.0	tr	1.5	tr	tr	0	0	0	7.5	7.0	14.0	9.0	1.5	0	
754	229.8(754)	N7	5Y3/1	95	532	ws	s	15.0	2.5	6.0	2.5	.5	1.5	tr	tr	0	0	0	2.0	10.5	14.5	4.5	tr	0	
763	232.6(763)	N7	5Y4/1	120	456	ws	A	16.5	5.0	8.0	na	tr	1.0	tr	0	0	0	0	2.0	10.5	11.0	12.5	tr	0	
771	235.0(771)	N6	5Y4/1	260	608	ws	s	8.5	8.5	9.0	.5	tr	.5	tr	0	0	0	0	5.5	14.0	19.5	10.5	tr	0	
1328	404.8(1328)	N7	5Y4/1	133	494	mvs	s	8.0	1.0	7.0	2.0	tr	1.0	tr	0	0	0	0	28.5	6.0	11.5	12.0	tr	0	
1331	405.7(1331)	N6-N7	5Y4/1	190	760	mvs	A	6.0	.5	9.0	.5	tr	.5	tr	0	0	0	0	22.5	4.5	8.0	5.5	1.5	0	
1343	409.4(1343)	N6-N7	5Y3/1	150	418	ws	s	10.5	3.5	9.0	tr	tr	1.0	tr	tr	0	0	0	16.5	6.0	11.5	9.5	.5	0	
1358	413.9(1358)	N6	5Y4/1	150	646	ps	s	9.0	tr	9.0	1.5	0	2.0	tr	0	0	0	0	22.0	3.5	14.0	2.0	tr	0	
1365	416.1(1365)	N6	5Y4/1	135	608	mvs	s	8.0	1.0	12.5	1.0	tr	1.0	tr	tr	0	0	0	21.0	5.0	9.0	5.0	tr	0	
1824	556.0(1824)	N6	5Y4/1	75	494	ws	A	29.5	8.0	2.0	.5	.5	.5	tr	tr	tr	0	0	0	5.0	10.5	6.5	.5	0	
Mean	---	---	---	153.5	576.9	---	---	12.14	3.74	7.91	1.71	0.15	0.96	0.1	0.5	0.02	0.0	0.0	12.59	8.77	12.23	8.05	0.43	0.0	
Stan. dev.	---	---	---	54.8	100.6	---	---	6.57	3.02	3.06	1.74	.18	.55	.0	.5	.04	.0	.0	9.94	5.46	3.16	3.52	.55	.0	
Ninuluk Formation																									
2049	624.5(2049)	N6-N7	5Y4/1	85	228	ws	A	20.0	5.0	0.5	0.5	tr	tr	tr	tr	tr	0	0	0	7.0	18.0	13.5	0.5	0	
2060	627.9(2060)	N6	5Y4/1	150	418	ws	A	17.0	3.5	1.5	1.5	tr	tr	tr	0	0	0	0	13.5	16.0	12.5	tr	0	0	
2068	630.3(2068)	N7	5Y4/1	160	342	ws	A	22.5	6.0	1.0	tr	1.0	.5	tr	0	tr	tr	0	0	15.0	18.0	16.5	tr	0	
2075	632.5(2075)	na	na	na	na	na	na	na	na	na	na	na	na	na	na	na	na	na	na	na	na	na	na	na	na
2080	634.0(2080)	N6-N7	5Y3/1	120	304	ws	s	10.5	3.0	.5	3.5	tr	tr	tr	0	tr	tr	0	0	6.0	9.5	9.5	tr	0	
2085	635.5(2085)	N6-N7	5Y3/1	115	760	mvs	A	9.5	3.5	1.0	1.0	tr	tr	tr	0	tr	0	0	tr	23.0	24.5	12.5	tr	0	
2093	638.0(2093)	N6	N3	95	684	ws	s	32.5	6.0	.5	.5	tr	.5	tr	tr	tr	0	0	0	8.5	21.5	10.5	4.5	0	
2110	643.1(2110)	N6-N7	N3	190	1026	ps	s	47.5	8.5	tr	tr	tr	0	tr	0	tr	0	0	0	13.0	8.5	10.5	1.0	0	
2117	645.3(2117)	N6	5Y4/1	228	1406	ps	s	43.0	10.5	tr	tr	tr	tr	tr	0	tr	0	0	0	17.0	8.0	12.5	1.0	0	
2120	646.2(2120)	N6-N7	N5	228	1786	ps	s	41.5	6.0	.5	.5	tr	0	tr	0	0	0	0	0	17.5	7.5	19.0	1.0	0	
2128	648.6(2128)	N7	5Y4/1	190	570	ws	s	41.5	8.0	1.0	tr	tr	0	tr	0	tr	0	0	tr	12.0	9.0	18.5	.5	0	
Mean	---	---	---	156.1	752.4	---	---	28.55	6.00	0.67	0.79	0.19	0.15	0.1	0.02	0.07	0.05	0.0	0.02	13.25	14.05	13.55	0.89	0.0	
Stan. dev.	---	---	---	52.1	512.6	---	---	14.34	2.43	.44	1.06	.28	.19	.0	.04	.05	.05	.0	.04	5.23	6.29	3.35	1.33	0.0	
Killik Tongue of the Chandler Formation																									
2200	670.6(2200)	N7	5Y5/1	100	266	ws	A	29.0	6.5	1.5	2.5	tr	0	tr	tr	tr	0	0	tr	9.0	10.0	1.5	2.0	0	
2235	681.2(2235)	N6	5Y4/1	190	532	ws	s	48.0	6.5	1.5	.5	tr	tr	tr	tr	0	0	0	.5	16.0	7.0	7.5	.5	0	
2298	700.4(2298)	N6-N7	N5	190	798	ws	s	50.5	6.0	tr	tr	tr	tr	tr	0	tr	0	0	0	14.5	2.5	9.0	tr	0	
2305	702.6(2305)	N7	5Y4/1	70	190	vws	s	39.5	10.0	2.0	3.0	tr	tr	tr	0	0	0	0	0	13.0	6.0	5.0	tr	0	
2378	724.8(2378)	N7	5Y4/1	175	456	ws	s	31.0	8.0	3.0	5.5	tr	tr	tr	0	tr	0	tr	0	22.5	6.5	8.5	tr	0	
2386	727.3(2386)	N7	5Y4/1	57	304	vws	A	44.5	4.0	2.5	1.0	tr	tr	tr	.5	tr	tr	0	0	14.0	7.5	4.0	1.0	0	
Mean	---	---	---	130.3	424.3	---	---	40.42	6.83	1.77	2.10	0.10	0.08	0.1	0.15	0.03	0.05	0.2	0.12	14.83	6.58	5.92	0.63	0.0	
Stan. dev.	---	---	---	61.7	222.1	---	---	8.90	2.02	1.00	2.01	.0	.04	.0	.18	.05	.05	.4	.19	4.43	2.44	2.92	.76	.0	
Grandstand Formation																									
2445	745.2(2445)	N6-N7	5Y4/1	150	1064	ws	s	41.5	14.0	1.5	0.5	tr	0	tr	0	0	0	0	0	tr	23.0	6.0	4.5	tr	0
2450	746.8(2450)	N6-N7	5Y4/1	133	646	ws	s	34.5	7.5	1.0	.5	.5	0	tr	0	0	tr	0	0	tr	19.5	10.0	6.5	1.0	0
2453	747.6(2453)	N6-N7	6Y4/1	114	532	ws	s	37.5	4.5	.5	na	tr	0	tr	0	0	0	0	.5	19.5	7.5	7.5	.5	0	
2460	749.8(2460)	N6-N7	5Y4/1	150	722	ws	s	42.5	5.5	tr	tr	tr	tr	tr	0	0	tr	0	0	0	20.0	8.5	4.0	tr	tr
2532	771.8(2532)	5Y7/1	10Y4/2	270	836	ws	s	32.0	8.5	.5	1.0	tr	0	tr	0	0	0	0	0	0	39.5	1.0	2.5	0	0
2813	857.4(2813)	N7	5Y4/1	190	608	ws	s	33.0	9.5	1.0	1.0	0	0	tr	tr	0	0	0	0	tr	27.5	5.0	5.0	tr	0
2824	860.8(2824)	N7	5Y4/1	228	570	ws	s	29.5	12.0	1.5	1.0	tr	0	tr	tr	tr	0	0	0	tr	27.5	4.5	3.5	tr	0
2832	863.2(2832)	N6-N7	5Y5/1	228	608	ws	s	50.0	10.5	.5	1.0	tr	0	tr	0	0	tr	0	0	0	14.5	1.0	5.5	0	0
2841	865.9(2841)	N7	5Y4/1	150	381	ws	s	31.5	8.5	.5	3.0	.5	0	tr	tr	0	0	0	0	tr	18.5	11.5	8.5	.5	0
2849	868.4(2849)	N7-N5	5Y5/1	209	608	ws	s	44.0	5.5	1.5	1.0	0	0	tr	tr										

of selected core samples from Umiat test well 11

Og, gray opaque mineral; G, garnet; Z, zircon; T, tourmaline; R, rutile; Lv, volcanic rock fragments; Ch, chert; Mp, phyllite and (or) schist; Mq, Oy, yellow opaque mineral; Det., detrital; grns., grains; aut., authigenic; min., minerals; C, calcite; Mx, matrix; Q, quartz; Dd, dolomite; I, illite; S, na, not analyzed; tr, trace; leaders (---), not applicable; np, not present; Stan. dev., Standard deviation; pct., percent; md., millidarcy

Authigenic minerals						Det. grns. and aut. min.	Mx	Rock name	X-ray mineralogy										Reservoir properties						
Or	Qg	Ch	Ka	D	Oy				Q	K	P	C	Dd	Cl	Ka	I	S	Ml	Ap (md)	Ep (pct.)	Vp (pct.)	Vp (um)	PWC (pct.)	Sample No.	
Tuluwak Tongue of the Prince Creek Formation																									
tr	0	0	0	1.5	0	7.5	26.5	Feldspathic phyllarenite	46	130	130	np	np	19	33	45	9	np	na	10.2	2.0	100	95	118	
na	na	na	na	na	na	na	na	na	43	44	38	np	np	20	17	51	12	np	21	13.1	na	na	na	128	
na	na	na	na	na	na	na	na	na	38	87	52	17	25	12	np	28	26	np	6.21	5.4	na	na	na	140	
0	0	0	0	5.0	tr	0	23.0	Volcanic litharenite	na	na	na	na	na	na	na	na	na	na	<1	17.85	1.0	50	95	233	
.5	0	0	tr	1.0	tr	5.0	33.0	Phyllarenite	na	na	na	na	na	na	na	na	na	na	0	13.94	tr	20	95	331	
tr	0	0	0	1.0	0	2.0	57.5	do	na	na	na	na	na	na	na	na	na	na	0	15.9	4.0	100	100	514	
na	na	na	na	na	na	na	na	na	42	23	82	7	27	17	np	29	9	np	na	16.8	na	na	na	519	
na	na	na	na	na	na	na	na	na	39	63	37	34	38	14	31	26	5	np	na	na	na	na	na	532	
0.18	0.0	0.0	0.03	2.13	0.05	3.63	35.0	---	na	na	na	na	na	na	na	na	na	na	0.03	14.47	1.78	67.50	96.25	---	
.22	.0	.0	.05	1.93	.06	3.30	15.56	---	na	na	na	na	na	na	na	na	na	na	.05	3.27	1.67	39.48	2.50	---	
Seabee Formation																									
0	0	0	0	1.0	tr	10.0	7.0	Phyllarenite	na	na	na	na	na	na	na	na	na	na	<1	14.9	2.5	50	95	545	
1.5	0	0	0	.5	tr	2.0	14.5	Feldspathic phyllarenite	40	12	62	np	31	17	12	46	3	np	5.1	18.25	7.0	70	95	746	
tr	0	0	0	2.0	tr	2.0	35.5	Phyllarenite	33	85	48	np	33	30	12	41	7	np	7.0	17.7	1.0	40	95	754	
tr	0	0	0	1.5	tr	14.0	17.0	Metarenite	32	29	32	17	17	21	np	71	3	np	.0	12.7	1.0	40	95	763	
.5	0	0	0	tr	tr	1.0	15.0	Phyllarenite	37	35	54	7	7	12	5	27	2	np	48	20.64	7.0	20	95	771	
tr	0	0	0	0	tr	.5	21.5	Volcanic litharenite	17	31	32	10	5	13	9	11	tr	np	27	18.4	1.0	60	75	1328	
0	0	0	0	tr	tr	41.5	.0	do	12	32	45	103	6	4	np	14	tr	np	0	.55	0	0	0	1331	
.5	0	0	0	0	tr	1.5	30.0	Phyllarenite	22	50	85	np	np	13	np	18	3	tr	0	6.46	0	0	0	1343	
tr	0	0	0	0	tr	1.5	33.5	Volcanic litharenite	14	49	39	np	np	19	np	14	tr	np	0	7.03	0	0	0	1365	
1.0	0	0	0	0	tr	.5	35.0	do	28	61	90	np	np	8	np	10	tr	11	0	10.1	0	0	0	1365	
0	0	0	0	4.0	tr	16.5	15.5	Phyllarenite	na	na	na	na	na	na	na	na	na	na	0	9.66	.5	15	75	1824	
0.35	0.0	0.0	0.0	0.84	0.1	8.27	20.41	---	na	na	na	na	na	na	na	na	na	na	7.93	12.40	1.82	26.82	56.82	---	
.49	.0	.0	.0	1.26	.0	12.46	11.84	---	na	na	na	na	na	na	na	na	na	na	15.55	6.24	2.67	26.29	45.68	---	
Minuluk Formation																									
0	tr	0	0	4.5	tr	21.5	8.5	Phyllarenite	39	8	28	31	23	14	16	47	np	np	0	10.58	0.5	23	0	2049	
0	tr	0	1.0	.5	tr	23.5	8.5	do	42	11	26	29	39	17	20	37	np	np	0	11.79	1.0	20	25	2060	
tr	tr	0	1.0	4.5	tr	8.0	5.0	do	61	48	28	19	26	13	11	20	np	np	0	13.32	1.0	40	0	2068	
na	na	na	na	na	na	na	na	na	59	6	32	20	34	23	28	53	np	np	na	na	na	na	na	2075	
0	0	0	0	1.5	tr	56.0	tr	Metarenite	30	7	33	134	57	13	17	34	np	np	0	7.39	0	0	0	2080	
tr	tr	0	3.5	4.0	tr	6.5	11.0	Phyllarenite	63	9	34	19	16	8	8	24	np	np	0	11.55	tr	30	50	2085	
0	0	0	0	tr	tr	15.0	tr	do	39	6	13	np	np	20	np	48	np	np	0	10.41	tr	20	60	2093	
0	.5	0	0	tr	tr	0	4.0	Metarenite	na	na	na	na	na	na	na	na	na	na	29	14.50	6.5	80	15	2110	
0	tr	0	0	1.0	tr	0	5.0	do	na	na	na	na	na	na	na	na	na	na	14	13.45	2.0	40	20	2117	
0	tr	0	tr	tr	tr	0	4.0	do	na	na	na	na	na	na	na	na	na	na	28	13.40	2.5	25	60	2120	
0	tr	0	0	1.0	tr	0	3.0	do	na	na	na	na	na	na	na	na	na	na	56	15.65	5.5	70	40	2128	
0.02	0.12	0.0	0.56	1.73	0.1	11.56	6.41	---	na	na	na	na	na	na	na	na	na	na	12.70	12.20	1.92	34.80	24.0	---	
.04	.14	.0	1.11	1.86	.0	18.01	4.35	---	na	na	na	na	na	na	na	na	na	na	19.28	2.38	2.31	24.14	24.24	---	
Killik Tongue of the Chandler Formation																									
0	tr	0	tr	1.0	tr	31.0	5.5	Phyllarenite	na	na	na	na	na	na	na	na	na	na	0	12.4	0.5	7	60	2200	
0	1.0	0	0	tr	tr	tr	3.5	Chert arenite	na	na	na	na	na	na	na	na	na	na	125	15.65	7.5	80	10	2235	
0	1.0	0	0	tr	tr	tr	3.0	do	na	na	na	na	na	na	na	na	na	na	na	550	19.80	13.5	80	<10	2298
0	.5	0	tr	1.0	tr	0	9.5	do	na	na	na	na	na	na	na	na	na	na	13	16.15	10.5	40	40	2305	
0	tr	0	0	.5	tr	0	7.0	do	121	8	23	np	np	6	18	9	np	np	102	19.6	7.5	50	40	2378	
0	.5	tr	.5	1.5	tr	tr	16.0	do	95	21	95	np	np	18	33	22	np	np	10	16.78	2.5	40	40	2386	
0.0	0.53	0.02	.12	0.70	0.1	5.22	7.42	---	na	na	na	na	na	na	na	na	na	na	133.33	16.73	7.0	49.50	33.33	---	
.0	.40	.04	.19	.56	.0	12.63	4.83	---	na	na	na	na	na	na	na	na	na	na	210.78	2.75	4.85	27.74	19.66	---	
Grandstand Formation																									
tr	tr	0	0	tr	tr	tr	3.0	Chert arenite	107	5	12	np	np	8	6	12	np	np	120	17.60	6.0	60	25	2445	
tr	1.0	0	0	.5	tr	0	9.5	do	127	np	56	np	np	7	4	11	np	np	81	16.45	8.0	40	25	2450	
tr	1.0	0	tr	3.0	0	0	12.0	do	88	5	17	np	np	10	6	15	np	np	18	14.83	6.0	50	25	2453	
0	tr	0	tr	2.5	1.0	tr	11.0	do	121	5	20	np	np	13	13	25	np	np	27	14.95	5.0	50	50	2460	
0	1.0	tr	0	0	.5	tr	1.5	do	na	na	na	na	na	na	na	na	na	na	235	18.96	12.0	100	<5	2532	
0	1.0	tr	.5	tr	.5	0	8.0	do	115	np	28	np	np	4	5	8	np	np	100	16.35	8.0	60	30	2813	
0	2.0	tr	2.5	tr	.5	1.0	3.0	do	123	7	24	np	np	4	5	4	np	np	158	17.35	11.5	75	<1	2824	
0	2.5	0	tr	tr	tr	0	3.0	do	150	6	30	np	np	4	6	4	np	np	280	17.1	11.5	120	<1	2832	
1.0	1.0	0	0	tr	0	tr	11.0	Phyllarenite	164	5	18	np	np	4	4	6	np	np	na	14.71	4.0	40	75	2841	
0	2.0	0	.5	tr	0	0	3.0	Chert arenite	123	5	13	np	np	3	5	4	np	np	400	19.25	10.5	100	<1	2849	
0	tr	0	0	3.5	0	0	19.5	Phyllarenite	na	na	na	na	na	na	na	na	na	na	0	11.96	3.5	12	55	2925	
0	1.0	0	.5	1.0	0	0	15.0	do	68	10	47	np	np	11	6	23	np	np	<1	13.5	5.0	30	25	2990	
0	1.5	0	.5	3.5	tr	0	8.5	do	74	25	44	np	np	13	10	26	np	np	2.3	12.85	5.5	50	25	2997	
0	tr	0	0	4.5	0	0	17.5	do	55	20	43	np	11	17	8	30	np	np	0	10.2	.5	17	40	3005	
0.09	1.03	0.02	0.34	1.36	0.21	0.10	8.96	---	na	na	na	na	na	na	na	na	na	na	101.53	15.43	6.93	57.43	27.16	---	
.26	.77	.04	.66	1.65	.30	.26	5.80	---	na	na	na	na	na	na	na	na	na	na	125.97	2.65	3.46	31.73	22.31	---	
0.14	0.42	0.01	0.25	1.30	0.13	5.64	13.30	---	na	na	na	na	na	na	na	na	na	na	54.13	14.06	4.12	44.76	40.67	---	
.31	.63	.03	.66	1.54	.17	11.85	11.91	---	na	na	na	na	na	na	na	na	na	na	112.37	4.09	3.96	31.17	35.50	---	

<sup>4</sup>A, alizarin red; s, sodium cobaltinitrite.  
<sup>5</sup>Includes some alkalic feldspar in some samples.

<sup>6</sup>Unsuccessful stain; counted with plagioclase.  
<sup>7</sup>Sample too friable to test.

perm-plug sample locations. No previous petrographic study of rocks from Umiat test well 11 exists, but Krynine (1947, 1948) and Krynine and Ferm (1952) studied rocks that are stratigraphically equivalent in other test wells in NPRA, including other Umiat wells. Sample depth, stratigraphic position (using the boundaries assigned by Collins, 1958), petrography, and reservoir properties of all samples are shown in table 2.

Two disc-shaped slices 20 mm in diameter were cut from the end of each perm plug and used to make one standard petrographic thin section per sample. Thin sections of samples with high contents of smectite were cut and ground in oil. The thin sections were impregnated with blue dye to show porosity. Thin sections of samples with high contents of carbonate minerals were stained with alizarin red dye; the remainder were stained with sodium cobaltinitrite for feldspar identification. Two hundred points per thin section were counted for modal analysis. Modal grain size of the sand fraction only was estimated using an ocular micrometer; and, similarly, sorting of the sand fraction only was estimated using the reference photographs of Beard and Weyl (1973). The rocks are named according to the classification of Folk and others (1970), with the addition of the term "metarenite" to describe a litharenite composed mainly of metamorphic rock fragments other than phyllite.

For each sample studied by X-ray diffraction techniques, the fraction that is less than 2  $\mu\text{m}$  (micrometers) was used to prepare an oriented clay mount which was subsequently glycolated at 60°C for 24 hours and heated to 300°C and 500°C respectively for 1 hour. X-ray diffraction patterns were run after each of these steps. In addition to analysis of the fraction that is less than 2  $\mu\text{m}$ , each sample was analyzed on a whole-rock basis in order to identify the major mineral assemblages. For each mineral identified, the height of a specified peak above background was measured in order to determine a peak height intensity. Table 2 shows the relative proportions according to peak height intensity between the identified clay minerals for each of the samples studied. Each X-ray diffraction trace was run at 2° 2 $\theta$  per minute with nickel-filtered CuK $\alpha$  radiation. Instrument conditions were 34 kilovolts, 18 milliamperes, and a counting rate of 3,000 counts per second.

Criteria used for clay-mineral identification are as follows: Kaolinite displays a sharp basal (001) peak at 7.13 Å and a (002) peak at 3.58 Å. The kaolinite was unaffected by glycol and collapsed after being heated for 1 hour at 550°C. Because all of the samples studied contained considerable amounts of well-crystallized chlorite, the (001) kaolinite peak could not be distinguished from the (002) peak of chlorite. Therefore,

resolution of the 3.54-Å chlorite peak from the 3.58-Å kaolinite reflection was used for positive kaolinite identification and measurement of peak intensity.

Chlorite gives a sharp (001) basal spacing at 14.2 Å. The intensity of this peak is unchanged upon glycolation or heat treatment at 550°C for 1 hour. A sharp, well-developed (002) reflection is present at 7.0 Å and is consistently more intense than the (001) peak; however, it interferes with the (001) kaolinite peak. Positive chlorite identification was based on the presence of a sharp (004) peak at 3.54 Å. Both the (002) and (004) reflections collapse upon heating at 550°C for 1 hour.

Illite is identified by a strong, well-ordered (001) reflection at 10.0 Å that is not affected by glycolation. Heat treatments to 500°C for 1 hour cause a sharpening of basal reflections.

Smectite shows a broad basal (001) reflection at 12.6 Å, which expands to 17.3 Å upon glycolation at 60°C for 24 hours. Because the smectite contains between 80 and 100 percent expandable layers, the (003) glycolated reflection at 5.68 Å was used to measure peak height intensity. Heat treatment above 300°C caused the smectite to collapse. A measure of crystallinity following the methods of Biscaye (1965) indicates that, in almost all of the samples studied, the smectite is well crystallized.

Interstratified minerals are recognized in only two of the samples studied. Glycolation and heat treatments indicate that the mixed layering is predominantly chlorite-smectite. Its presence is indicated by an incomplete collapse of the smectite peak upon heating at 550°C for 1 hour.

The following criteria were used to identify the major minerals in the whole-rock fraction. Quartz identification was based on the presence of the 4.27-Å reflection. The strongest (101) quartz peak, at 3.35 Å, interferes with the (003) peak of illite at 3.33 Å and therefore was not used for measuring peak height intensity.

Both alkalic feldspar and plagioclase feldspar were recognized in all of the samples studied. The peak position used to identify alkalic feldspar ranged from 3.20 Å to 3.25 Å, and the plagioclase reflection ranged from 3.18 Å to 3.19 Å.

Calcite and dolomite were identified in samples from the Tuluvak Tongue of the Prince Creek Formation and from the Seabee and Ninuluk Formations. Calcite was identified by a strong sharp peak at 3.03 Å and dolomite by a sharp symmetrical peak at 2.89 Å. Siderite was tentatively identified in some samples by a reflection near 2.79 Å; however, its presence was somewhat uncertain. Neither magnesian calcite nor ankerite was recognized in any of the samples studied.

GRANDSTAND FORMATION AND KILLIK TONGUE OF THE CHANDLER FORMATION

Rock samples analyzed from the Grandstand Formation and Killik Tongue are petrographically similar. They are light-gray, well-sorted, very fine grained to fine-grained chert arenites and phyllarenites relatively poor in quartz and rich in lithic fragments such as chert, phyllite, and metaquartzite (figs. 15-19). Detrital grains are mainly angular to subangular. The amount of matrix is highly variable, and, except in sample No. 2200, carbonate is present in small amounts. Many of the samples from the Grandstand Formation and Killik Tongue have excellent porosity and permeability (figs. 20-23).

Quartz grains are generally strained and quartz individuals in polycrystalline quartz grains generally have slightly sutured boundaries. Most plagioclase grains exhibit albite twinning and appear to be sodic plagioclase. The plagioclase is unzoned and generally unaltered. Grains of alkalic feldspar are blocky and mostly unaltered. The feldspar is generally untwinned, although a few grains exhibit grid twinning. Some grains are perthitic. X-ray diffraction analysis indicates that alkalic feldspar is significantly less abundant in the Nanushuk Group than it is in the Colville Group.

Detrital chert is dominantly microcrystalline, with the individual crystals averaging about 3-12  $\mu\text{m}$  in diameter. The

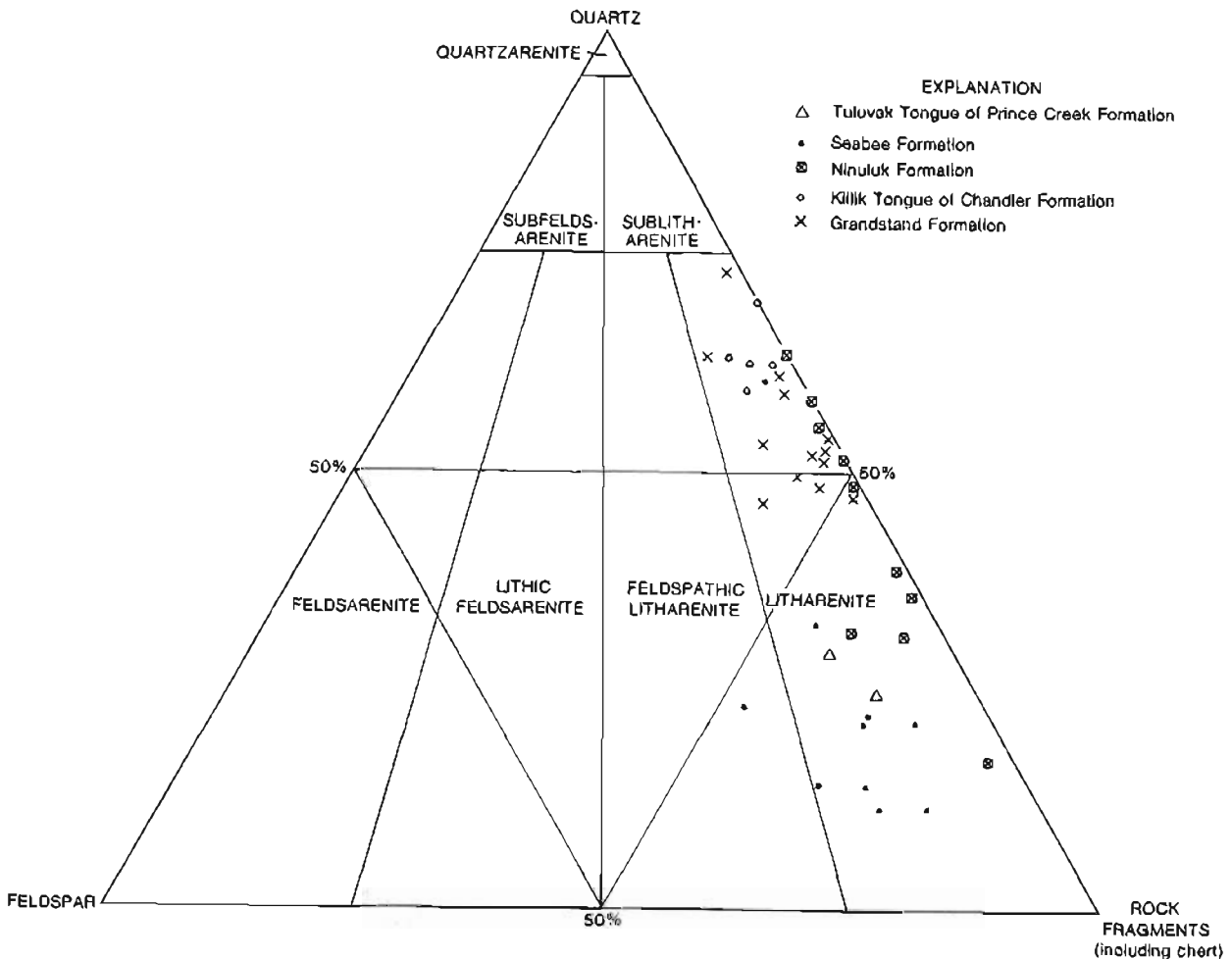


Figure 15.--Primary arenite triangle (Folk and others, 1970) showing composition of samples listed in table 2. Each symbol indicates the formation from which the sample came.

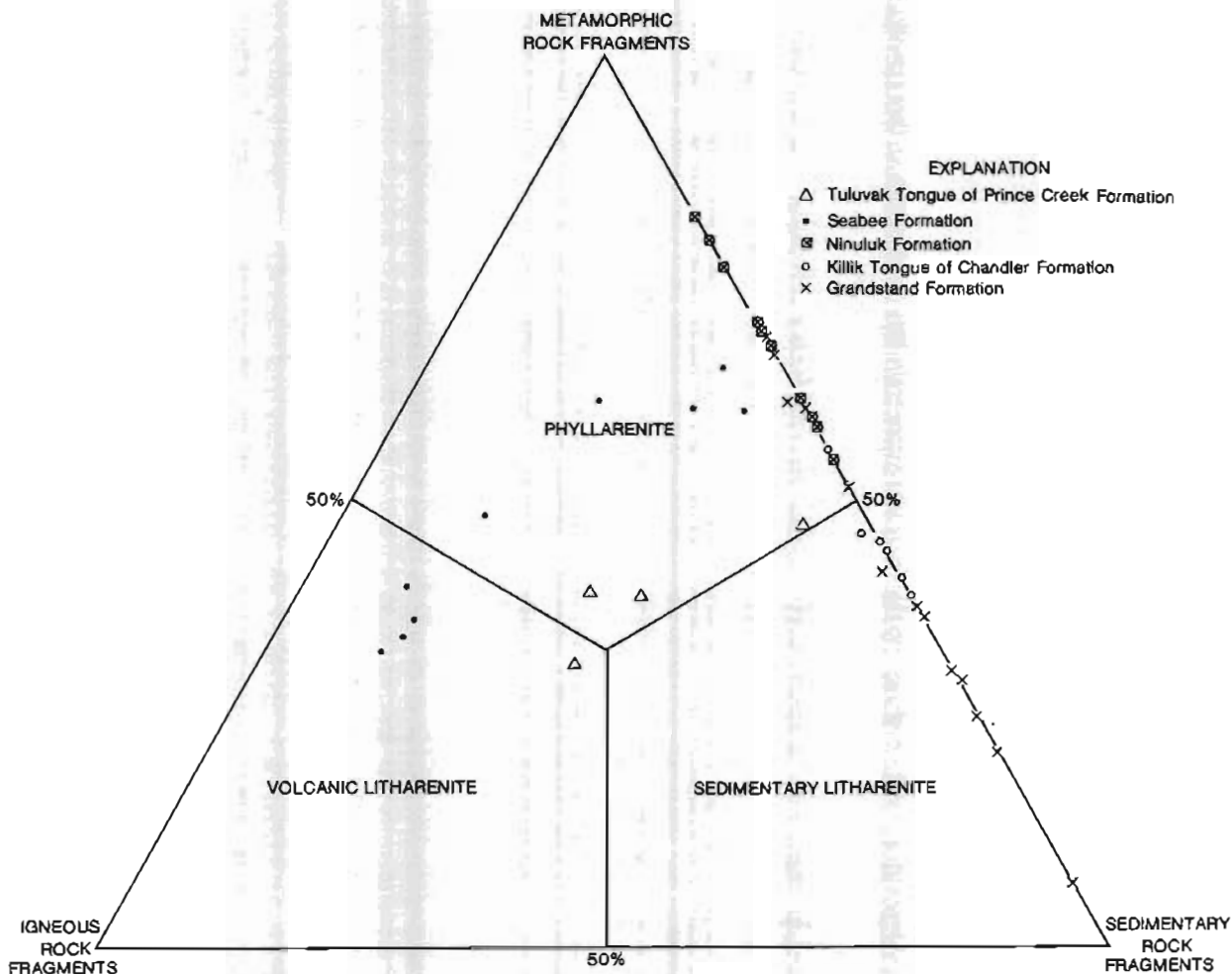


Figure 16.—Litharenite triangle (Folk and others, 1970) showing composition of samples listed in table 2. Each symbol indicates the formation from which the sample came.

chert grains are colorless to yellow to dark brown, and some grains are highly charged with inclusions, including clay(?) and euhedral crystals of pyrite and dolomite. Patches of chalcedonic chert, both length-slow and length-fast varieties, occur in a few microcrystalline chert grains; a very few grains are wholly chalcedonic chert. In rare cases chert grains are slightly deformed, but in general they behave as noncompressible (nonductile) detrital grains. Some grains that otherwise appear to be chert contain abundant and, in some cases, subparallel flakes of sericite. These grains of "sericitized chert" may represent altered or even slightly metamorphosed chert, or they may actually be grains of a low-grade metamorphic rock such as slate.

Metamorphic rock fragments include both phyllite and metaquartzite. The phyllite is characteristically composed of subparallel flakes (average size  $3 \times 15 \mu\text{m}$ ) of sericite and,

more rarely, chlorite, and equant to slightly elongate anhedral crystals of quartz. Similar fragments with mica flakes larger than  $140 \mu\text{m}$  are extremely rare and are classified as schist in this report. In sample Nos. 2298, 2305, 2445, 2450, and 2453, some phyllite fragments contain small prismatic crystals of what appears to be clinozoisite. In general, the phyllite grains are highly compressible (ductile) and are mashed and stretched between noncompressible detrital grains (figs. 24, 25). Grains composed of foliated quartz individuals have been classified as metaquartzite in this report, whereas grains composed of unfoliated quartz individuals have been classified as polycrystalline quartz grains. The metaquartzite is similar to the phyllite, except that the metaquartzite contains greater than 50 percent quartz and the quartz individuals are generally larger and more definitely stretched. Most metaquartzite

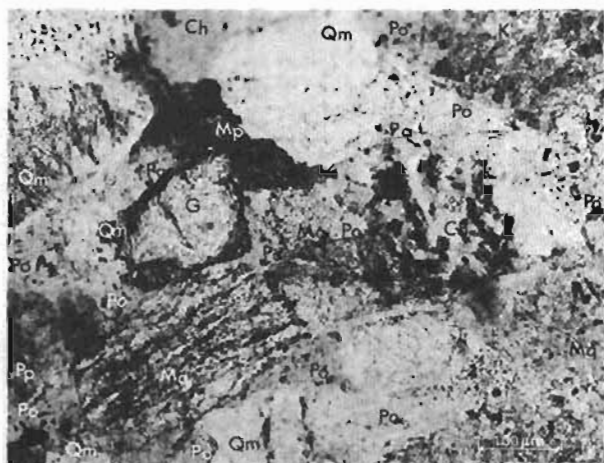


Figure 17.--Grandstand Formation, 860.8 m (2824 ft). Chert arenite showing excellent porosity and permeability. Note variety of detrital grains and mashed phyllite grain. Ch, chert; K, alkalic feldspar; G, garnet; Mp, phyllite or schist; Mq, metaquartzite; Po, pore; Qm, monocrystalline quartz; Pq, polycrystalline quartz. Photomicrograph, plane polarized light.

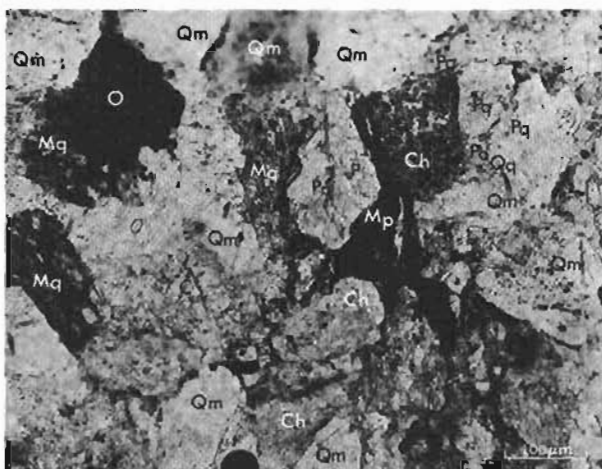


Figure 19.--Grandstand Formation, 913.5 m (2997 ft). Phyllarenite with poor porosity and permeability. Note variety of detrital grains, mashed phyllite, and slightly deformed metaquartzite (near center). C, calcite; Ch, chert; P, plagioclase feldspar; Mp, phyllite or schist; Mq, metaquartzite; O, opaque mineral; Po, pore; Qm, monocrystalline quartz; Pq, polycrystalline quartz; Qg, quartz overgrowth. Photomicrograph, plane polarized light.

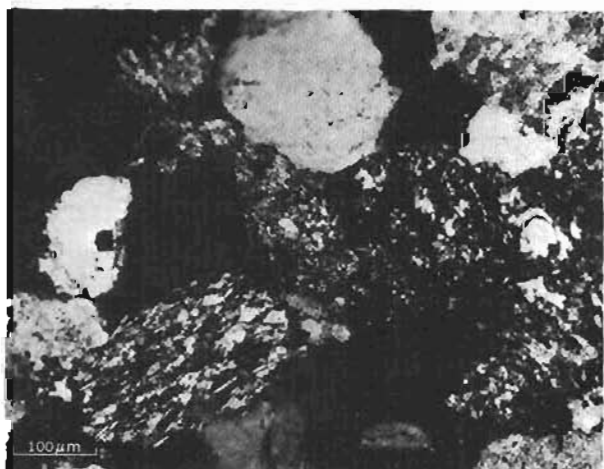


Figure 18.--Grandstand Formation, 860.8 m (2824 ft). Chert arenite showing excellent porosity and permeability. Note variety of detrital grains and mashed phyllite grain. Photomicrograph same as figure 17 but with crossed nicols.

grains contain a considerable amount of sericite as thin undulating laminae or as flakes bent around quartz crystals, but some grains are nearly pure quartz. A few grains of graphitic metaquartzite occur in almost every sample.

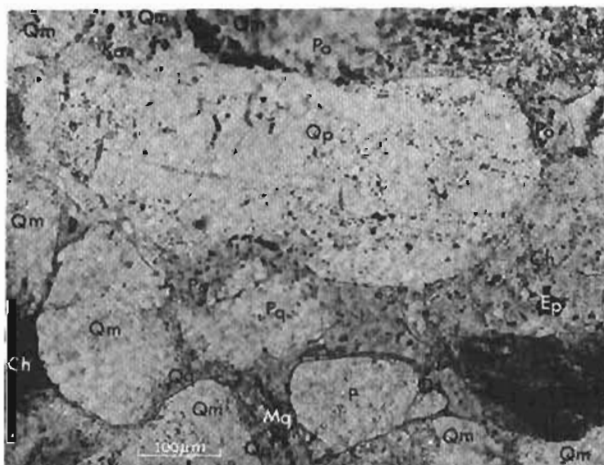


Figure 20.--Grandstand Formation, 868.4 m (2849 ft). Note numerous intergranular pores, a few of which are bounded by quartz overgrowths. Ch, chert; Ep, euhedral pyrite; P, plagioclase feldspar; Ka, kaolinite; Mq, metaquartzite; Ot, open throat; Po, pore; Qm, monocrystalline quartz; Pq, polycrystalline quartz; Qg, quartz overgrowth. Photomicrograph, plane polarized light.

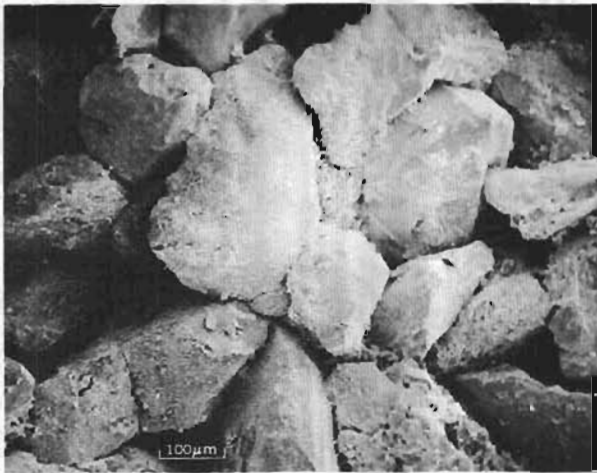


Figure 21.--Grandstand Formation, 868.4 m (2849 ft). Note excellent intergranular porosity. Scanning electron micrograph.

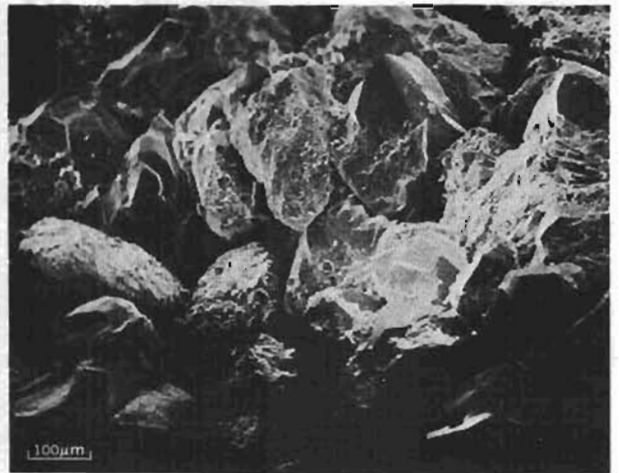


Figure 23.--Killik Tongue of the Chandler Formation, 700.4 m (2298 ft). Note intergranular pores and quartz grains with quartz overgrowths. The pillow-shaped grain at left center may be a phyllite grain. Scanning electron micrograph.

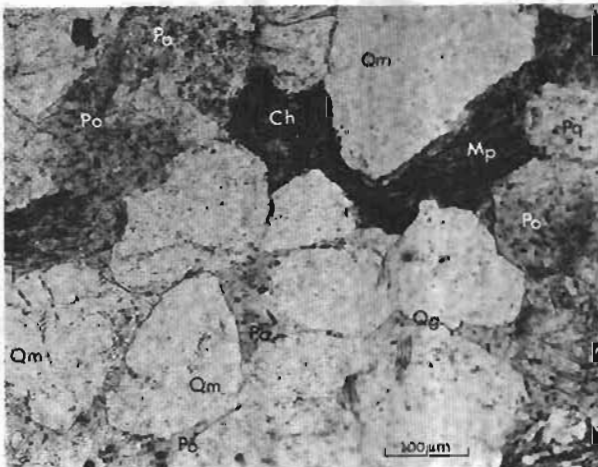


Figure 22.--Killik Tongue of the Chandler Formation, 700.4 m (2298 ft). Note intergranular pores, many of which are bounded by quartz overgrowths. Deformed chert and phyllite plug intergranular pores at lower left. Ch, chert; Mp, phyllite; Po, pore; Qm, monocrystalline quartz; Pq, polycrystalline quartz; Qg, quartz overgrowth. Photomicrograph, plane polarized light.

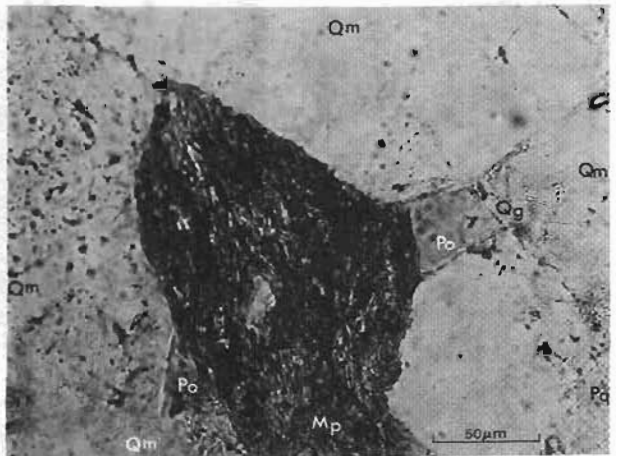


Figure 24.--Grandstand Formation, 868.4 m (2849 ft). Phyllite grain partially squeezed into intergranular pore. Quartz overgrowth also partially fills pore. Sericite of phyllite grain appears to slightly etch quartz grains, suggesting some recrystallization of sericite. Mp, phyllite; Po, pore; Qm, monocrystalline quartz; Pq, polycrystalline quartz; Qg, quartz overgrowth. Photomicrograph, plane polarized light.

Most metaquartzite grains behave as noncompressible grains, but some that have a high content of sericite are slightly compressible.

Volcanic rock fragments are present in trace amounts in several samples; they consist of plagioclase microlites (average 20x60  $\mu\text{m}$ ) in a random or subparallel arrangement set in a chloritic groundmass. The groundmass is more abundant than plagioclase in some fragments

and less abundant in others. Biotite is present as pleochroic pale-brown to dark-brown flakes (100 to 400  $\mu\text{m}$  long) with frayed ends; some are partially altered to chlorite. What appears to be detrital chlorite occurs as

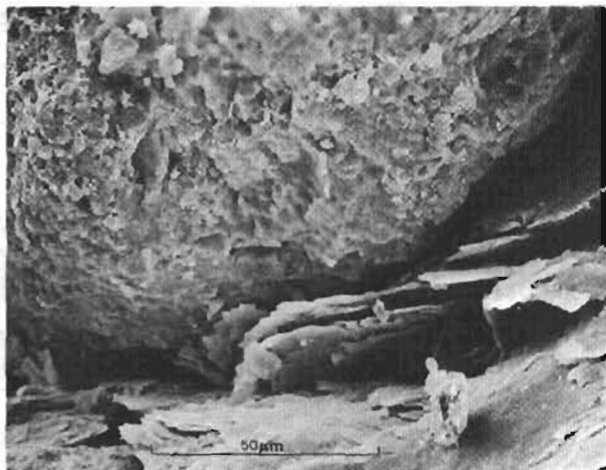


Figure 25.—Grandstand Formation, 745.2 m (2445 ft). Deformation of compressible grain, possibly phyllite, by noncompressible grain. Scanning electron micrograph.

flakes composed of a single crystal and as flakes composed of a scaly mass of almost cryptocrystalline crystals; optical properties indicate that at least some of the chlorite is penninite.

Organic matter occurs as highly deformed masses and stringers as much as 4 mm long that totally lack cellular form. As seen in thin section the material is nearly opaque, but very thin edges are deep orange. Other detrital components occur in small amounts in the samples and are shown in table 2.

#### Matrix

As seen in thin section, matrix (material smaller than 30  $\mu\text{m}$ ) consists mainly of randomly oriented to subparallel flakes of sericite and some chlorite, and tiny grains of quartz. Much of this material appears to be detrital and probably represents "hash" resulting from the abrasion and disintegration of phyllite and metaquartzite fragments. However, many detrital grains are etched and slightly embayed by the matrix, indicating that at least some of the matrix phyllosilicates are authigenic. In addition, coatings as much as 10  $\mu\text{m}$  thick of subparallel flakes of authigenic(?) sericite, chlorite, and (or) illite occur locally along some detrital grain contacts.

X-ray diffraction analysis indicates the presence of illite, chlorite, and kaolinite in the fraction that is less than 2  $\mu\text{m}$  in size; however, they appear to be less abundant than in the overlying formations. No smectite was detected. Clay material identified as illite in all samples from Umiat test well 11 has a sharp, well-ordered 10-A peak, suggesting that much of this material may be detrital sericite rather than authigenic illite. Similarly,

material identified as chlorite in all the samples has a sharp, well-ordered peak suggesting that at least some of the chlorite is detrital metamorphic rather than sedimentary in origin.

#### Authigenic Minerals

Quartz overgrowths on free surfaces of detrital quartz grains are a ubiquitous but minor authigenic mineral (figs. 22, 23). They are as much as 15  $\mu\text{m}$  thick and, as seen in thin section, have straight or sawtooth edges. Locally the contact between the overgrowth and the detrital grain is marked by opaque dust or authigenic(?) illite. Some overgrowths are etched by matrix phyllosilicates. The overgrowths project into, but rarely completely fill, intergranular pores. Other authigenic minerals that occur in small amounts include kaolinite, which occurs as intergrown masses of vermicular crystals (5-15  $\mu\text{m}$  in length) that completely fill some pores; chert; pyrite; and possibly some smaller flakes of chlorite.

Several kinds of carbonate minerals occur in the samples. Sparry colorless carbonate crystals (100-150  $\mu\text{m}$  in diameter) and clusters of two to four such crystals, in sample Nos. 2925, 2990, 2997, and 3005, are unstained by alizarin red and are apparently dolomite. The crystals have shapes suggestive of rhombs, but the edges of the crystals are irregular and replace adjacent detrital silicate grains. Tiny (1-20  $\mu\text{m}$  in diameter) yellow authigenic crystals of another carbonate unstained by alizarin red are very common in these and other samples from the Grandstand Formation and Killik Tongue; they appear to be siderite. These crystals are generally subhedral to euhedral and occur as single crystals scattered evenly through the rock or as equidimensional clusters as much as 250  $\mu\text{m}$  across. The single crystals occur along grain boundaries and pore walls, and, locally, replace quartz, chert, and phyllite; in deeper samples from the Grandstand Formation, they coat dolomite crystals. In sample No. 2925 siderite individuals smaller than 7  $\mu\text{m}$  in diameter are spherical and composed of radiating crystals.

Calcite occurs mainly as sparry anhedral to rhomb-shaped individuals (50-150  $\mu\text{m}$  in diameter) that may represent recrystallized detrital carbonate grains (fig. 26). The grains are composed of one crystal or as many as 15-20 small anhedral crystals. Many of the grains exhibit twinning. The twin lamellae are unbent, suggesting that recrystallization of the original carbonate occurred after compaction. Calcite is less common as large optically continuous (poikilotopic) crystals as much as 800  $\mu\text{m}$  across that slightly replace detrital silicates.

Both types of calcite are present in sample No. 2200, but the detrital variety is more abundant. With the exception of sample No. 3005, no carbonates were detected by X-ray

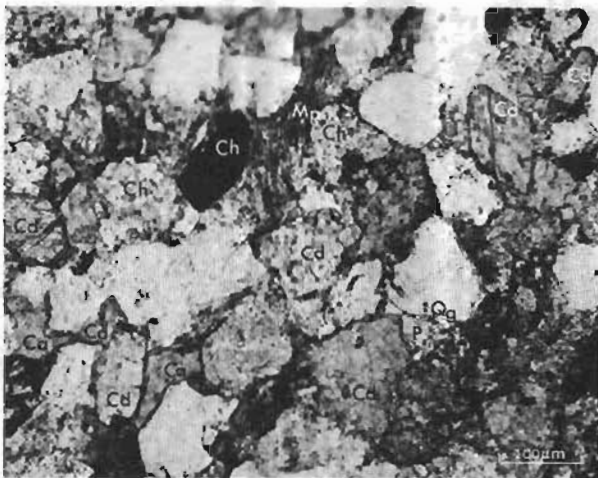


Figure 26.—Killik Tongue of the Chandler Formation, 670.6 m (2200 ft). Sparry anhedra to euhedral calcite crystals that may represent recrystallized detrital carbonate grains. Authigenic calcite fills intergranular pores and partially replaces detrital silicate grains in lower left-hand corner. Ca, authigenic calcite; Cd, recrystallized detrital calcite; Ch, chert; Mp, phyllite; Po, pore; Qg, quartz overgrowth. Photomicrograph, plane polarized light.

diffraction analysis, possibly due to their presence in very small amounts or their somewhat erratic distribution; sample No. 2200 was not analyzed.

#### Porosity

Porosity and permeability values are high for the Grandstand and Killik samples studied (table 2). Most porosity is primary and intergranular; secondary porosity due to leaching of feldspar grains is minor. Partial leaching of feldspar grains was noted in sample No. 2841. Visible pores (pores visible at magnifications to about 800x) have an average size of about 50  $\mu\text{m}$ . They are mainly triangular, equant, or crescent-shaped spaces between noncompressible grains such as quartz, feldspar, and chert. Many pore walls are formed of straight-edged quartz overgrowths, and these are generally free of phyllosilicate coatings. Less than 50 percent of the length of most other pore walls is coated with phyllosilicate coatings.

#### NINULUK FORMATION

The sandstone samples studied from the Ninuluk Formation are similar to those from the underlying Grandstand Formation and Killik Tongue in that they are mainly light gray,

very fine grained to fine-grained sandstones relatively poor in quartz and rich in chert and metamorphic rock fragments. Unlike those from the two lower units, however, they tend to be more poorly sorted, even bimodal; and they contain significantly more metamorphic rock fragments than chert fragments (figs. 15, 16). Fragments of metaquartzite are especially common, and are more abundant than phyllite in the deeper samples. The Ninuluk samples contain less detrital quartz than samples from the Grandstand and Killik, and the shallower samples contain a considerable amount of carbonate (table 2).

Grains in many of the samples are very tightly packed owing to the high content of metamorphic rock fragments (fig. 27). Sample No. 2110 contains laminae of fine sand and medium sand; and sample No. 2117, although unstratified, is bimodal fine and coarse sand.

#### Detrital Grains

With some exceptions the detrital components are petrographically identical to those of the underlying Grandstand Formation and Killik Tongue. Some phyllite fragments in sample Nos. 2080-2128 contain relatively large flakes of sericite (as large as 100  $\mu\text{m}$  in diameter); in addition, some contain biotite, and others contain clinozoisite(?). Free flakes of biotite in sample No. 2080 and in



Figure 27.—Ninuluk Formation, 637.9 m (2093 ft). Very tightly packed phyllarenite. Note abundant phyllite grains wedged between noncompressible detrital grains and lack of pores. Matrix in lower left corner may represent highly deformed phyllite grain(s) (pseudomatrix). Ch, chert; Mx, matrix; Mp, phyllite; Mq, metaquartzite; M, muscovite. Photomicrograph, plane polarized light.

stratigraphically higher samples are pleochroic pale yellow to dark reddish brown rather than light brown to dark brown.

#### Matrix

In thin section the matrix material in the Ninuluk is the same as that in the Grandstand and Killik. X-ray diffraction analysis, indicates the presence of illite, chlorite, and kaolinite, and the absence of smectite, in the fraction that is less than 2  $\mu\text{m}$ .

#### Authigenic Minerals

Authigenic cement in sandstones studied consists of calcite, quartz, siderite, and, possibly, chlorite. Quartz overgrowths are notably less abundant in the Ninuluk Formation than in the Grandstand Formation and Killik Tongue. A colorless overgrowth on feldspar was noted in sample No. 2068. Sparse, green, finely crystalline aggregates of chlorite may be authigenic.

As was the case in samples from the Grandstand and Killik, calcite in the Ninuluk Formation occurs mainly as anhedral to euhedral individuals that may be recrystallized detrital carbonate grains. These grains average 70-150  $\mu\text{m}$  in diameter and are generally composed of several to many anhedral sparry crystals that have an average size of 30-50  $\mu\text{m}$  in diameter (some average only 3-5  $\mu\text{m}$  in diameter). Many of the grains exhibit twinning. Much calcite, though, is definitely authigenic, especially in sample No. 2080. This calcite replaces detrital silicate and detrital calcite grains along grain boundaries.

Siderite crystals in sample No. 2068 occur in great numbers along the boundaries of detrital silicate grains and preferentially replace phyllite fragments. Locally they replace calcite. They do not occur on free surfaces of quartz overgrowths, but do occur along the contact between detrital quartz and quartz overgrowth.

X-ray diffraction analysis indicates considerable amounts of calcite and dolomite, and in four samples (Nos. 2049, 2068, 2080, 2093) a siderite reflection was tentatively identified. No mineral in thin section was positively identified as dolomite, even though the sections had been stained with alizarin red. Abundance of metamorphic rock fragments, chert, and detrital carbonate grains and the low content of quartz in the shallower samples suggest that the source rocks for these sandstones were dominantly limestone and low-grade metamorphic rocks. These were most probably pre-Cretaceous rocks that are present in the Brooks Range to the south (Brosge and Tailleux, 1971; Grybeck and others, 1977; Barrsch-Winkler, in Ahlbrandt, 1979).

#### Porosity

Porosity is mostly intergranular. Visible pores average about 35  $\mu\text{m}$  in size and are triangular, equant, or elongate intergranular spaces that have not been filled with matrix, deformed phyllite grains, or authigenic carbonate.

#### Colville Group

#### SEABEE FORMATION AND TULUVAK TONGUE OF THE PRINCE CREEK FORMATION

Except for sample No. 1824 which is similar to samples from the Ninuluk Formation, the samples from the Seabee Formation and Tuluvak Tongue of the Prince Creek Formation are light-gray, very fine grained to fine-grained sandstones characterized by an abundance of volcanic rock fragments, high content of detrital plagioclase feldspar, low content of detrital quartz, and generally abundant chloritic and smectitic matrix of authigenic origin (figs. 15, 16, 28). Calcite is abundant in some samples.

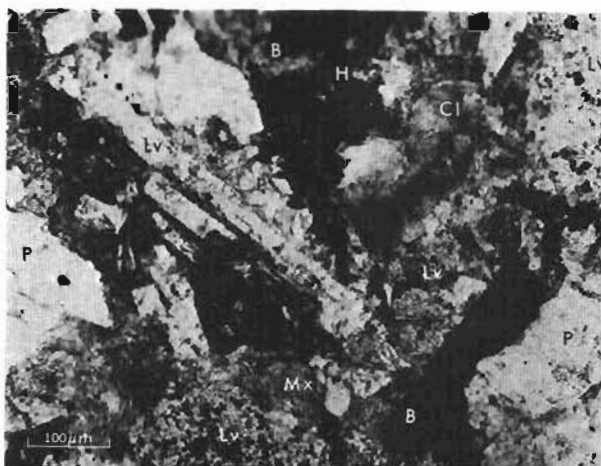


Figure 28.--Seabee Formation, 409.3 m (1343 ft). Tightly packed phyllarenite with authigenic chlorite matrix. Large volcanic rock fragment contains rather large plagioclase crystals and is somewhat atypical. Chlorite occurs as masses of intergrown flakes (lower center) and as radial growths that fill intergranular pores (upper right and in fig. 32). Note slightly deformed biotite flake at lower right. B, biotite; Cl, authigenic chlorite; P, plagioclase feldspar; H, hematite stain; Mx, matrix of chlorite; Lv, volcanic rock fragment. Photomicrograph, plane polarized light.

## Detrital Grains

Quartz, chert, phyllite, and metaquartzite all appear to be the same petrographically as in the Nanushuk Group. No grains of volcanic quartz were noted. Quartz is slightly more abundant and volcanic and metamorphic rock fragments are less abundant in the Tuluvak Tongue than in the Seabee Formation.

The dominant volcanic rock type is a quartz-free intermediate rock that has an extremely high content of plagioclase (fig. 29). Average composition of 20 randomly selected grains in sample No. 1343 is 94 percent plagioclase microlites, 5 percent chloritic material, and 1 percent opaque mineral. Mean size of the grains is 240  $\mu\text{m}$  in diameter and maximum is 500  $\mu\text{m}$ ; roundness of the grains is about equally divided between subangular, subrounded, and rounded. Plagioclase microlites are generally unaltered and have an average size of 16x60  $\mu\text{m}$ ; many, though, have a much more acicular habit. Extinction angle of albite twins of the microlites is  $0^\circ$ . The microlites have a random orientation in about two thirds of the grains and a subparallel orientation in the remainder. Untwinned, compositionally zoned blocky microlites in some grains take a slight sodium cobaltinitrite stain and may be alkalic feldspar. Very finely crystalline chloritic material occurs in the triangular and linear

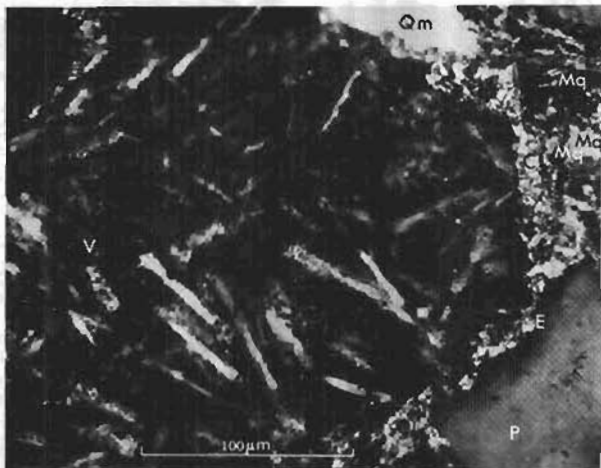


Figure 29.—Seabee Formation, 409.3 m (1343 ft). Typical volcanic rock fragment. At right edge of photograph, note authigenic chlorite matrix (masses of intergrown flakes) between volcanic rock fragment and other detrital grains. Surfaces of detrital grains are etched by chlorite. Cl, massive chlorite; E, etching; P, plagioclase feldspar; Mq, metaquartzite; Qm, monocrystalline quartz. Photomicrograph, crossed nicols.

interstices (average 15  $\mu\text{m}$  in length) between plagioclase microlites and appears to be highly altered aphanitic groundmass. Minute yellow pinpoints of sodium cobaltinitrite stain in the groundmass of some grains may indicate the presence of groundmass alkalic feldspar or, instead, may represent stained alteration products. No unaltered ferromagnesian minerals were noted, but rare, small, equant masses of chloritic material may represent highly altered pyroxene or amphibole microlites. In sample No. 1331 many grains are partially replaced by calcite, and in sample No. 514 the altered groundmass in most volcanic rock fragments appears to be smectitic rather than chloritic.

In addition to the volcanic rock fragments described above, grains of a somewhat different volcanic rock occur in trace amounts in sample Nos. 1328-1365. This rock (actually several different rock types may be represented) typically contains about 60 percent plagioclase microlites and 40 percent dark-yellow-brown to nearly opaque groundmass. The rock may only be a variant of the more abundant plagioclase-rich volcanic rock.

Most, if not all, of the plagioclase in the sandstones is of volcanic origin and may, in part, represent phenocrysts too large to appear in the sand-sized volcanic rock fragments. The plagioclase is generally unaltered, but some grains are highly sericitized, and in sample No. 1331 many grains are partially replaced by calcite. Most grains are angular to subangular and appear to be broken fragments. Albite twinning is common, and some grains are compositionally zoned. Maximum extinction angles measured on albite twins suggest that the plagioclase is andesine to sodic labradorite. Rectangular inclusions (15-25  $\mu\text{m}$ ) of unaltered brown glass were noted in a few grains. In samples rich in smectite, many of the plagioclase grains and some quartz grains are highly fractured and shattered (fig. 30). Rare grains have leached pores.

The alkalic feldspar, likewise, may be largely volcanic in origin. An optic angle of 15-30 $^\circ$  was measured on one alkalic feldspar in sample No. 771, but this grain also contained irregular patches of plagioclase. Other alkalic feldspar grains are also perthitic. Most grains are blocky and untwinned, although a few grains that have grid twinning were noted. Some grains are slightly altered, but most are fresh.

Biotite is pleochroic brown, but in some samples two varieties seem to be present: one, pleochroic pale yellow brown to very dark brown; and the other, medium orange brown to dark orange brown. In many samples biotite flakes (or possibly fragments of a biotite schist) are extremely altered and replaced by siderite and penninite. The siderite occurs as tiny (15  $\mu\text{m}$ ) crystals that have grown in



Figure 30.--Seabee Formation, 235.0 m (771 ft). Phyllarenite with authigenic smectite matrix. Note intergranular pore and smectite coatings on surfaces of detrital grains. Plagioclase (two grains?) in lower left corner is highly fractured and shattered; smectite coats some fractures, but not others, in the plagioclase. Ch, chert; P, plagioclase feldspar; Mx, matrix; Mq, metaquartzite; Po, pore; S, smectite. Photomicrograph, plane polarized light.

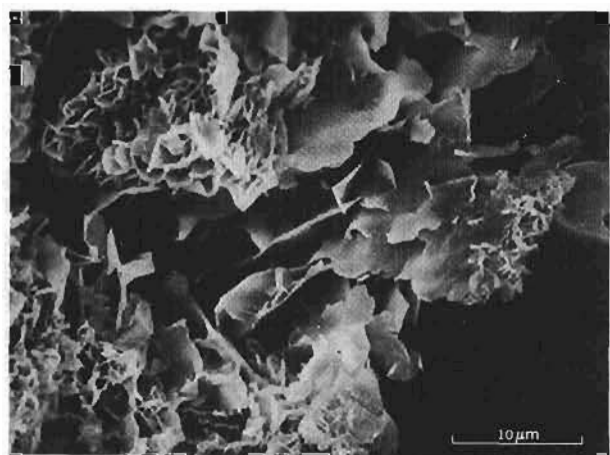


Figure 31.--Seabee Formation, 409.3 m (1343 ft). Mass of intergrown flakes of authigenic phyllosilicate, presumably chlorite, filling an intergranular pore. Note clusters of smaller flakes attached to larger flakes, suggesting two stages of chlorite growth. Scanning electron micrograph.

great profusion along biotite cleavage planes, completely shredding the biotite fragments. In samples rich in smectite, many biotite flakes exhibit kink folding.

#### Matrix and Authigenic Minerals

As seen in thin section, an authigenic phyllosilicate that has the optical properties of prochlorite makes up over half of the matrix in sample Nos. 1343-1365 and about one fourth of the matrix in sample No. 1328. The remainder of the matrix material in these samples appears to be mainly detrital sericite with possibly some authigenic illite. The prochlorite occurs as masses as much as 250  $\mu\text{m}$  across of intergrown flakes (as much as 30  $\mu\text{m}$  long) that fill intergranular spaces (figs. 28, 29, 31) and also as radial (fan-shaped) growths of flakes projecting from pore walls (fig. 32). Commonly, the chlorite etches adjacent detrital grains.

Much of the matrix in sample Nos. 118-771 is also authigenic, but the authigenic phyllosilicate in these samples has the optical properties of smectite rather than prochlorite and also occurs in a somewhat different manner. Much of the smectite, especially in the shallower samples, occurs as clumpy masses of intergrown flakes (flakes average 0.1-5  $\mu\text{m}$  in length) that fill intergranular pores or merge to form a continuous matrix in which detrital grains "float" (figs. 33, 34). No volcanic glass shards or relicts of altered glass shards were noted in the matrix. The smectite is also present, especially in the

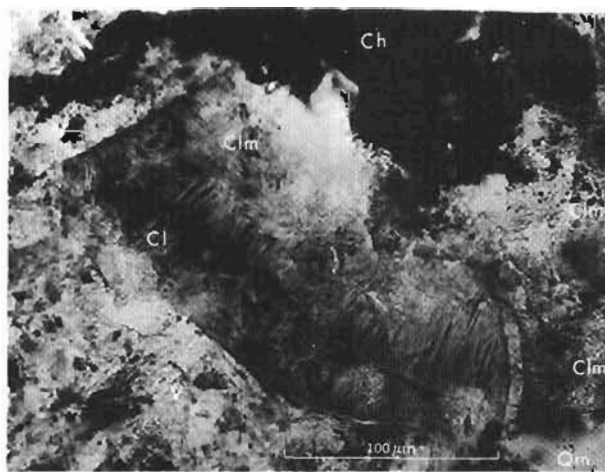


Figure 32.--Seabee Formation, 409.3 m (1343 ft). Chlorite-filled pore seen in figure 28. Note radial (fan-shaped) growths of flakes projecting into elongate intergranular pore. Flakes from opposite walls do not everywhere touch, leaving a long medial opening. At right edge chlorite occurs as a mass of intergrown flakes. Ch, hematite-stained chert; Clm, massive chlorite; Cl, chlorite; Qm, monocrystalline quartz; Lv, volcanic rock fragment. Photomicrograph, plane polarized light.



Figure 33.—Tuluwak Tongue of Prince Creek Formation, 156.7 m (514 ft). Phyllarenite with authigenic smectite matrix. Smectite occurs as clumpy masses that fill intergranular spaces and as continuous matrix between detrital grains. Note bifurcating and anastomosing fractures in matrix; also note variety of detrital grains. B, biotite; C, calcite; Ch, chert; F, feldspar; P, plagioclase feldspar; Mx, matrix; Mp, phyllite; Mq, metaquartzite; Qm, monocrystalline quartz; S, smectite matrix. Photomicrograph, plane polarized light.

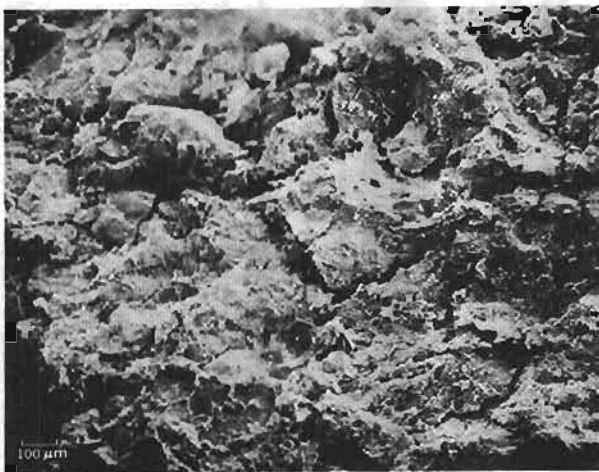


Figure 34.—Tuluwak Tongue of Prince Creek Formation, 156.7 m (514 ft). Dense masses and coatings of smectite with bifurcating and anastomosing fractures. Scanning electron micrograph.

deeper samples, as a discrete coating as much as 10 µm thick of overlapping flakes (as much as 15 µm long) on surfaces of detrital grains (figs. 30, 35) and, more rarely, as radial

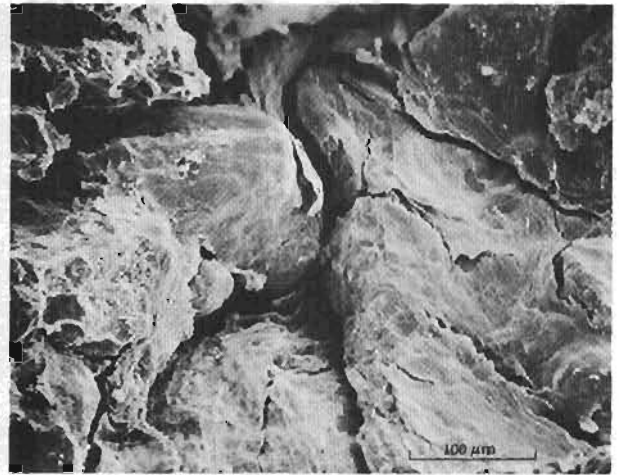


Figure 35.—Seabee Formation, 229.8 m (754 ft). Dense masses and coatings of smectite with bifurcating and anastomosing fractures. Note thick coating on rounded grain to left of center. Scanning electron micrograph.

growths of flakes (as much as 12 µm long) on intergranular pore walls (fig. 36). The coatings are present both on free surfaces of grains and on surfaces where grains are in contact. Etching of detrital silicate grains by the smectite is very common. Besides smectite, the matrix in sample Nos. 118-771 also contains some detrital and (or) authigenic(?) sericite, chlorite, and illite.

X-ray diffraction analysis indicates the presence of illite, chlorite, smectite, and kaolinite in the fraction that is less than 2 µm in size. Larger amounts of smectite are present in sample Nos. 118-771. Two samples in the Seabee Formation contain interstratified smectite-chlorite.

Calcite in samples containing only small amounts of calcite appears to be the same as the possibly detrital variety occurring in samples from the Nanushuk Group. In samples with relatively large amounts of calcite (Nos. 118, 545, 763, 1331), the calcite occurs mainly as irregular, optically continuous (poikilotopic) crystals (as large as 1 mm) that fill intergranular pores and replace detrital silicate grains along grain boundaries. Free surfaces of calcite crystals that partially fill pores are coated with smectite in some samples. X-ray diffraction analysis indicates small amounts of calcite and dolomite.

#### Porosity

Intergranular spaces in sample Nos. 134-1365 are completely plugged with the authigenic prochlorite, and no visible pores were noted in these samples; similarly, no visible pores are present in sample No. 1331 owing to complete

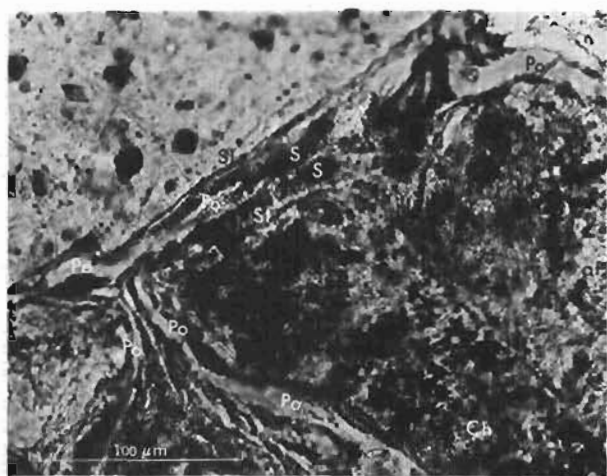


Figure 36.--Seabee Formation, 229.8 m (754 ft). Smectite coatings on detrital grains. To left of center, the sequence of coatings includes inner layered coating next to chert grain, outer radial coating, medial pore, outer radial coating, inner layered coating, and feldspar grain. At lower left a layered coating has pulled away from adjoining grains. Ch, chert; aF, altered feldspar; Po, pore; S, smectite; Sl, layered smectite. Photomicrograph, plane polarized light.

cementation by calcite. Authigenic prochlorite is less abundant in sample No. 1328, and visible pores in this sample are the result of incomplete filling of intergranular spaces by prochlorite. Many visible pores in sample Nos. 118-771 are normal intergranular spaces incompletely filled by matrix material, but a large number of the open spaces seen in thin section are unusual bifurcating and anastomosing fractures as much as 30  $\mu$ m wide and 400  $\mu$ m long that cut through and split the clumpy smectitic matrix (figs. 33-35). These fractures appear to have been caused by a swelling or a "pulling apart" of the rock. The fracturing was probably caused by swelling and shrinking of the smectite due to wetting and drying, but freeze and thaw of ice crystals may have been a contributing factor, also. The questions of when the fracturing occurred and whether or not the fracturing actually exists in the subsurface are moot ones. It is conceivable that the swelling and shrinking of the smectite were not caused by natural processes, but rather were caused by man-related processes such as drilling or sample preparation. The shattered plagioclase grains and kink-folded biotite flakes common in the smectite-rich samples suggest that expansion (and presumably contraction) has occurred at least once under conditions of considerable confining pressure, but whether or not the cracks in the smectite

matrix occurred during the same episode is not known.

#### FACTORS AFFECTING POROSITY AND PERMEABILITY

Several factors were identified petrographically as having effects on porosity and permeability. First of all there seems to be no discernible relationship between compaction, as influenced by depth of burial, and porosity and permeability. In fact, deeper samples from Umiat test well 11 are just as porous and actually more permeable than shallower samples owing to abundant intergranular porosity in the deeper samples and abundant matrix in the shallower samples (figs. 37, 38). Modal grain size appears to be a minor factor in its effect on porosity and permeability. In all formations, porosity and permeability tend to increase with increasing modal grain size (figs. 39, 40). In general, a minimum grain size of about 175  $\mu$ m appears to be necessary for good (>50 md) permeability.

Composition of the rock has a major

#### EXPLANATION

- + Tuluvak Tongue of Prince Creek Formation
- Seabee Formation
- ▲ Ninuluk Formation
- ◊ Killik Tongue of Chandler Formation
- △ Grandstand Formation

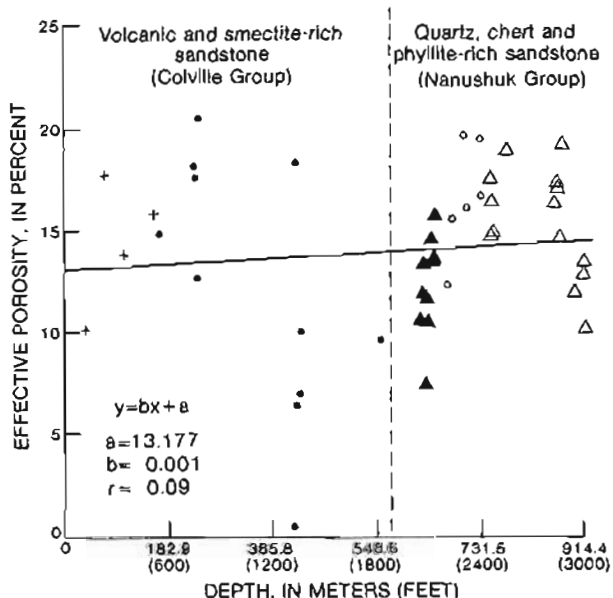


Figure 37.--Effective porosity versus depth. The solid line is the line defined by linear-regression analysis on all the data points. The equation of the solid line and the values of a, b, and r (correlation coefficient) are shown on the graph.

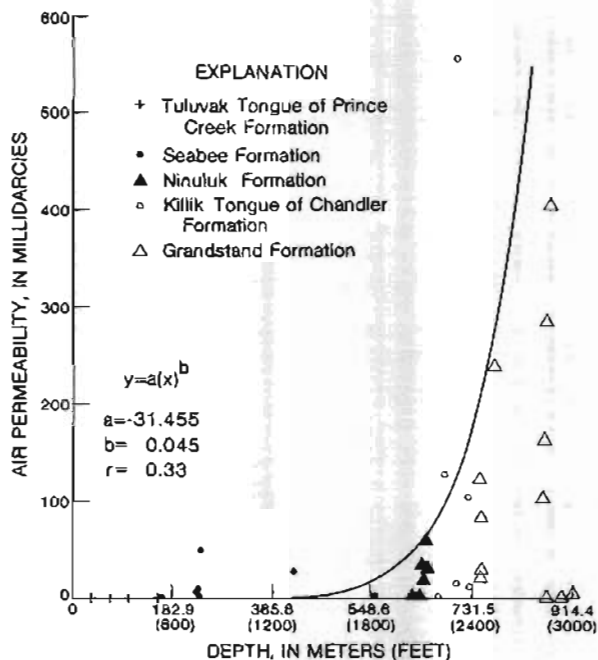


Figure 38.--Air permeability versus depth. The solid line is the least-squares fit to a power equation for all the data points. The least-squares program was modified to calculate data points equal to zero. The equation of the solid line and the values of a, b, and r (correlation coefficient) are shown on the graph.

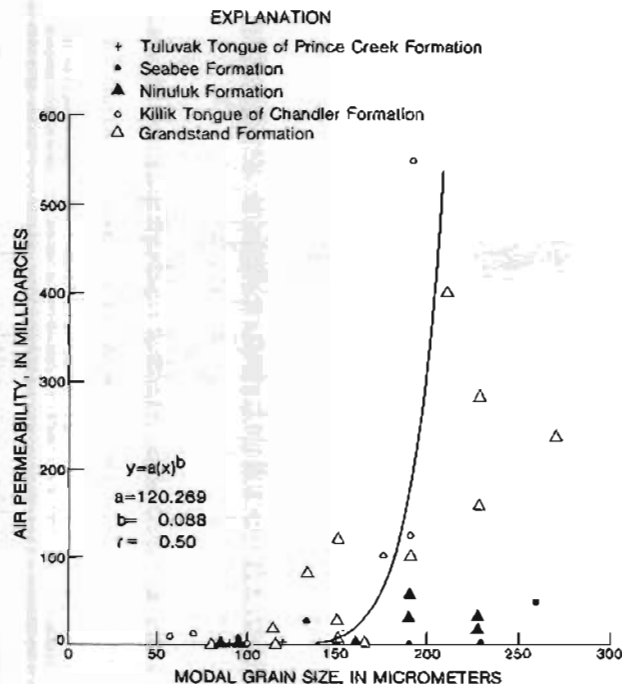


Figure 40.--Air permeability versus modal grain size. The solid line is the least-squares fit to a power equation for all the data points. The least-squares program was modified to calculate data points equal to zero. The equation of the solid line and the values of a, b, and r (correlation coefficient) are shown on the graph.

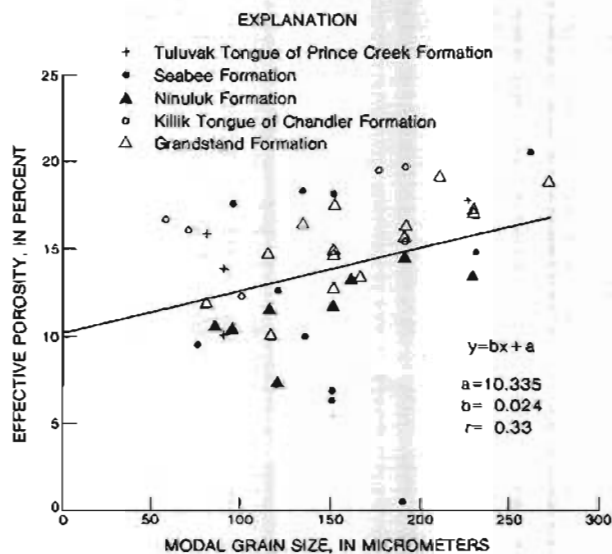


Figure 39.--Effective porosity versus modal grain size. The solid line is the line defined by linear-regression analysis on all the data points. The equation of the solid line and the values of a, b, and r (correlation coefficient) are shown on the graph.

effect on porosity and permeability. The relationship between permeability and composition is shown on figures 41 and 42. Samples classed as sedimentary litharenite generally have greater permeability than those classed as volcanic litharenite or phyllarenite. As can be seen in figures 43 and 44, rocks that have a high content of compressible grains (phyllite, schist, mica, and, rarely, chert and micaceous metaquartzite) generally have low porosity and permeability values. Similarly, rocks that have a high matrix content or carbonate cement also generally have low porosity and permeability values (figs. 45, 46). It is also apparent in figures 43-46 that an increase in the amount of compressible grains or matrix has a much greater effect on permeability than on porosity.

Other factors specifically affecting permeability, as pointed out by Krynine and Fern (1952), include the modal size of visible pores and the percent of pore wall coated by phyllosilicate. A decrease in the former or an increase in the latter will cause a decrease in permeability. Estimated values for these parameters are given in table 2 for each sample.

Some of the specific petrographic factors





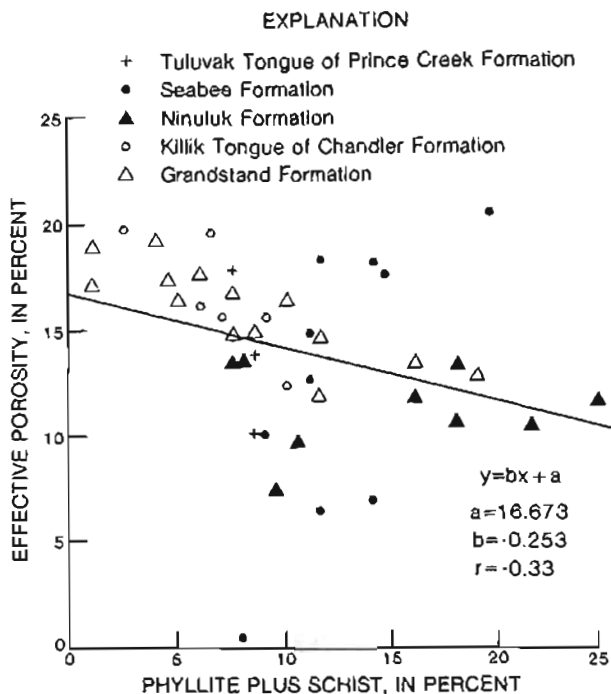


Figure 43.—Effective porosity versus percent phyllite plus schist. The solid line is the line defined by linear-regression analysis on all the data points. The equation of the solid line and the values of a, b, and r (correlation coefficient) are shown on the graph.

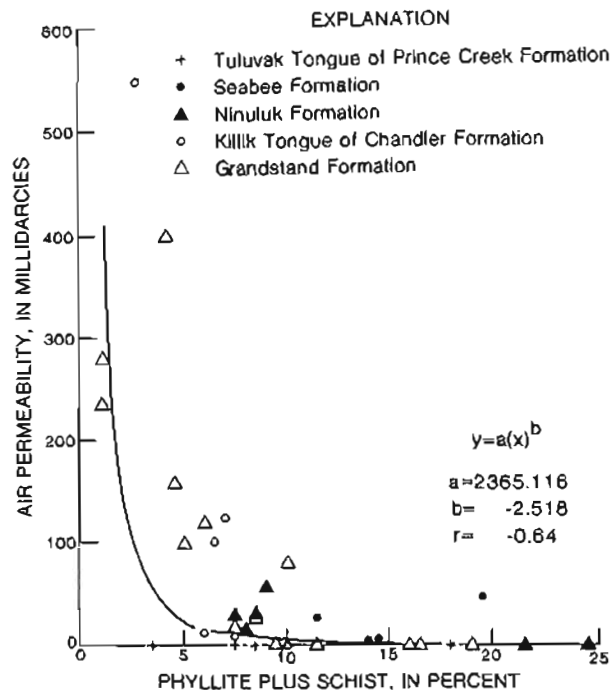


Figure 44.—Air permeability versus percent phyllite plus schist. The solid line is the least-squares fit to a power equation for all the data points. The equation of the solid line and the values of a, b, and r (correlation coefficient) are shown on the graph.

air permeability of most sandstone units of each formation (table 3).

Well logs available for the analysis included spontaneous potential (SP); 16-in. short normal (SN); 64-in. long normal (LN) (from 33-1003 m); Microlog (ML) (2-in. normal and 1½-in. inverse, from 33-1003 m); Lateral (from 52-448 m); and temperature survey (from 0-104 m). Except for the SP log in the permafrost zone (0-229 m), the log quality was fairly good.

The porosity of sandstone beds in the Grandstand Formation was estimated from the well-log-analysis methods using combinations of SN and SP, and ML and SP. Both gave rather inconsistent results compared to previously reported core-analysis values (Collins, 1958). However, plots of core porosity vs. the resistivity of 16-in. short normal ( $R_{16}''$ ) or the resistivity of 64-in. long normal ( $R_{64}''$ ) and plots of log air permeability ( $K_a$ ) vs. core porosity showed rather consistent linear relationships. Thus, such correlations were used to determine the porosity of sand members when core data were not available.

Formation-water resistivity was estimated from formation-water analysis and well-log analysis. This formation-water resistivity

was used in the estimation of water saturation in the Grandstand Formation.

#### Average Porosity of Each Formation

*Correlation between core porosity and normal-log resistivities.*—Plots of core porosity and normal-log resistivities were made to determine any consistent relationships between them for the purpose of estimating porosity of the sand intervals for which core data were not available.

Only the better developed sands (less shaly) that were greater than 3 m in thickness were selected. Two intervals were analyzed separately: 0-235 m (within the permafrost zone) and 610-917 m.

Figures 47 through 50 show the correlation between core porosity and normal-log resistivity. A roughly linear relationship exists between the core porosity and the normal-log resistivity:

1. The  $R_{64}''$  ranges from 10 to 90 ohm-m in the permafrost zone and from 40 to 80 ohm-m in the deeper zone. The slope of the correlation is much lower in the permafrost zone.

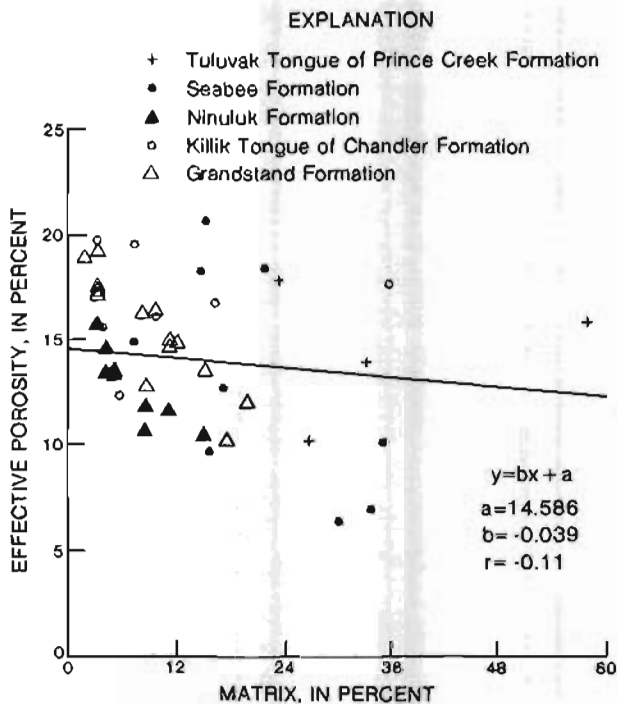


Figure 45.--Effective porosity versus percent matrix. The solid line is the line defined by linear-regression analysis on all the data points. The equation of the solid line and the values of a, b, and r (correlation coefficient) are shown on the graph.

2. The  $R_{16''}$  ranges from 15 to 45 ohm-m in the permafrost zone and from 40 to 60 ohm-m in the deeper zone. Again the slope of the correlation is much lower in the permafrost zone.

Lines shown on figures 47 through 50 are fit to the data using the least-squares method. The correlations were used to estimate the porosity of the uncored intervals (table 4). The significance of the linear relationships and the lower slope of correlation for the permafrost zone have not been investigated.

*Average porosity of each formation.*--The weighted average porosity of the formations penetrated by Umiat test well 11 are tabulated in table 4; they are averages of core porosity and porosity obtained from the aforementioned correlation method. Only the better developed sandstone beds (thickness greater than 3 m picked from SP and ML) are included in computing the average porosity. The weighted average porosity is 14.6 percent for the Tuluvak Tongue, 11.5 percent for the Seabee Formation, 12.6 percent for the Ninuluk Formation, 16.4 percent for the Kilik Tongue, 15.6 percent for the upper part of the Grandstand Formation, and 15.1 percent for the lower part of the Grandstand Formation.

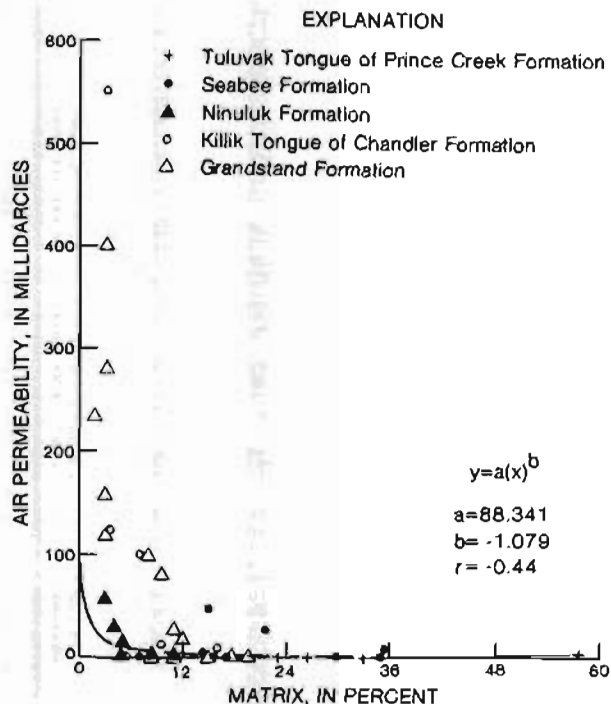


Figure 46.--Air permeability versus percent matrix. The solid line is the least-squares fit to a power equation for all the data points. The equation of the solid line and the values of a, b, and r (correlation coefficient) are shown on the graph.

*Porosity from well-log analysis.*--The porosity of Grandstand Formation sandstone was estimated by well-log analysis. The porosity was obtained by two analysis methods: one using SN and SP, and the other using ML and SP. The porosity obtained from SN and SP is consistently higher than the core-analysis porosity. The porosity obtained from ML and SP does fall in the range of core porosity, however (fig. 51). The unsatisfactory scattering of the comparison data indicates inconsistency in either the well-log-analysis porosity or the core-analysis porosity.

If core-analysis porosity is assumed to be accurate, the average porosity of the formation can be obtained from core-analysis data and, where cores are not available, from the correlation of core porosity and  $R_{64''}$ .

#### Average Permeability of Each Formation

*Correlation between core porosity and air permeability.*--Espach (1951) showed that, for Umiat test wells 2 and 3, a log  $K_a$  vs. core porosity plot results in a linear relationship. A similar core permeability and porosity plot was made for Umiat test well 11. Data used in this plot are shown in table 5 and the resulting plot, in figure 52. In figure 52, samples A,

Table 3.--Core-analysis and well-log data

[Leaders (—) indicates no data;  $R_{64}''$ , resistivity of 64-in. long normal;  $R_{16}''$ , resistivity of 16-in. short normal]

Depth (meters)	Air permeability (md)	Effective core porosity (percent)	Average effective porosity <sup>1</sup> (percent)	$R_{64}''$ (ohm-m)	$R_{16}''$ (ohm-m)
Tulvak Tongue of the Prince Creek Formation					
36.0	—	10.2	11.7	90	35
39.0	<1	13.1	11.7	90	35
42.7	6.2	15.4	15.4	45	17
71.0	<1	17.9	14.8	35	18
74.1	0	11.8	14.8	35	18
100.9	0	13.9	13.9	86	45
156.2	0	15.9	16.4	35	30
158.2	—	16.8	16.4	35	30
160.3	26	18.0	16.4	35	30
Seabee Formation					
166.1	<1	14.9	16.4	35	30
227.4	5.1	18.1	18.0	23	16
229.8	7.0	17.7	18.0	23	16
232.6	0	12.7	16.7	15	10
235.0	48	20.6	16.7	15	10
404.8	27	18.4	8.5	35	30
407.7	0	.6	8.5	35	30
409.4	0	6.5	8.5	35	30
413.9	0	7.0	8.6	36	33
416.1	0	10.1	8.6	36	33
556.0	0	9.7	9.7	50	35
Ninuluk Formation					
624.5	0	10.6	11.3	75	60
627.9	0	11.8	11.3	75	60
632.5	0	13.1	11.3	75	60
638.0	0	10.4	11.3	75	60
643.1	29	14.5	14.5	55	50
646.2	28	13.4	14.5	55	50
652.0	51	15.5	15.5	55	50
Kililik Tongue of the Chandler Formation					
670.6	0	12.4	12.4	80	55
700.4	550	19.8	18.0	55	46
702.6	13	16.2	18.0	55	46
724.8	102	19.6	18.2	53	46
727.3	10	16.8	18.2	53	44
Grandstand Formation (upper part)					
745.2	120	17.6	16.5	60	50
746.8	81	16.5	16.5	60	50
749.8	27	15.0	16.5	60	50
771.6	235	19.0	19.0	40	40
Grandstand Formation (lower part)					
857.4	100	16.4	16.9	45	50
860.8	158	17.4	16.9	45	50
863.2	280	17.1	17.1	35	40
865.9	—	14.7	17.0	40	42
868.4	400	19.3	17.0	40	42
911.4	<1	13.5	12.2	50	53
935.5	2.3	12.9	12.2	56	55
935.9	0	10.2	12.2	56	55

<sup>1</sup>Two or more consecutive equal values are the average effective porosity of the interval.

B, and C are excluded owing to their abnormally low permeabilities in contrast to their high porosities (depth between 702-730 m).

The correlation indicates a linear relationship between the permeability and the porosity for (1) rocks having depths less than 405 m, and (2) rocks having depths greater than 644 m, excluding data points A, B, and C on figure 52 (lower sandstones in Kililik Tongue).

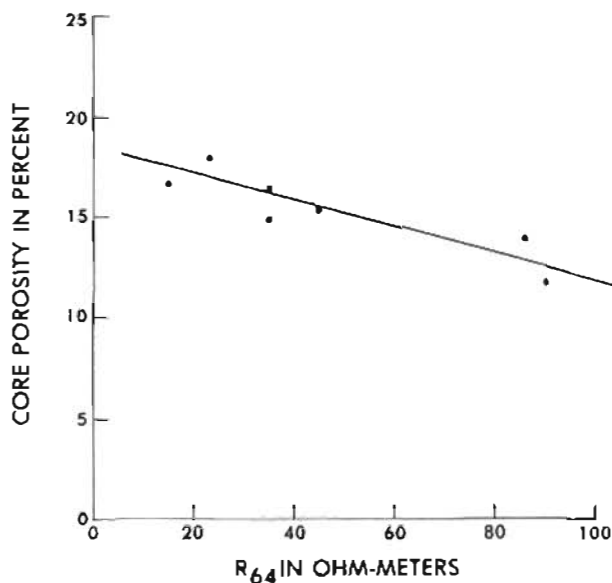


Figure 47.--Correlation of core porosity and  $R_{64}''$  for beds stratigraphically above 610 m (2000 ft) (in the permafrost zone).

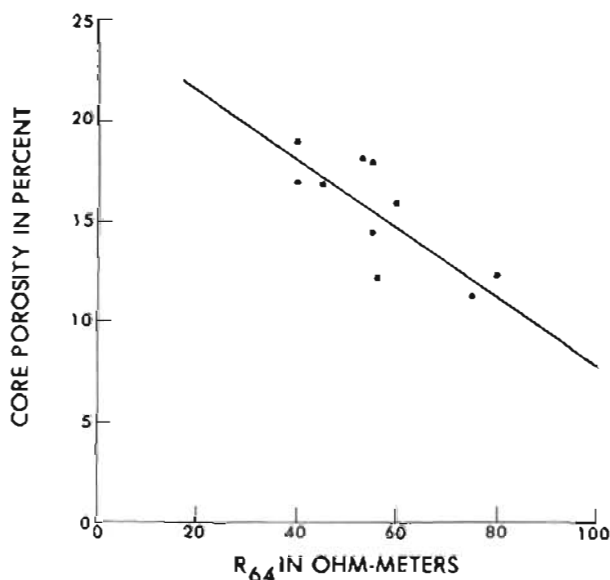


Figure 48.--Correlation of core porosity and  $R_{64}''$  for beds stratigraphically below 610 m (2000 ft) (below the permafrost zone).

These plots also indicate that permeability at depths less than 405 m will be less than 1 md if the porosity is less than 11.5 percent and that the permeability at depths greater than 644 m will be less than 1 md if the porosity is less than 9 percent.

On the basis of these correlations, it appears that an average permeability can be

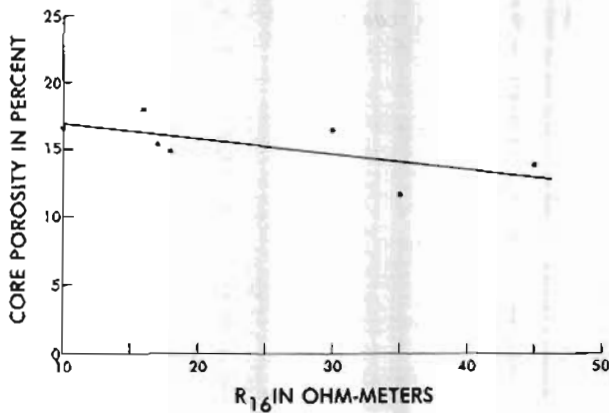


Figure 49.—Correlation of core porosity and  $R_{16}$  for beds stratigraphically above 610 m (2000 ft) (in the permafrost zone).

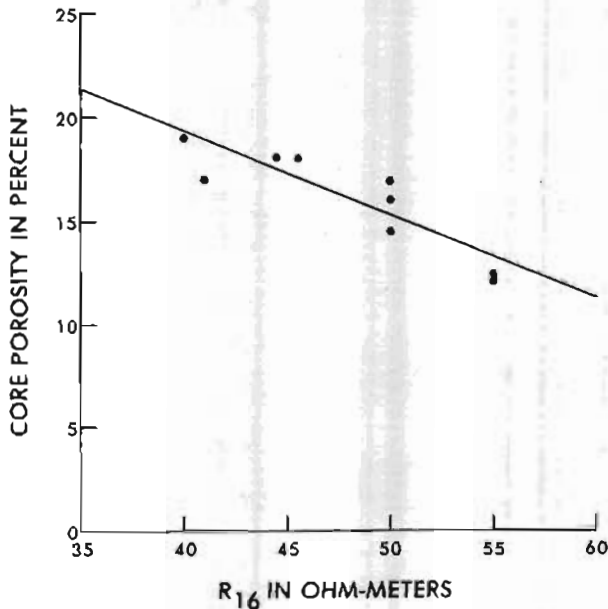


Figure 50.—Correlation of core porosity and  $R_{16}$  for beds stratigraphically below 610 m (2000 ft) (below the permafrost zone).

estimated with reasonable accuracy for the Tuluva Tongue, the Seabee Formation, the Killik Tongue, and the Grandstand Formation.

*Average permeability of each formation.*-- The average permeability of each sandstone is obtained from the permeability vs. core porosity correlations. The weighted average permeability is calculated for each formation and tabulated in table 6. The weighted average permeability for the Tuluva is 3.9 md; Seabee, 3.1 md; Ninuluk, 10.7 md; Killik 96.2 md; upper part

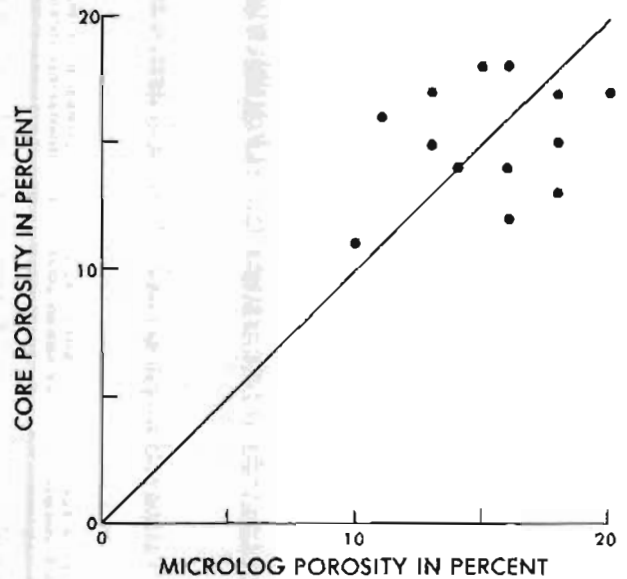


Figure 51.—Correlation of core and microlog porosities.

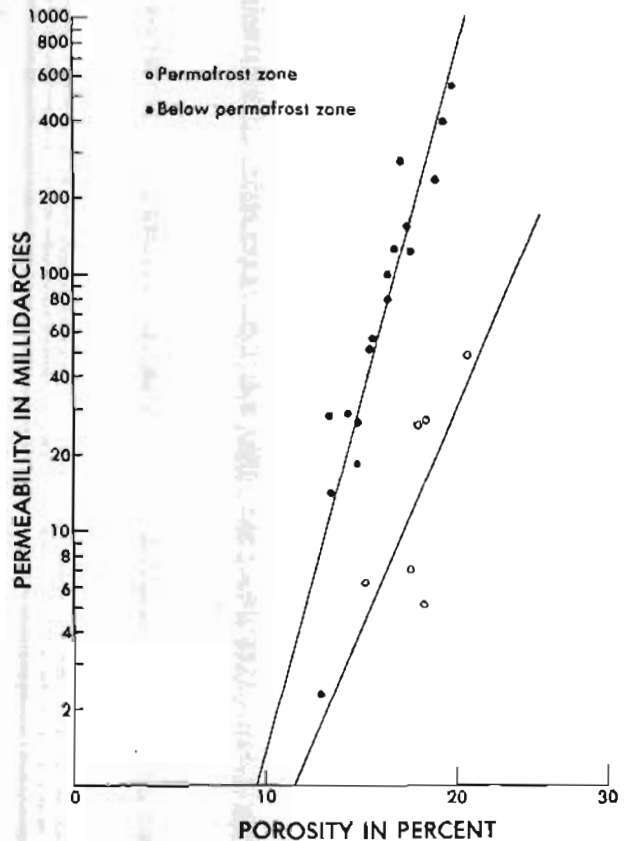


Figure 52.—Correlation of core permeability and porosity.

Table 4.--Weighted average porosity, Umiat test well 11  
[Leaders (---) indicate no value]

Interval m	Thickness h m (ft)		Arithmetic average porosity $\phi$ (percent)	Cumulative thickness $\Sigma h$ m (ft)		Storage capacity h(ft) x $\phi$	Cumulative storage capacity $\Sigma h$ (ft) x $\phi$	Formation average porosity = $\frac{\Sigma h \phi}{\Sigma h}$
Tuluvak Tongue of the Prince Creek Formation								
30.5-44.2	13.7	(45)	12.9	13.7	(45)	580.5	580.5	---
67.1-76.2	9.1	(30)	14.8	22.9	(75)	444.0	1,024.5	---
97.5-103.6	6.1	(20)	13.9	29.0	(85)	278.0	1,302.5	---
123.4-128.0	4.6	(15)	<sup>1</sup> 14.2	33.5	(110)	213.0	1,515.5	---
155.5-166.1	10.6	(35)	16.4	44.2	(145)	574.0	2,089.5	---
176.8-179.8	3.0	(10)	<sup>1</sup> 17.0	47.2	(155)	170.0	2,259.5	14.6
Seabee Formation								
224.0-236.2	12.2	(40)	17.3	12.2	(40)	692.0	692.0	---
400.8-417.6	16.8	(55)	8.5	29.0	(95)	467.5	1,159.5	---
551.7-562.4	10.7	(35)	9.7	39.6	(130)	339.5	1,499.0	11.5
Ninuluk Formation								
623.3-638.6	15.2	(50)	11.3	15.2	(50)	565.0	565.0	---
641.6-652.3	10.7	(35)	14.5	25.9	(85)	507.5	1,072.5	12.6
Killik Tongue of the Chandler Formation								
669.0-675.1	6.1	(20)	12.5	6.1	(20)	250.0	250.0	---
698.0-704.1	6.1	(20)	18.0	12.2	(40)	360.0	610.0	---
722.4-730.0	7.6	(25)	18.2	19.8	(65)	455.0	1,065.0	16.4
Grandstand Formation (upper part)								
743.7-749.8	6.1	(20)	16.0	6.1	(20)	320.0	320.0	---
751.3-757.4	6.1	(20)	11.0	12.2	(40)	220.0	540.0	---
768.1-775.7	7.6	(25)	19.0	19.8	(65)	475.0	1,015.0	15.6
Grandstand Formation (lower part)								
855.0-861.1	6.1	(20)	16.9	6.1	(20)	338.0	338.0	---
862.6-876.3	13.7	(45)	17.0	19.8	(65)	765.0	1,103.0	---
876.3-883.9	7.6	(25)	<sup>1</sup> 14.6	27.4	(90)	365.0	1,468.0	---
905.3-917.5	12.2	(40)	12.2	45.7	(150)	732.0	2,200.0	---
923.5-938.8	15.3	(50)	<sup>1</sup> 16.5	61.0	(200)	825.0	3,025.0	---

<sup>1</sup>Obtained from core-analysis porosity vs.  $R_{64}$  correlation.

of the Grandstand, 167.0 md; and lower part of the Grandstand, 58.6 md.

#### Formation-Water Resistivity

From formation-water analysis.--  
Formation-water analysis is available for water samples taken from Formation Test No. 8 (724-735 m), No. 9 (746-751 m), and No. 11

(864-869 m). The total equivalent sodium chloride concentration of these waters was calculated to determine the formation-water resistivities (tables 7-9). The formation-water resistivity ranges from 1.6 to 1.8 ohm-m at temperatures from 13 to 17°C.

From well-log analysis.--Three well-log analysis methods were used to estimate the formation-water resistivity. These methods

Table 5.--Core permeability and porosity data

Depth (meters)	Air permeability (md)	Core porosity (percent)
Tuluwak Tongue of the Prince Creek Formation		
42.7	6.2	15.4
160.3	26.0	18.0
227.4	5.1	18.3
229.8	7.0	17.7
235.0	48.0	20.6
Seabee Formation		
404.3	27.0	18.4
Ninuluk Formation		
640.1	29.0	14.5
645.3	14.0	13.5
646.2	28.0	13.4
648.6	56.0	15.7
652.0	51.0	15.5
Killik Tongue of the Chandler Formation		
681.2	125.0	16.7
700.4	550.0	19.8
702.6	13.0	16.2
724.8	102.0	19.6
727.3	10.0	16.8
Grandstand Formation (upper part)		
745.2	120.0	17.6
746.8	81.0	16.5
747.7	18.0	14.8
749.8	27.0	15.0
771.6	235.0	19.0
Grandstand Formation (lower part)		
857.4	100.0	16.4
860.8	158.0	17.4
863.2	280.0	17.1
868.4	400.0	19.3
913.5	2.3	12.9

include (1) using SP and  $R_{16}''$ , (2) using  $R_{16}''$  and  $R_{64}''$ , and (3) using core porosity and  $R_{64}''$ .

Results of these analyses are shown in tables 10-12. As shown, the formation-water resistivity ranges from 0.65 to 0.90 ohm-m for method (1), is 2.3 ohm-m for method (2), and is 1.03 ohm-m for method (3). The average formation-water resistivity as determined from these three methods is 1.33 ohm-m.

**Water saturation by Ri and Tixier methods.**--Both Ri and Tixier methods were used to evaluate the water saturation in the sandstones deeper than 723 m (lower part of the Killik Tongue and Grandstand Formation). The Ri method gives 100 percent water saturation (SW) for all the zones analyzed and the Tixier method gives SW ranging from 65 to 80 percent. All of these saturation values indicate nonproductive water-bearing zones at Umiat test well 11.

Results of Porosity and Permeability Analyses

The weighted average porosity for the Tuluwak Tongue is 14.6 percent; Seabee Formation, 11.5 percent; Ninuluk Formation, 12.6 percent; Killik Tongue, 16.4 percent; upper part of the Grandstand Formation, 15.6

Table 6.--Weighted average permeability [Leaders (---) indicate no value; av. perm., average permeability]

Depth m	Thickness m (ft)	Average porosity (%) (percent)	Average permeability (md)	Formation weighted av. perm. (md)
Tuluwak Tongue of the Prince Creek Formation				
30.5-44.2	13.7 (45)	12.9	1.7	---
67.1-76.2	9.1 (30)	14.8	3.2	---
97.5-103.6	6.1 (20)	13.9	2.5	---
123.4-128.0	4.6 (15)	14.2	3.0	---
155.5-166.1	10.6 (35)	16.4	7.1	---
176.8-179.8	3.0 (10)	17.0	9.0	---
3.9				
Seabee Formation				
224.0-236.2	12.2 (40)	17.3	10.0	---
400.8-417.6	16.8 (55)	8.5	0	---
551.7-562.4	10.7 (35)	9.7	0	---
3.1				
Ninuluk Formation				
623.3-636.2	15.3 (50)	11.3	2.8	---
641.6-652.3	10.7 (35)	14.5	22.0	---
10.7				
Killik Tongue of the Chandler Formation				
669.0-675.1	6.1 (20)	12.5	5.0	---
698.0-704.1	6.1 (20)	18.0	210.0	---
722.4-730.0	7.6 (25)	18.2	241.7	---
96.2				
Grandstand Formation (upper part)				
748.7-749.8	6.1 (20)	16.0	59.0	---
751.3-757.4	6.1 (20)	11.0	2.5	---
768.1-775.7	7.6 (25)	19.0	385.0	---
167.0				
Grandstand Formation (lower part)				
855.0-861.1	6.1 (20)	16.9	70.0	---
862.6-876.3	13.7 (45)	17.0	180.0	---
786.3-883.9	7.6 (25)	14.6	23.0	---
905.3-917.5	12.2 (40)	12.2	5.2	---
923.5-938.8	15.3 (50)	16.5	70.0	---
58.6				

<sup>1</sup>From core porosity vs.  $R_{64}''$  correlation.  
<sup>2</sup>Average of core permeabilities.

Table 7.--Water analysis and formation-water resistivity from 724-725 meters

Ionic constituents	Concentration (ppm)	Conversion factor	Equivalent NaCl conc. (ppm)
Ca <sup>++</sup>	30	0.95	28.9
Mg <sup>++</sup>	9	2.00	18.0
Na	2,190	1.00	2,190.0
CO <sub>3</sub>	96	1.26	120.9
HCO <sub>3</sub>	2,960	.27	799.2
SO <sub>4</sub>	21	.50	10.5
Cl	1,600	1.00	1,600.0
Total <sup>1</sup>			4,767.1

<sup>1</sup>The formation-water resistivity for 4,767.1 ppm NaCl equivalent solution is 1.6 ohm-m at an estimated formation temperature of 13°C.

Table 8.--Water analysis and formation-water resistivity from 746-751 meters

Ionic constituents	Concentration (ppm)	Conversion factor	Equivalent NaCl conc. (ppm)
Ca <sup>+</sup>	8	0.95	7.6
Mg <sup>+</sup>	3	2.00	6.0
Na	2,030	1.00	2,030.0
CO <sub>3</sub> <sup>-</sup>	390	1.26	491.4
HCO <sub>3</sub> <sup>-</sup>	3,120	.27	842.2
SO <sub>4</sub> <sup>-</sup>	28	.50	14.0
Cl <sup>-</sup>	865	1.00	865.0
		Total <sup>1</sup>	4,256.4

<sup>1</sup>The formation-water resistivity for 4,256.4 ppm NaCl equivalent solution is 1.8 ohm-m at an estimated formation temperature of 13°C.

Table 9.--Water analysis and formation-water resistivity from 864-869 meters

Ionic constituents	Concentration (ppm)	Conversion factor	Equivalent NaCl conc. (ppm)
Ca <sup>+</sup>	14	0.95	13.3
Mg <sup>+</sup>	4	2.00	8.0
Na	2,190	1.00	2,190.0
CO <sub>3</sub> <sup>-</sup>	126	1.26	158.8
HCO <sub>3</sub> <sup>-</sup>	2,240	.27	604.8
SO <sub>4</sub> <sup>-</sup>	19	.50	9.5
Cl <sup>-</sup>	1,950	1.00	1,950.0
		Total <sup>1</sup>	4,934.4

<sup>1</sup>The formation-water resistivity for 4,934.4 ppm NaCl equivalent solution is 1.6 ohm-m at an estimated formation temperature of 13°C.

Table 10.--Formation-water resistivity from well-log analyses using SP and R<sub>16"</sub>

Interval (in meters)	SP (-mv)	R <sub>16"</sub> (ohm-m)	T <sub>p</sub> percent	R <sub>m</sub> (ohm-m)	R <sub>mf</sub> (ohm-m)	R <sub>w</sub> (ohm-m)
723-730	40	45	55	3.6	2.6	0.90
744-750	45	50	56	3.6	2.6	.65
863-877	48	43	62	3.6	2.8	.68

Table 11.--Formation-water resistivity from well-log analyses using R<sub>16"</sub> and R<sub>64"</sub>

Interval (meters)	R <sub>16"</sub> (ohm-m)	R <sub>64"</sub> (ohm-m)	$\frac{R_{16''}}{R_{64''}}$
723-730	45	52	0.87
744-750	50	58	.83
752-758	68	90	.75
836-862	50	45	1.11
843-877	45	40	1.13
914-932	43	40	1.08

Maximum  $\frac{R_{16''}}{R_{64''}} = 1.13 = \frac{R_{mf}}{R_w} = \frac{2.6}{2.3} = 1.13$

Table 12.--Formation-water resistivity from well-log analyses using core porosity and R<sub>c</sub> method

Interval (meters)	Core porosity (percent)	P = $\phi^{-2}$	R <sub>w</sub> <sup>1</sup> = $\frac{R_c}{P}$
723-730	18.2	30	1.73
744-750	16.0	39	1.49
752-758	11.0	83	1.68
836-862	16.9	36	1.25
863-877	17.0	35	1.60
924-932	16.6	39	1.03

<sup>1</sup>Minimum R<sub>w</sub> = P<sub>w</sub> = 1.03 ohm-m.

percent; and lower part of the Grandstand Formation, 15.1 percent. The weighted average permeability (air) for the Tuluva Tongue is 3.9 md; Seabee Formation, 3.1 md; Ninuluk Formation, 10.7 md; Killik Tongue, 96.2 md; upper part of the Grandstand Formation, 167.0 md; and lower part of the Grandstand Formation, 58.6 md. The formation water is rather fresh, about 5,000 ppm dissolved solids, with formation-water resistivity of 1.6 ohm-m at 13°C. At Umiat test well 11, the sandstones in the Killik Tongue and Grandstand Formation are non productive water-bearing rocks.

### SUMMARY

Cretaceous sandstones in the Umiat Anticline contain the largest volume of oil discovered to date in NPRA. Umiat test well 11, although dry and abandoned, penetrated the most complete sequence of Cretaceous rocks in the Umiat area. Each of the formations penetrated by the well was studied to identify the factors influencing porosity and permeability. Selected cores and core samples were studied to determine environments of deposition and sedimentary petrology, and electric logs were examined to determine porosity and permeability of uncored zones and to determine whether water saturation could be estimated.

The Grandstand Formation and Killik Tongue of the Chandler Formation at Umiat contain numerous sandstone beds deposited in a shallow, near-shore-marine prograding environment (delta-front sediments deposited northeast of delta-plain facies). The source terrane was southwest of Umiat and consisted of low-grade metamorphic rocks and possibly sandstone and cherty limestone. Sandstone samples studied petrographically are light-gray, well-sorted, very fine grained to fine-grained chert arenites and phyllarenites relatively poor in quartz and rich in lithic fragments such as chert, phyllite, and metaquartzite. Samples with the best permeability have relatively low content of phyllite and matrix, probably due to deposition in high-energy nearshore environments. High-energy nearshore environments (foreshore-shoreface) predominate throughout the Grandstand Formation, Killik Tongue, and Ninuluk Formations, as determined from sedimentologic core analyses.

A roughly linear relationship was established between core porosity and normal-log resistivity, and this relationship was used to estimate the porosity of uncored intervals. The weighted average porosity for the lower part of the Grandstand Formation is 15.1 percent and for the upper part is 15.6 percent. A linear relationship was also established between permeability and porosity for rocks at depths less than 404.8 m and for rocks at depths greater than 643.1 m. The weighted average permeability for sandstones

of the lower part of the Grandstand is 58.6 md and for the upper part is 167.0 md. Weighted average porosity for sandstones of the Killik Tongue is 16.4 percent and the weighted average permeability is 96.2 md.

The Ninuluk Formation was deposited, in large part, in a transgressive, shallow-marine foreshore environment which lay to the east of a delta-plain environment. Sandstone samples studied petrographically are similar to those of the Grandstand Formation and Killik Tongue, but are more poorly sorted and contain significantly more metamorphic rock fragments. A change in source area between the time of deposition of the Killik Tongue and that of the Ninuluk Formation may have occurred, or a reduction in degree of destruction and winnowing of metamorphic fragments relative to underlying sediments may have taken place. Samples from the upper part of the Ninuluk contain considerable detrital and authigenic calcite. Well-log analysis indicates that the weighted average porosity for the sandstone beds in the Ninuluk Formation is 12.6 percent and the weighted average permeability is 10.7 md.

At Umiat test well 11 the Seabee Formation consists largely of shale and was deposited in an open-marine environment. Like those from the Nanushuk Group, sandstone samples studied petrographically contain fragments of low-grade metamorphic rocks and chert but, in addition, contain abundant fragments of intermediate volcanic rocks. This dramatic change in composition may be the result of a change in paleodrainage from a nonvolcanic to a volcanic area, or may represent the initiation of volcanic activity in the original source terrane. Although core analyses of sedimentologic characteristics are not conclusive, the position of a sandstone unit with mudstone clasts at the base, graded bedding, and occasional ripple laminations in a black marine-shale sequence suggests deposition as a marine-basin (turbidite) sandstone. The presence of abundant authigenic chlorite and smectite in sandstones of the Seabee Formation reduces permeability and makes these sandstones inadequate reservoir rocks. Well-log analysis indicates that the weighted average porosity for sandstone beds in the Seabee Formation is 11.5 percent and the weighted average permeability is 3.1 md.

The Tuluvak Tongue of the Prince Creek Formation consists of sandstone, siltstone, shale, bentonite, and coal deposited in a delta-plain, delta-front environment. The source terrane was to the west-southwest of the Umiat area. Sandstone samples studied petrographically are similar to those of the Seabee Formation, except that they contain slightly more quartz and less volcanic and metamorphic rock fragments, suggesting a slight change in source area and (or) a waning of volcanic activity. Abundant

authigenic smectite in these sandstones reduces permeability to very low values. Well-log analysis indicates that the weighted average porosity for sandstone beds in the Tuluvak Tongue is 14.6 percent and the weighted average permeability is 3.9 md.

#### REFERENCES CITED

- Ahlbrandt, T. S., ed., 1979, Preliminary geologic, petrologic, and paleontologic results of the study of Nanushuk Group rocks, North Slope, Alaska: U.S. Geological Survey Circular 794, 163 p.
- Beard, D. C., and Weyl, P. K., 1973, Influence of texture on porosity and permeability of unconsolidated sand: American Association of Petroleum Geologists Bulletin, v. 57, p. 349-369.
- Biscaye, Pierre, 1965, Mineralogy and sedimentation of recent deep-sea clay in the Atlantic Ocean and adjacent seas and oceans: Geological Society of America Bulletin, v. 76, p. 803-832.
- Brosge, W. P., and Tailleux, I. L., 1971, Northern Alaska petroleum province, in Cram, I. H., ed., Future petroleum provinces of the United States--Their geology and potential: American Association of Petroleum Geologists Memoir 15, p. 68-99.
- Brosge, W. P., and Whittington, C. L., 1966, Geology of the Umiat-Maybe Creek region, Alaska: U.S. Geological Survey Professional Paper 303-H, p. 501-638.
- Chapman, R. M., Detterman, R. L., and Mangus, M. D., 1964, Geology of the Killik-Ertivluk Rivers region, Alaska: U.S. Geological Survey Professional Paper 303-F, p. 325-407.
- Collins, F. R., 1958, Test wells, Umiat area, Alaska, with Micropaleontologic study of the Umiat field, northern Alaska, by H. R. Bergquist: U.S. Geological Survey Professional Paper 305-B, p. 71-206.
- Detterman, R. L., 1956a, New and redefined nomenclature of the Nanushuk group, in Gryc, George, and others, Mesozoic sequence in Colville River region, northern Alaska: American Association of Petroleum Geologists Bulletin, v. 40, no. 2, p. 233-244.
- 1956b, New member of Seabee Formation, Colville group, in Gryc, George, and others, Mesozoic sequence in Colville River region, northern Alaska: American Association of Petroleum Geologists Bulletin, v. 40, no. 2, p. 253-254.
- Detterman, R. L., Bickel, R. S., and Gryc, George, 1963, Geology of the Chandler River region, Alaska: U.S. Geological Survey Professional Paper 303-E, p. 223-324.

- Espach, R. H., 1951, Recoverable petroleum reserves in the Umiat structure, Naval Petroleum Reserve No. 4, Alaska: U.S. Bureau of Mines Petroleum and Natural Gas Branch Open-file report.
- Fisher, W. L., Brown, L. F., Jr., Scott, A. J., and McGowan, J. H., 1969, Delta systems in the exploration for oil and gas—A research colloquium, August 27-29, 1969: University of Texas Bureau of Economic Geology, 78 p., 168 figs.
- Folk, R. L., 1974, Petrology of sedimentary rocks: Austin, Texas, Hemphill Publishing Company, 182 p.
- Folk, R. L., Andrews, P. B., and Lewis, D. W., 1970, Detrital sedimentary rock classification and nomenclature for use in New Zealand: New Zealand Journal of Geology and Geophysics, v. 13, p. 937-968.
- Goddard, E. N., and others, ed., 1970, Rock-color chart: Boulder, Colorado, Geological Society of America.
- Grybeck, Donald, Beikman, H. M., Brosgé, W. P., Tailleux, I. L., and Mull, C. G., 1977, Geologic map of the Brooks Range, Alaska: U.S. Geological Survey Open-File Report 77-166B, 2 sheets, scale 1:1,000,000.
- Gryc, George, Patton, W. W., Jr., and Payne, T. G., 1951, Present Cretaceous stratigraphic nomenclature of northern Alaska: Washington Academy of Science Journal, v. 41, no. 5, p. 159-167.
- Krynine, P. D., 1947, Reservoir characteristics indicated by thin-section analyses of sand cores from Umiat Test Well No. 1: U.S. Geological Survey, Geological Investigations, Naval Petroleum Reserve No. 4 and adjacent areas, Alaska, Regular Report 9, 11 p., 1 fig., 3 pls.; released as an open-file report in 1954.
- 1948, Petrography and reservoir characteristics of selected Tertiary and Cretaceous sandstone cores from Naval Petroleum Reserve No. 4: U.S. Geological Survey, Geological Investigations, Naval Petroleum Reserve No. 4 and adjacent areas, Alaska, Regular Report 20, 47 p.; released as an open-file report in 1954.
- Krynine, P. D., and Fern, J. C., 1952, Petrography and reservoir characteristics of Umiat Test Well 9: U.S. Geological Survey, Geological Investigations, Naval Petroleum Reserve No. 4 and adjacent areas, Alaska: Special Report 34, 31 p., 13 figs.; released as an open-file report in 1954.
- Payne, T. G., and others, 1951, Geology of the Arctic slope of Alaska: U.S. Geological Survey Oil and Gas Investigations Map OM-126, 3 sheets, scale 1:1,000,000.
- Robinson, R. M., and Collins, F. R., 1959, Core test, Sentinel Hill area and test well, Fish Creek area, Alaska: U.S. Geological Survey Professional Paper 305-I, p. 485-521.
- Schrader, F. C., 1902, Geological section of the Rocky Mountains in northern Alaska: Geological Society of America Bulletin, v. 13, p. 233-252.
- Whittington, C. L., 1956, Revised stratigraphic nomenclature of Colville group, in Gryc, George, and others: American Association of Petroleum Geologists Bulletin, v. 40, no. 2, p. 244-253.